SYNTHESIS OF HIGH-VALUE CHEMICALS AND MATERIALS FROM RENEWABLE RESOURCES

Thesis

Submitted in partial fulfilment of the requirements for the degree of

DOCTOR OF PHILOSOPHY

by

HARSHITHA N ANCHAN

DEPARTMENT OF CHEMISTRY

NATIONAL INSTITUTE OF TECHNOLOGY KARNATAKA,

SURATHKAL, MANGALURU-575025

DECEMBER, 2023

SYNTHESIS OF HIGH-VALUE CHEMICALS AND MATERIALS FROM RENEWABLE RESOURCES

Thesis

Submitted in partial fulfilment of the requirements for the degree of

DOCTOR OF PHILOSOPHY

by

HARSHITHA N ANCHAN

Reg. No: 197028CY002

DEPARTMENT OF CHEMISTRY

NATIONAL INSTITUTE OF TECHNOLOGY KARNATAKA,

SURATHKAL, MANGALURU-575025

DECEMBER, 2023

DECLARATION

By the Ph.D. Research Scholar

I hereby declare that the Research Thesis titled **"Synthesis of high-value chemicals and materials from renewable resources"**, which is being submitted to the ***National Institute of Technology, Karnataka, Surathkal***, in partial fulfilment of the requirements for the award of the Degree of ***Doctor of Philosophy in Chemistry*** is a bonafide report of the research work carried out by me. The materials contained in this Research Thesis have not been submitted to any University or Institution for the award of any degree.

HARSHITHA N ANCHAN
Registration No.: 197028CY002
Department of Chemistry

Place: NITK Surathkal

Date: 04-12-2023

CERTIFICATE

This is to *certify* that the Research Thesis titled **"Synthesis of high-value chemicals and materials from renewable resources"**, submitted by **HARSHITHA N ANCHAN** (Registration Number: 197028CY002) as the record of the research work carried out by her, is *accepted* as the *Research Thesis submission* in partial fulfilment of the requirements for the award of the degree of **Doctor of Philosophy**.

SDutta
07/12/2023

रसायन शास्त्र विभाग ★ Chemistry Dept. ★ मंगलूरु MANGALURU 575 025 ★ राष्ट्रीय प्रौद्योगिकी संस्थान कर्नाटक सूरत्कल NITK SURATHKAL

Dr. Saikat Dutta
(Supervisor)
Associate Professor
Department of Chemistry
NITK Surathkal-575025

08/12/2023

Chairman-DRPC

विभागाध्यक्ष / H.O.D.
रसायन शास्त्र विभाग/ Chemistry Dept.
राष्ट्रीय प्रौद्योगिकी संस्थान कर्नाटक, सूरत्कल
NITK SURATHKAL
मंगलूरु-५७५ ०२५, कर्नाटक
MANGALURU-575 025, KARNATAKA

ACKNOWLEDGMENT

It is indeed a great pleasure to express my gratitute and indebtdness to my Ph.D. advisor, Dr. Saikat Dutta, for his unwavering support, valuable guidance and constant encouragement throughout the research program. I would like to express my gratitude to his sincerity, dignity, and decency towards work. The association with my guide will remain memoriable one throughout my entire life.

I would like to extend my heartfelt gratitude to my colleagues and fellow researchers Dr. Navya Subray Bhat, Ms. Nivedha Vinod, Mr. Gopikrishnan K., Mr. Poornachandra S. P., Mr. Abhishek Kumar Yadav, Mr. Sandeep Yadav, Ms. Megha B. N, Mr. Prajwal, Mr. Panchakshari, Ms. Snehal Jhadhav, and Ms. Muskan. They have been an integral part of my Ph.D. journey and an insightfull discussions with them have enriched my research experience and helped me to overcome challenges. I would like to express my deep appreciation to Dr. Anjana A V., Mr. Mukesh P, Mr. Manu, and Mr. Lakshmisagar G. for their assistance throughout my Ph.D. program. I would like to offer a special note of appreciation to my husband, Sharath Kumar for being my pillar of strength throughout my Ph.D. journey.

I am thankful to the RPAC members, Dr. Beneesh P.B, Department of Chemistry, and Dr. Saumen Mandel, Department of Metallurgical and Materials Engineering, for their insightful suggestions on my work. Their expertise and insights have been instrumental in shaping this thesis. I would also like to thank HOD, Department of Chemistry, Prof. Darshak R Trivedi and former HODs Prof. Uday Kumar Dalimba and Prof. Arun M Isloor. I also extend my appreciation to CSIR-UGC for financial support in terms of scholarship and contingency during my Ph.D. I am very grateful to all faculties, students, and staff members in the Department of Chemistry, NITK for all the support during my Ph.D.

Finally, I would like to thank my parents, family and friends for their constant support, motivation, prayers and sacrifices.

Harshitha N Anchan

ABSTARCT

Over the past three decades, significant research has been focused on producing fuels and chemicals from renewable carbon resources to reduce the carbon footprint and its disastrous environmental impact. In this regard, the non-food terrestrial lignocellulosic biomass has emerged as the source of biogenic carbon since they are geographically diverse, available in plenty, inexpensive, and a component in many waste streams. Catalytic synthesis of organic chemicals from the carbohydrate fraction of biomass (e.g., cellulose, hemicellulose) through the furanic platforms has received particular attention. Acid-catalyzed dehydration of hexose sugars (e.g., glucose) and pentose sugars (e.g., xylose) derived from the cellulose and hemicellulose fractions lead to 5-(hydroxymethyl)furfural (HMF) and furfural (FUR), respectively. HMF and FUR have been established as commercially viable renewable chemical intermediates for synthesizing transportation fuels, organic chemicals, and synthetic polymers of commercial significance. The commercial production of HMF remains a challenge due to its inherent hydrophilicity and poor thermal and hydrolytic stability. In this regard, the hydrophobic congeners of HMF, such as 5-(acetoxymethyl)furfural (AcMF), have received much interest in recent years. The current focus is on the efficient production of AcMF and expanding its derivative chemistry. Several classes of products of commercial significance have been produced from FUR, HMF, and even AcMF. However, synthesizing densely-functionalized heterocycles from biorenewable furfurals is underexplored. The synthesis of heterocycles is a crucial area of synthetic organic chemistry since they are known for their biological activities and are found in many pharmaceuticals. Morita-Baylis-Hillman reaction, Biginelli reaction, and Hantzsch reaction can create remarkable structural complexities in a single step using structurally simple and easily available starting materials under catalytic conditions. Moreover, they are atom-economical, high-yielding, scalable, and lead to important structural motifs for high-value applications (e.g., pharmaceuticals). The substrate scope of these green transformations is typically limited to FUR. Therefore, a systematic study of these transformations using the 5-substituted-2-furaldehydes will not only improve the substrate scope of these reactions but also lead to novel products with interesting properties and expand the derivative chemistry of these biorenewable chemicals. In

addition to the production of chemicals, the biogenic carbon in terrestrial cellulosic biomass can be transformed into renewable materials. For example, activated carbon (AC) can be produced by carbonizing biomass followed by activation. AC has a variety of conventional and emerging applications ranging from energy storage to catalyst support to water purification. Renewable synthesis of AC helps to mitigate the issue of managing waste biomass while generating value-added commodities. Therefore, producing valuable chemicals and materials from biomass is of interest from both academic and industrial perspectives.

Keywords: *Morita-Baylis-Hillman, Biginelli reaction, Hantzsch reaction, Activated Carbon, 5-(Acetoxymethyl)furfural.*

TABLE OF CONTENTS

CHAPTER 2: LITERATURE REVIEW, SCOPE, AND OBJECTIVES OF THE WORK

CHAPTER 3: RENEWABLE SYNTHESIS OF NOVEL ACRYLATES FROM BIOMASS-DERIVED 5-SUBSTITUTED-2-FURALDEHYDES BY MORITA-BAYLIS-HILLMAN REACTION

LIST OF FIGURES

CHAPTER 1

CHAPTER 3

CHAPTER 4

CHAPTER 5

CHAPTER 6

LIST OF SCHEMES

CHAPTER 1

CHAPTER 2

CHAPTER 3

CHAPTER 4

LIST OF TABLES

CHAPTER 2

CHAPTER 3

CHAPTER 4

CHAPTER 6

ABBREVIATIONS

A-15	Amberlyst-15
ALA	δ-Aminolevulinic acid
AC	Activated carbon
AcMF	5-(Acetoxymethyl)furfural
AkMF	5-(Alkyloxymethyl)furfural
AMF	5-(acyloxymethyl)furfurals
BET	Brunauer-Emmett-Teller
BMF	5-(Bromomethyl)furfural
BuMF	5-(Butyloxymethyl)furfural
BzMF	5- (benzoyloxymethyl)furfural
CBzMF	5-[(4-Chlorobenzoyloxy)methyl]furfural
CMF	5-(Chloromethyl)furfural
ChCl	Choline chloride
CNH	Cashew nut husk
CNS	Cashew nut shell
DABCO	1,4-Diazabicyclo[2.2. 2]octane
DBU	1,8-Diazabicyclo [5.4.0]undec-7-ene
DFF	2,5-Diformylfuran
DHMF	2,5-Dihydroxymethylfuran
DHPM	3,4-Dihydropyrimidin-2-(*1H*)-one
DI	Deionized
DIPEA	Diisopropylethylamine
DMAP	4-(Dimethylamino)pyridine
DMF	2,5-Dimethylfuran
DHP	1,4-Dihydropyridine
EDX	Energy-dispersive X-ray analysis
EMF	5-(Ethoxymethyl)furfural
FAL	Furfuryl alcohol
FDCA	2,5-Furandicarboxylic acid

FESEM	Field emission scanning electron microscopy
FFCA	5-Formyl-2-furancarboxylic acid
FMF	5-(Formyloxymethyl)furfural
FTIR	Fourier transform infrared
FUR	Furfural
GAAS	Gluconic acid aqueous solution
GMF	Glucosyloxymethyl furfural
HMF	5-(Hydroxymethyl)furfural
HMFA	5-Hydroxymethyl-2-furoic acid
HQD	Hydroxyquinuclidine
IN	Iodine number
LA	Levulinic acid
MB	Methylene blue
MBH	Morita-Baylis-Hillman
MSA	Methanesulfonic acid
MMF	5-(Methoxymethyl)furfural
MsMF	5-(Mesitylmethyl)furfural
5MF	5-Methylfurfural
NMR	Nuclear magnetic resonance
NBzMF	5-[(4-Nitrobenzoyloxy)methyl]furfural
PTSA	p-Toluenesulfonic acid
PrMF	5-(Propionyloxymethyl)furfural
PXRD	Powder X-ray diffraction
RT	Room temperature
SEM	Scanning electron microscopy
SMF	5-(Succinyloxymethyl) furfural
TEA	Triethylamine
THF	Tetrahydrofuran
TLC	Thin-layer chromatography

SYMBOLS

°C	Degree Celsius
wt%	Weight percent
min	Minute
h	Hour
s	Second
mL	Milliliter
mmol	Millimole
eq.	Equivalent
mg	Milligram
L	Liter
M	Molar
Å	Angstrom
mol%	Mole percent
MHz	Megahertz
Δ	Delta
Hz	Hertz
%	Percent
ppm	Parts per million
cm^{-1}	Reciprocal centimeter

CHAPTER 1

GENERAL INTRODUCTION

1.1 INTRODUCTION

Over the past three decades, significant research has been focused on producing fuels and chemicals from renewable carbon resources to reduce the carbon footprint and its disastrous environmental impact. The global demand for crude oil is increasing every day, and an effective alternative for petrochemicals is bio-based chemicals sourced from biomass (Figure 1.1). Non-food lignocellulosic and algal biomasses have been entrusted as renewable and economically feasible carbon-based feedstock to produce bioproducts of industrial significance (Bozell 2008). In a biorefinery concept, in analogy to a petrorefinery, a handful of simpler chemicals are produced initially, acting as chemical platforms, which are then synthetically upgraded into structurally and functionally diverse compounds of commercial significance (Cherubini 2010). However, one of the most intricate technological hurdles in biorefinery stems from the molecular-level differences between biomass and fossilized sources (Fernando et al. 2006). Petroleum is primarily composed of molecular hydrocarbons, which are fractionated and selectively oxygenated by catalytic processes. In contrast, biomass is made of complex, recalcitrant, and highly oxygenated biopolymers. Besides, biomass contains varying amounts of moisture, extractives, and inorganic components that often require pretreatments (e.g., drying) (Vassilev et al. 2010). Converting biopolymers like cellulose into fuels and chemicals necessitates a cascade of depolymerization, deoxygenation, and defunctionalization steps. Apart from direct combustion, biomass value addition strategies can be broadly classified into (1) thermochemical, (2) chemical-catalytic, and (3) biotechnological routes (Tursi 2019). The chemical-catalytic upgrading of biomass is of particular interest in the biorefinery realm since they are fast, selective, routinely used catalytic processes, and work under relatively less energy-intensive reaction conditions (Jing et al. 2019). In addition, they adopt similar strategies exercised in the petrorefineries and could be integrated into the prevalent infrastructure.

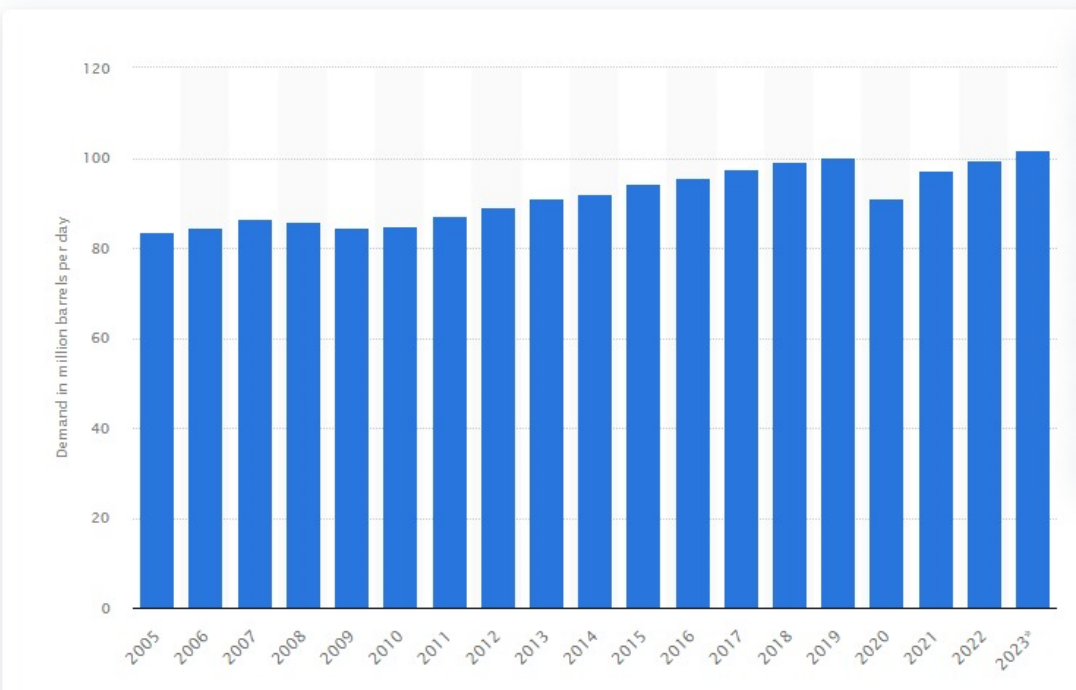

Figure 1.1 Demand for crude oil worldwide from 2005 to 2022, with a forecast for 2023 (Image credit: Global crude oil demand 2023 | Statista).

1.2 VALORIZATION OF LIGNOCELLULOSIC BIOMASS

The percentage of cellulose, hemicellulose, and lignin in terrestrial and algal biomass depends on the types of biomass, seasonal parameters, and storage conditions. The lignocellulosic biomass mostly contains biopolymers like cellulose, hemicelluloses, and lignin, along with smaller quantities of extractives (e.g., triglyceride, protein) and inorganic impurities (i.e., ash) (Figure 1.2). The choice of valorization technology for biomass must consider its composition to ensure efficiency.

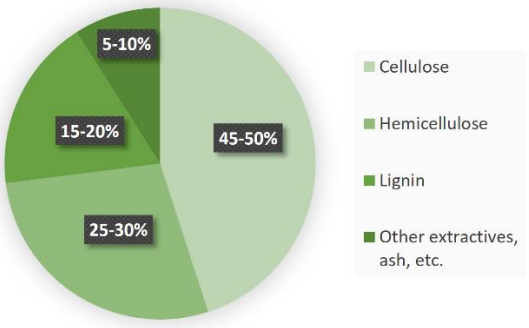

Figure 1.2 Composition of terrestrial lignocellulosic biomass.

1.2.1 Biotechnological transformation

At the last stage of their metabolic cycle, the bacteria release one or more compounds while feeding on lignocellulose. Biochemical conversions use the selective breakdown of the biopolymers into simple organic molecules using isolated enzymes in live microorganisms. The processes operate under ambient conditions and are very selective. Many high-value compounds, including lactic acid and succinic acid, are commercially produced, following the biotechnological pathway (Gao et al. 2011). A well-known example of the biotechnological value addition of biomass is the fermentation of glucose to produce ethanol. The biochemical conversion process, however, is subject to stringent health and environmental safety regulations. Additionally, the procedure necessitates continuous observation of the reaction parameters, such as temperature, nutrients, product concentration, and reaction broth pH (Kumar et al. 2016).

1.2.2 Thermolytic conversion

The breakdown of the biopolymers by heat produces a complex mixture of small organic molecules with a wide range of structures and functional groups. Regardless of whether a catalyst is present, the heat energy supplied causes depolymerization, dehydration, condensation, and various C-C and C-O bond scissions. This type of conversion includes processes such as gasification, pyrolysis, and hydrothermal liquefaction. Gasification, which involves heating biomass to temperatures in the range of 800-1300 °C in the presence of steam or limited oxygen, transforms solid biomass primarily into CO and H_2. The thermal breakdown of biomass without oxygen is known as pyrolysis. The result of pyrolysis is a mixture of gas, liquid, and solid char; the amount of each component depends on the conditions of the process (e.g., catalyst, temperature, pressure, and precursor). Although thermal processes are quick, they are almost non-selective, producing a complex mixture of chemicals that are unstable. Biomass is thermochemically transformed into liquid fuels by hydrothermal liquefaction when it is processed long enough in a hot, pressurized water environment to liquefy the solid biopolymeric structure primarily into liquid components (Maqsood et al. 2021; Tezer et al. 2022; Xu and Li 2021).

1.2.3 Chemocatalytic conversion

This strategy transforms biopolymers into value-added chemicals using stoichiometric chemical reagents, reagentless organic synthesis, or by choosing a catalytic pathway. Reagentless organic synthesis uses heat, light, sound, and electricity to produce the desired product. Catalytic transformations can be broadly categorized into homogeneous and heterogeneous based on the catalyst phase used in the reaction medium. Catalysts must be inexpensive, recyclable, robust, selective, and environmentally friendly. Although homogeneous catalysts are efficient, these systems have limitations, such as separating the catalyst from the products, acid recovery, and reactor corrosion issues when running in extreme circumstances. Some of these acids do not produce desired by-products, making them non-selective, reducing the yield of the desired molecule. Therefore, heterogeneous catalysts must be used in place of homogenous catalysts. Most heterogeneous catalysts convert cellulose and inexpensive platform chemicals with a significant rise in desired product yield. The issue of stability is one issue that plagues the use of heterogeneous catalysts. Product recovery efficiency depends on the production method and technique employed to extract the product. When conducting synthetic organic transformations, green chemistry principles must be consulted (Dutta 2023a; Nzediegwu and Dumont 2021).

1.3 FURFURAL

One of the simple and classic examples of the chemocatalytic strategy is that the furfural (FUR) can be produced from lignocellulosic materials rich in pentosan polymers (e.g., xylan) by acidic degradation (Scheme 1.1). The reaction involves acid-catalyzed hydrolysis of pentosan into pentoses (e.g., xylose) and then successive dehydration to FUR. The commercial utility of FUR was first discovered in 1921. FUR is well known for its thermosetting properties, corrosive resistance, and physical strength, so it has a broad spectrum of applications in non-petroleum-derived chemicals. Catalytic hydrogenation of FUR leads to furfuryl alcohol (FAL) used as a chemical intermediate in the paint industry. 2-Furoic acid, a flavoring agent and a starting material for various pharmaceuticals is produced by oxidizing FUR. The ring oxidation of FUR leads to 2- furanone, which gets further oxidized into maleic and succinic acid. The decarbonylation and ring-hydrogenation of FUR leads to

tetrahydrofuran. The levulinate class of products can be accessed via the ring-opening hydrolysis of FAL. FUR has also been used as a chain extender in making diesel-like fuel (Choudhary et al. 2012; Lange et al. 2012).

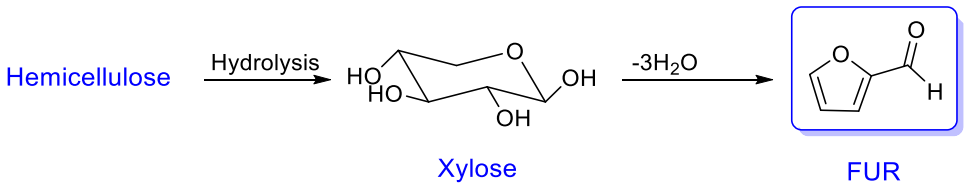

Scheme 1.1 Transformation of hemicellulose to FUR.

1.4 5-(HYDROXYMETHYL)FURFURAL

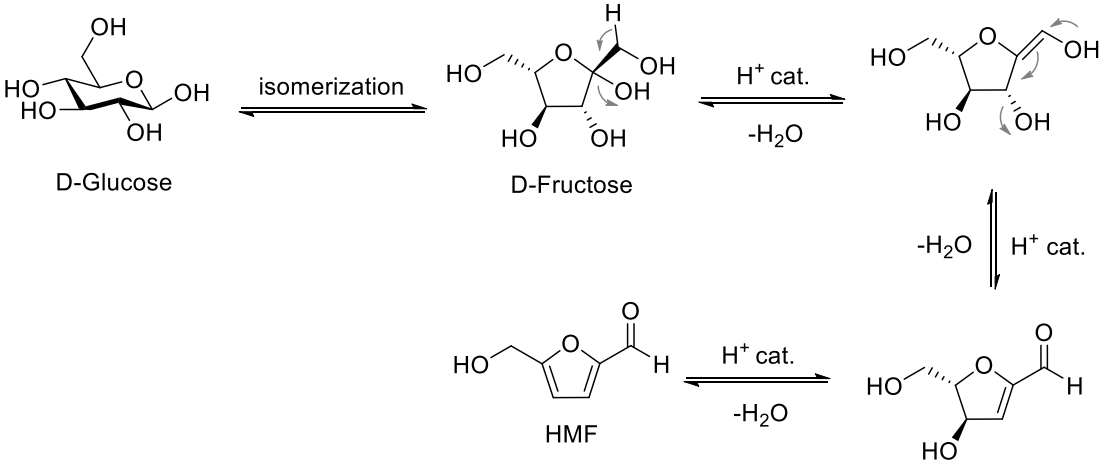

Scheme 1.2 Acid-catalyzed dehydration of glucose to HMF.

Another example of chemo catalytic value addition is the acid-catalyzed hydrolysis of cellulose and hemicellulose, followed by the dehydration of the resulting hexose sugars into 5-(hydroxymethyl)furfural (HMF) (Rosatella et al. 2011) (Scheme 1.2). The elegant process sequentially eliminates three water molecules from a hexose sugar-like fructose. This transformation reduces the oxygen content of the feed by 50 mol% and increases the energy density from 16.3 kJ/g in fructose to 22.1 kJ/g in HMF (Verevkin et al. 2009). Importantly, all the carbon atoms and some of the key functionalities of the parent sugar molecule are preserved in HMF. The functional groups in HMF are indispensable for its downstream synthetic upgrading into value-added chemicals and commodity products. 2,5-Dimethylfuran (DMF) is produced through the selective hydrogenation of HMF. DMF is a potential high-octane fuel with many physical and chemical characteristics of petrol. 2,5-Diformylfuran (DFF)

and 2,5-furandicarboxylic acid (FDCA) are produced when HMF is selectively oxidized. DFF and FDCA are both considered renewable monomers. For instance, poly(ethylene furoate), a renewable substitute for poly(ethylene terephthalate), is made using FDCA. HMF has been successfully transformed into several other important chemicals, such as levulinic acid (LA), 5-(alkoxymethyl)furfural (AkMF), and δ-aminolevulinic acid (ALA) (Scheme 1.3). HMF was first reported as early as 1895, produced by the hydrolysis and dehydration of inulin (a β-2,1-fructan) in aqueous oxalic acid (Düll 1895). HMF is known to form in baked items and other foodstuffs and is responsible for their smoky odor (Shapla et al. 2018). HMF has received renewed attention since the early 1990s due to increased volatility in the petroleum market and public consensus for a sustainable future. Multiple comprehensive reviews have summarized the enormous research on the production and synthetic upgrading of HMF (Kong et al. 2018; Xia et al. 2018).

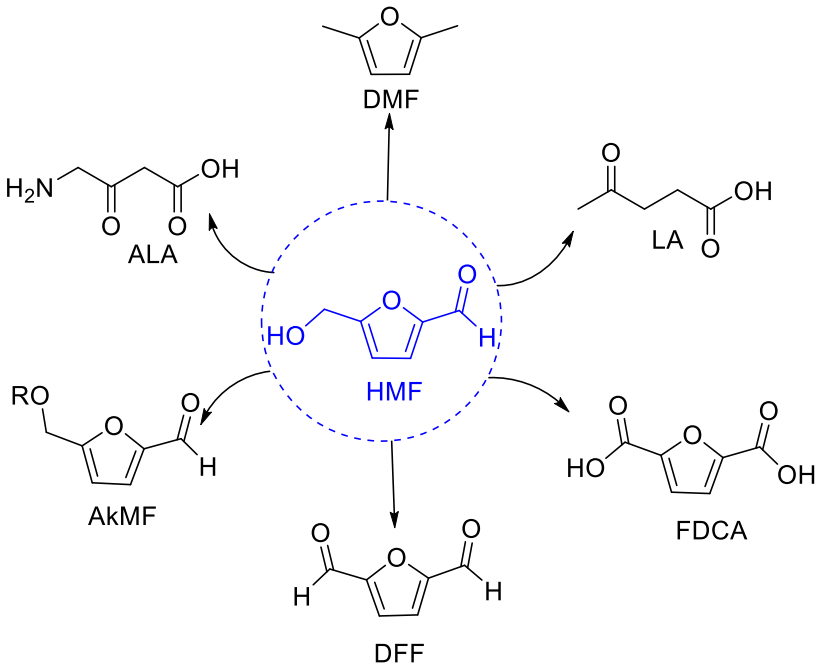

Scheme 1.3 Some of the commercially relevant renewable chemicals produced from HMF.

1.5 HYDROPHOBIC ANALOGS OF HMF

However, even after years of dedicated research fueled by huge commercial prospects, the production of HMF has yet to reach the commercialization stage. The challenges associated with the isolation and purification of hydrophilic HMF from the

aqueous or polar reaction media must be surmounted for the process scale-up (Rosenfeld et al. 2020). Besides, HMF is inherently unstable in aqueous acid and has poor storage stability due to the accessibility of several decomposition pathways with low kinetic barriers. Though high yields of HMF can be ensured from simple sugars like fructose, special reaction conditions and reagents are often required to transform the complex carbohydrates and cellulosic biomasses to HMF in acceptable yields (Menegazzo et al. 2018). The hydrophilicity of HMF is responsible for most shortcomings it encounters as a renewable chemical building block. Therefore, a hydrophobic analog of HMF that can be produced directly from biomass efficiently would undoubtedly alleviate those issues. The hydrophobic analogs could be sequestered in an organic solvent as soon as they form and shielded from acid-promoted decomposition pathways in the aqueous phase. The hydrophobic nature of the compounds decreases their miscibility in water, thereby improving the hydrolytic and storage stability. The hydrophobic analogs of HMF, with superior thermal, hydrolytic, and storage stability, have been proposed as suitable replacements in derivative chemistries of HMF (Anchan and Dutta 2021). The most significant advantage of hydrophobic derivatives is their straightforward isolation from the aqueous or polar reaction media by solvent-solvent extraction. The hydrophobic character lowers solubility in the aqueous medium and slows the hydrolysis reaction. All the hydrophobic alternatives of HMF can be produced in high yield directly from biomass. Mechanistically, protonation of the hydroxymethyl group in HMF followed by the nucleophilic substitution with a halide ion produces 5-(chloromethyl)furfural (CMF) or 5-(bromomethyl)furfural (BMF). The acid-catalyzed dehydration of hexoses (e.g., fructose) into HMF presumably occurs in the aqueous phase. Owing to its hydrophilicity, the distribution coefficient of HMF is generally low even in polar solvents (e.g., R = 0.6 for HMF in 1:1 (v/v) (water-ether) (Gomes et al. 2015). Therefore, a significant proportion of HMF remains in the aqueous acid, where it continues to degrade into unwarranted side products. When HMF gets converted into CMF, it gets transported into the organic layer and stays there due to the significantly more hydrophobicity of the latter. The equilibrium concentration of HMF and CMF depends on the type of organic solvent used and the chloride ion availability in the aqueous and organic phases. HMF can undergo rehydration, followed by ring opening

to form LA. Alternatively, it can undergo several not well-studied decomposition reactions forming humin. Therefore, a key strategy to ensure a good yield of CMF is to sequester it into the organic phase as soon as it forms and minimizes the hydrolysis of CMF back into HMF. The preparation of CMF and BMF from biomass-derived carbohydrates generally requires concentrated acids (i.e., HCl, HBr) to be used. Strong, corrosive, and volatile mineral acids used in the process can lead to engineering challenges and environmental concerns (Oriez et al. 2019). The synthetic upgrading of CMF or BMF must be designed to recover and recycle HCl or HBr, which is vital from both the economic and environmental perspectives.

Alkyl ethers of HMF can be produced by the acid-catalyzed alcoholysis of biomass-derived carbohydrates. In this regard, the C1-C4 monohydric alkyl alcohols are most employed since they are commercially available in bulk quantities, inexpensive, and biorenewable. Among the alkyl ethers of HMF, 5-(ethoxymethyl)furfural (EMF) has the most literature presence. Other alkyl ethers of HMF, such as 5-(methoxymethyl)furfural (MMF) and 5-(butyloxymethyl)furfural (BuMF), have also been studied in detail, but their literature presence is relatively sparse compared to EMF. Various acid catalysts, including mineral acids, solid Brønsted acids, metal oxides and salts, zeolites, acidic ionic liquids, and ion-exchange resins, have been used to produce EMF. The reaction conditions include conventional as well as microwave heating, the use of ionic liquid, and supercritical solvents (Yu et al. 2021; Zuo et al. 2023).

There have been significant interests in producing non-halogenated, hydrophobic derivatives of HMF, and the esters of HMF with biogenic carboxylic acids (e.g., formic acid, acetic acid) are some of the prime candidates for that. Dehydration of sugars and carbohydrates in formic acid and acetic acid forms 5-(formyloxymethyl)furfural (FMF) and 5-(acetoxymethyl)furfural (AcMF), respectively. Both esters of HMF are significantly more stable than HMF and consist of C, H, and O only. The major challenge in producing FMF or AcMF is the low Brønsted acidity of carboxylic acids. The reactions generally require relatively harsh reaction conditions to ensure faster kinetics but lead to low selectivity and yield. Direct esterification of HMF to HMF esters under different catalytic conditions has been reported (Hu et al. 2017; Kumar et al. 2018a). FMF was obtained in 92% yield

when HMF was reacted with formic acid for 6 h at 120 °C (Xiong et al. 2018). AcMF can be conveniently prepared from HMF using a bimetallic catalyst (Pérez-Bustos et al. 2019; Ramírez Bocanegra et al. 2021). Enzymatic transformations of HMF into its esters using lipase as an efficient and environmentally-benign biocatalyst have also been reported (Krystof et al. 2013). However, the approaches from HMF are unlikely to be economically competitive, as mentioned earlier. By integrating the dehydration of carbohydrates and the subsequent esterification of the resulting HMF with an organic acid, anhydride, or acid halides, HMF esters may be produced. The HMF esters were produced as early as the twentieth century (Jogia et al. 1985). However, their applications as sweet-modulating agents, monomers, fragrances, fuel additives, surfactants, and fungicides have recently gained prominence (Liu and Wang 2018; Mascal 2017; Peng et al. 2019).

In this section, the preparation of other hydrophobic derivatives of HMF directly from biomass feedstock is discussed. For example, the one-pot preparation of 5-methylfurfural (5MF) from carbohydrates has been realized. Sugars like fructose can be transformed into 5MF by one-pot dehydration and metal-free hydrogenolysis using iodide as the catalyst (Peng et al. 2019). Carbohydrates have been converted into 5MF in a reaction medium of aqueous HI with or without noble metal-based catalysts (Yang et al. 2012; Yang and Sen 2011). Recently, L-rhamnose has been dehydrated into 5MF in a nearly quantitative yield using $AlCl_3$ as a catalyst (Feng et al. 2020).

Strong Brønsted acid, Lewis acid, or a combination of the two is used as catalysts for preparing the hydrophobic analogs of HMF. Sometimes, the acid catalyst acts as the reagent (e.g., HCl for CMF, HBr for BMF). For the preparation of AcMF and FMF, an external acid catalyst is often used in addition to acetic acid or formic acid to make the reaction work faster under milder conditions and to afford better yields. Over the past few years, extensive research has been conducted to synthesize hydrophobic congeners of HMF directly from biomass resources.

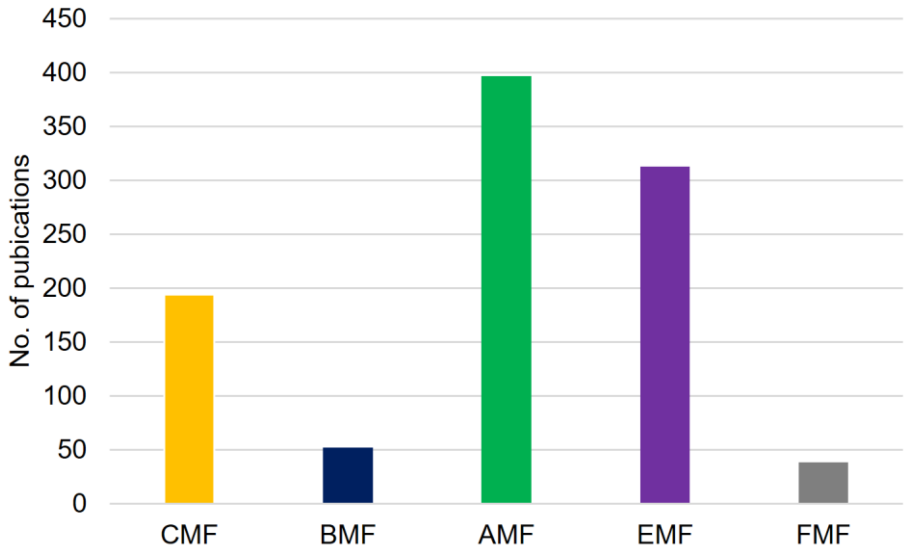

Figure 1.3 Number of journal articles and patents published during 2000-2020 for some selected hydrophobic analogs of HMF (Structure search in the SciFinder, Accessed on January 14, 2021).

Purified HMF can be converted efficiently into hydrophobic analogs and vice versa. For example, HMF can be transformed into CMF by reacting with chlorinated reagents, and the latter can be hydrolyzed to the former in boiling water (Mascal and Nikitin 2010; Sanda et al. 1992). However, converting the isolated HMF into these derivatives has no substantial economic advantages since the former must be produced from biomass in the first place. A SciFinder search revealed the total number of publications (journal articles and patents) published on various hydrophobic derivatives of HMF during 2000–2020 (Figure 1.3). EMF and AcMF have significantly more literature references than all others combined due to their natural occurrence in foodstuffs and potential applications such as biofuel.

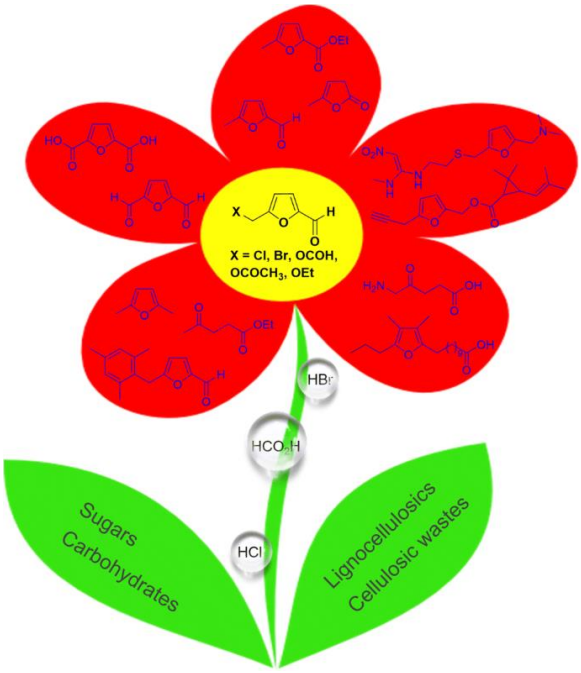

Figure 1.4 Synthesis and application of hydrophobic analogs of HMF.

The halogenated congeners such as CMF and BMF serve as chemical platforms to produce various value-added chemicals such as 5MF, ranitidine, prothrin, DMF, ALA, and many other value-added chemical compounds. Furthermore, the non-halogenated analogs of HMF, such as AcMF, FMF have been successfully transformed into DMF, DFF, FDCA, 5-formyl-2-furancarboxylic acid (FFCA), 2,5-dihydroxymethylfuran (DHMF), 5-hydroxymethyl-2-furoic acid (HMFA), and diesel fuel precursor such as 5-(mesitylmethyl)furfural (MsMF). Several research articles show the enormous application and derivative chemistry of hydrophobic congeners of HMF (Anchan and Dutta 2021; Mascal 2019).

1.6 FURAN-BASED HETEROCYCLES

The chemistry of heterocycles is a crucial subfield of synthetic organic chemistry with applications in agrochemicals and pharmaceuticals. A large fraction of all pharmaceuticals and agrochemicals contains at least one heterocyclic ring. Pharmaceutically important molecules containing a furan moiety include furosemide, ranitidine, amiodarone, and psoralen. The well-documented class of heterocyclic compounds, such as 3,4-Dihydropyrimidin-2-(*1H*)-one (DHPM) and 1,4-dihydropyridine (DHP), synthesized using Biginelli and Hantzsch reactions, have shown remarkable biological properties (Crespo et al. 2013). However, the

comprehensive investigation of biomass-derived 5-substituted-2-furaldehydes as substrates for synthesizing several classes of heterocyclic compounds is virtually unexplored. In this regard, the systematic investigation will help unravel these biorenewable compounds' reactivity patterns and broaden the scope of their derivative chemistry. The research discussed in this thesis will assist in ideating novel structural moieties using biorenewable chemicals and exploring their potential applications.

1.7 ACTIVATED CARBON

Lignocellulosic biomass wastes can also be converted into value-added materials with a wide range of commercial significance. Converting biomass waste into materials such as activated carbon (AC) will help to mitigate environmental issues, such as waste accumulation, landfilling, air pollution, and water pollution. The highly porous AC has a well-established market as adsorbent and catalyst support. The mass-scale use of AC as an adsorbent can be traced back to World War II when it was used as the active component in gas masks. AC has been widely employed as catalyst support for chemical reactions, for air and water purification, as a decolorizing agent, a formulating agent in personal care products and pharmaceuticals. Even though AC can be produced from anthropogenic carbon like coal and peat, the synthesis of AC from biomass is recommended from a sustainability perspective (González-García 2018; Ioannidou and Zabaniotou 2007).

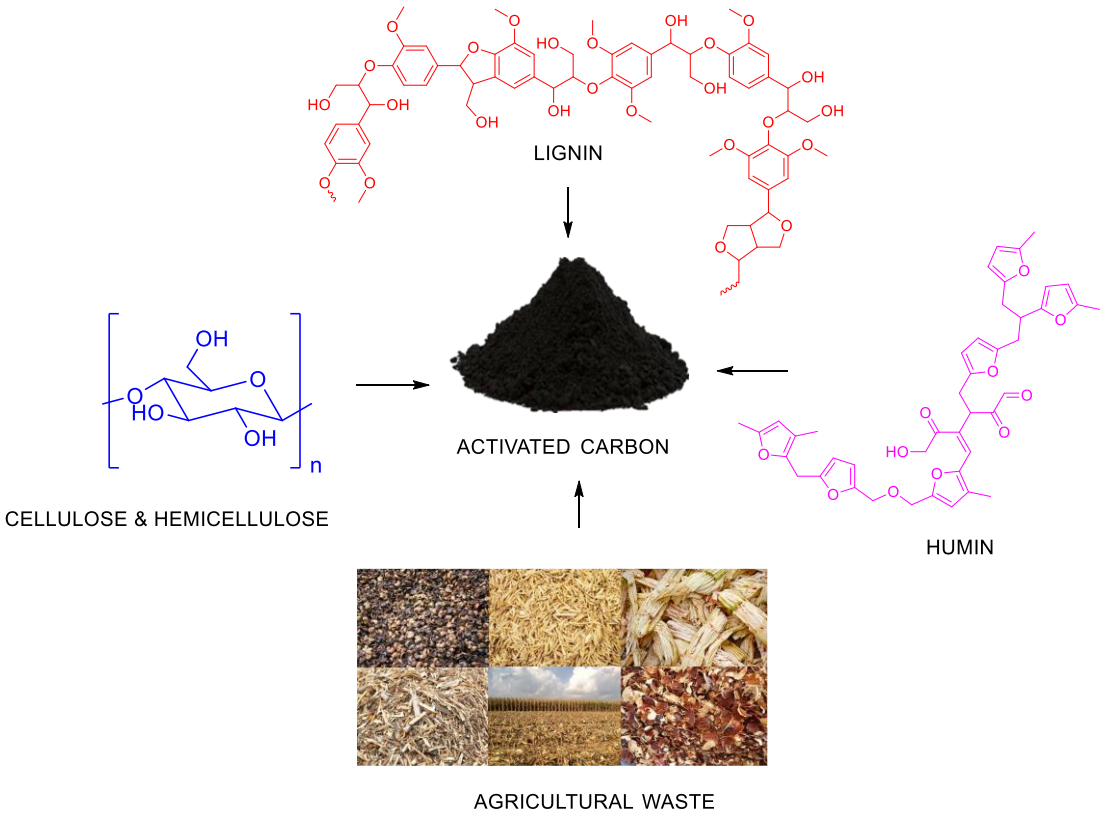

Figure 1.5 Various precursors for the preparation of AC.

1.8 TYPES OF ACTIVATION

The methods for activating AC can be classified as chemical and physical methods. In some instances, physical and chemical activation processes are combined (Gao et al. 2020; Heidarinejad et al. 2020)

1.8.1 Physical activation

In the physical method, the first step involves the carbonization of precursor in an inert atmosphere, and the second step is activation using steam, CO_2, or air mixture at elevated temperatures in the range of 800-1100 °C. This method is generally considered green as it is a chemical reagent-free process. However, this method has certain disadvantages, such as high energy consumption, low adsorption capacity of the synthesized carbons, and long activation time (Bouchelta et al. 2008; Yang and Lua 2003).

1.8.2 Chemical activation

In this method, the carbonization and activation process take place simultaneously. Here the precursors are activated using chemical activating agents,

such as KOH, H_3PO_4, and $ZnCl_2$ (Tadda et al. 2016). The chemical activating agents promote deoxygenation processes (e.g., dehydration) in the precursor. Chemical activation is advantageous over physical activation due to its lower carbonization temperature and shorter time of activation. ACs can be prepared from various carbonaceous materials such as coal, wood, nutshells, fruit peels and agricultural by-products or wastes using chemical activation method (Xu et al. 2014).

1.9 TYPES OF CHEMICAL ACTIVATING AGENTS

The activating agents react with cellulose, hemicellulose, lignin, and polysaccharides in the precursors leading to different activation mechanisms. Different types of activating agents include acidic, alkaline, and neutral activating agents (Gao et al. 2020; Karapınar 2022).

1.9.1 Acidic activating agents

Examples of acidic activating agents include H_3PO_4, HCl, H_2SO_4, and HNO_3. Oxidation, dehydration, and swelling play key roles in carbonization and activation. For instance, the precursor loses hydrogen and oxygen as water vapor when H_3PO_4 is present. In contrast, they are removed as volatile carbon-containing molecules without H_3PO_4. As the activating agent, H_3PO_4 can penetrate the precursor, reacting with biopolymers like cellulose, hemicellulose, and lignin. Interestingly, H_3PO_4 has a higher thermal conductivity than air, water vapor, or CO_2, making it a superior heat transfer medium (Sujiono et al. 2022).

1.9.2 Basic activating agents

Alkaline activating agents are further divided into strongly alkaline activating agents (e.g., KOH, NaOH), moderately alkaline activating agents (e.g., K_2CO_3), and weakly alkaline activating agents (e.g., K_2SiO_3). Among these, KOH is the most widely used activating agent owing to its effectiveness (Wazir et al. 2022).

1.9.3 Neutral activating agents

Metal salts like $ZnCl_2$, $FeCl_3$, $MgCl_2$, and even KCl have been employed as neutral activating agents. The neutral activating agent's primary pore-forming mechanism is oxidation, and gasification. By engaging in reduction processes with carbon atoms, the positive ions (such as Fe^{3+}, Mg^{2+}, Na^{+}, etc.) at their oxidation states could remove some of the carbon atoms and leave behind channels (Susanti et al. 2022).

1.9 APPLICATIONS OF AC

The high surface area, high microporosity, and presence of surface functional groups all contribute to the adsorptive properties of AC. Because of this, AC has tremendous growth and adoption in the industrial sectors for both gaseous and aqueous phase applications (González-García 2018).

- AC purifies contaminated water by removing the compounds that cause unwanted color, odor, and taste. It also helps in the removal of pesticides, heavy metals, and any other organic impurities.
- AC is also employed in gas purification to eliminate undesirable impurities such as volatile organic compounds. Mercury, furans, dioxins, and a few other dangerous substances are removed from the flue gas with its assistance.
- AC also helps solvent recovery, which can significantly affect solvent reutilization on an industrial scale.
- AC is used as a support for heterogeneous catalysts to carry out various chemical transformations.
- Other applications include gold recovery in mining and the food and beverage industry to eliminate undesired odor, color, and taste.

Figure 1.6 Applications of activated carbon (AC).

CHAPTER 2

LITERATURE REVIEW, SCOPE AND OBJECTIVES OF THE WORK

2.1 LITERATURE REVIEW

There are the latest comprehensive reviews, research publications, and other scientific articles on Morita Baylis Hilman (MBH) reactions, Biginelli reactions, Hantzsch reactions, synthesis of 5-(acetoxymethyl)furfural (AcMF), and the production and application of activated carbon (AC) from cashew wastes. This chapter provides an overview of the literature, current status, opportunities, and challenges in these research fields.

2.1.1 Literature review on MBH

The Baylis–Hillman reaction has been attracting the attention of synthetic and medicinal chemists in recent years; it not only helps in generating new ideas for novel methodologies and molecules, but it also provides intellectual challenges in understanding and addressing current needs in the fields of organic and medicinal chemistry, according to a recent tutorial review (Basavaiah and Tilak Naganaboina 2018; Basavaiah and Veeraraghavaiah 2012; Santos et al. 2023).

Early in 1989, MBH adduct from furfural (FUR) and 5-methyfurfural (5MF) was synthesized at room temperature (RT) using methyl acrylate as activated alkene and 2-HQD (hydroxyquinuclidine) as the catalyst, affording 65% and 33% yield, respectively (Drewes et al. 1989). 2,5-Diformyfuran (DFF) gave both mono- and bis-condensation MBH products resulting in 50-60% yield, respectively, using methyl acrylate as activated olefin and 1,4-diazabicyclo[2.2.2]octane (DABCO) as the catalyst. Mono condensation product was obtained in 4 h in the presence of THF as the solvent, whereas forming the bis-condensation product required 27 h to complete under solventless conditions (Fort et al. 1992b).

Various MBH adducts were synthesized by reacting substituted benzaldehydes and FUR with acrylic esters in slight excess (1.3 eq) using DABCO (10 mol%) as the catalyst. Using FUR and methyl acrylate, a 76% yield of the corresponding MBH adduct was obtained after 24 h of reaction. Using n-butyl acrylate and FUR, a 88% yield of the MBH adduct was isolated after 72 h (Fort et al. 1992a).

Using 1,4-dioxane-H_2O (1:1, v/v) solvent system, MBH products from FUR and 5-(hydroxymethyl)furfural (HMF), were obtained at RT in 85% and 62% yields using methyl acrylate as activated alkene and DABCO as the catalyst (Yu et al. 2001). Another research group reported using dimethylformamide as the solvent and

$Sc(OTf)_3$/HQD as the catalyst to produce nearly 88% yield of the MBH adduct from FUR and ethyl- or methyl acrylate (Shang et al. 2009).

A set of 2-(2-furyl)hydroxymethyl-2-cycloalkenones were synthesized in 70-88% yield at RT using precursors such as FUR, HMF and glucosyloxymethyl furfural (GMF), activated alkene such as cyclopentenone and cyclohexenone in the presence of DPI as the catalyst in aqueous medium (Wang et al. 2019b). Biobased solvents, such as ethanol, isopropanol, methyl-THF, and tetrahydrofurfuryl alcohol, have been used to produce the MBH adducts from HMF and GMF (Tan et al. 2013, 2015). The MBH products were employed as the starting material in Achmatowicz reaction to create substituted pyran-3-ones with a unique substitution pattern. The reactions were carried out at room temperature under ultrasound irradiation in methanol (Scheme 2.1). In the presence of Lewis bases such as DABCO and 1,8-diazabicyclo[5.4.0]undec-7-ene (DBU), the MBH adduct of FUR with methyl, ethyl, butyl, and *tert*-butyl acrylate (1.2 eq.) afforded 80-98% yields. Similarly, the MBH adduct of 5MF with methyl- and butyl acrylate provided 98% and 90% yields, respectively, in 24-80 h (Guidotti and Coelho 2015).

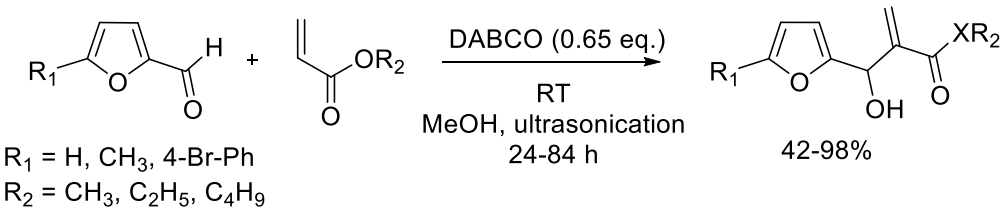

Scheme 2.1 Synthesis of MBH adducts under ultra-sonication in methanol.

The Baylis-Hillman reaction of FUR, HMF and GMF, was examined under solventless conditions. Using 1.5 eq. of methyl acrylate, ethyl acrylate and acrylonitrile, FUR gave 86%, 74% and 93% yields of the corresponding MBH adduct, respectively. HMF as the substrate afforded 91%, 88% and 71% yields of the MBH adducts (Wang et al. 2019a).

Using the Baylis-Hillman process, two dense diol monomers, 2-hydroxyethyl 2-(furan-2-yl(hydroxy) methyl)acrylate and methyl 2-(hydroxy(5-(hydroxymethyl)furan2-yl)methyl)acrylate, were synthesized from renewable FUR and HMF in 56% and 57% yield (Scheme 2.2). These products were utilized to make oligomers of linear polyurethane (Huang et al. 2019).

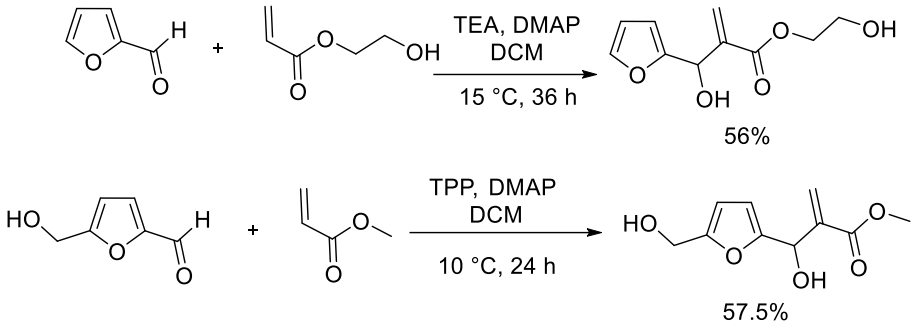

Scheme 2.2 Synthesis of MBH adducts from FUR and HMF using DMAP as the organocatalyst.

A set of amphiphiles using HMF, GMF, and 5-(succinyloxymethyl)furfural (SMF) have been synthesized in 49-93% yields. Starting from HMF, in the presence of DABCO (1 eq.) and corresponding acrylates (butyl and hexyl acrylate) gave H4 and H6 in 62% and 56% yields. The reaction was carried out at RT for 2 days in EtOH/H_2O (1:1). H6 was also synthesized in 49% yield under solvent less condition using DABCO (0.8 eq.) and acrylate (1.5 eq.) in 7 h. GMF based adducts G6, G8, G12, G16 were obtained in 58%, 56%, 53%, and 57% yields respectively in 5 days. G6 used solvent less condition with 3 eq. of acrylate and G8, G12, G16 used ethanol as the solvent in the presence of 0.8 eq. of DABCO and 1.1 eq. of acrylate. SMF adducts HS8, HS12, and HS16 were obtained in 91%, 93%, and 72% yields using 2.4 eq. of DABCO and 2 eq. of alkyl acrylate under solvent less condition in 64 h (Scheme 2.3).

H4N and H6N were obtained in 53% and 60% yields starting from HMF, acrylamide (2 eq. butyl or hexyl) and 3-HQD (1 eq.) in 1:1 2-MeTHF/H_2O after 3 days (Ontiveros et al. 2021).

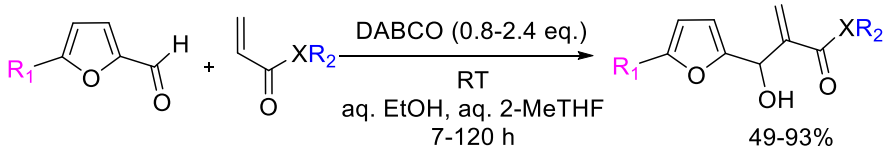

R_1 = CH_2OH (H4, H6 (X=O), H4N, H6N (X=NH)), CH_2O-glucosyl (G6, G8, G12, G16 (X=O)), $CH_2OCOCH_2CH_2CO_2H$ (HS8, HS12, HS16 (X=O))
R_2 = C_4H_9, C_6H_{13}, C_8H_{17}, $C_{12}H_{25}$, $C_{16}H_{33}$
X = O, NH

Scheme 2.3 Synthesis of MBH adducts using HMF, GMF and SMF using ethanol.

In this regard the MBH reaction of renewable 5-substituted-2-furfuraldehydes with acrylate reagents are underexplored and it is important to synthesis novel compounds in addition to expanding the derivative chemistry of biorenewable furaldehydes.

2.1.2 Literature review on Biginelli (synthesis of 3,4-Dihydropyrimidin-2-(1H)-ones (DHPMs)) and Hantzsch (synthesis of 1,4-dihydropyridines (DHPs)) reaction

Well-known heterocyclic substances with promising biological properties include DHPMs and DHPs. Therefore, there are many research publications and reviews that demonstrate the high-yielding synthesis of DHPMs and DHPs in the literature. The synthesis of DHPMs and DHPs from biorenewable FURs is described in more detail in the section that followed.

There are numerous literature on the preparation of DHPMs and DHPs from aldehydes, focusing on design, efficiency, selectivity, and recyclability of the catalyst. Numerous homogeneous and heterogeneous catalysts were used for synthesizing DHPMs and DHPs successfully. For benzaldehyde derivatives, strong acid catalysts were effective; however, moderate acids were preferred for FUR derivatives. The reactions were examined under various conditions, such as traditional or microwave heating, various temperature ranges, and time periods with or without the use of solvents such water, ethanol, methanol, and acetonitrile. In the literature, biorenewable FURs are rarely used as substrate. In this context, it is crucial to create mild, affordable, non-toxic, green, recyclable catalyst that can convert biorenewable FURs into DHPMs and DHPs.

Table 2.1 Literature reports of synthesis of DHPM from FURs

Substrate	Reaction Conditions	Product	Yield (%)	Reference
FUR	$ZrCl_4$, EtOH, EAA, urea, reflux, 6 h	DHPM	84	(Reddy et al. 2002)
FUR	12-Molybdophosphoric acid (2 mol%), AcOH, EAA, urea, reflux, 5 h,	DHPM	60	(Heravi et al. 2006)

FUR	DPA (10 mol%), EAA, urea, 70 °C, 20 min	DHPM	96	(Ghassamipour and Sardarian 2010)
FUR	Fe_3O_4@mesoporousSBA-15, EAA, urea, 90 °C, 5 h	DHPM	78	(Mondal et al. 2012)
FUR	nanocomposite ferrite (10 mol %), 2 drops HCl in EtOH (5 mL), EAA, urea, 60 °C, 1.2 h	DHPM	89	(Joshi et al. 2013)
FUR	$SiO_2/CuCl_2$ (0.05 g) and diphenic acid (0.02 g), EAA, urea, 40 °C, 1.5 h	DHPM	92	(Kour et al. 2014)
FUR	[Btto][p-TSA] (0.15 mmol), EAA, urea, 90 °C, 30 min	DHPM	79	(Zhang et al. 2015)
FUR	PSBIL (50 mg) in 5 mL EtOH, EAA, urea, 110 °C, 18 h	DHPM	84	(Khiratkar et al. 2016)
FUR	$GaCl_3$, EAA, urea, 80 °C, 6 h	DHPM	92	(Yuan et al. 2017)
FUR	Dendrimer-PWA^n, EAA, urea, 80 °C, 35 min	DHPM	92	(Safaei-Ghomi et al. 2018)
HMF	$ZnCl_2$,EAA, urea, 80 °C, 16 h	DHPM	82	(Fan et al. 2018)
FUR	Fe_3O_4@SiO_2@Polyionene/Br^-, EAA, urea, 100 °C, 60 min	DHPM	89	(Dezfoolinezhad et al. 2019)
FUR	BNPs@$SiO_2(CH_2)_3NHSO_3H$, EAA, urea, 80 °C, 55 min	DHPM	95	(Khodamorady et al. 2020)
FUR	20% PMo_7W_5/kaolin, EAA, urea, 80 °C, 15 min	DHPM	80	(S. Aher et al. 2021)
FUR	[BCMIM][Cl], EAA, urea, 80 °C, 17 min	DHPM	91	(Madivalappa Davanagere and Maiti 2021)
FUR	[BCMIM][Cl], EAA, thiourea, 80 °C, 22 min	DHPM	90	(Madivalappa Davanagere and Maiti 2021)

FUR	TiO_2, EAA, urea, Light (60 W), 18 h	DHPM	70	(Gawhale et al. 2022)
FUR	[Gly-H][OTs] (25% mol), EAA, urea, 110 °C, 17 min	DHPM	71%	(Hataminejad et al. 2023)
FUR	Cysteine (20 mol%), H_2O:EtOH, (3:1), EAA, urea, 70 °C, 30 min	DHPM	96%	(Hosseini Nasab et al. 2023)

Abbreviations: DPA: dodecylphosphonic acid;[Btto][p-TSA]: 1-Butyl-1,3-thiazolidine-2-thione *p*-toluenesulfonate;PSBIL: polymer-supported benzimidazolium based ionic liquid; PWA^n: $H_3PW_{12}O_{40}$ nanoparticles;BNPs@$SiO_2(CH_2)_3NHSO_3H$: Boehmite nanoparticles functionalized with silylpropyl sulfamic acid;[BCMIM][Cl]: 1,3-bis(carboxymethyl)imidazolium chloride;[Gly-H][OTs]: glycine-based ionic liquid.

Table 2.2 Literature reports on synthesis of DHP from FURs

Substrate	**Reaction Conditions**	**Product**	**Yield (%)**	**Reference**
5MF	MIL-101-SO_3H MO (20 wt%), EtOH, EAA, ammonium acetate, 60 °C, 8 h	DHP	93	(Devarajan and Suresh 2019)
FUR	$HClO_4$-SiO_2, EAA, ammonium acetate, 80 °C, 52 min	DHP	86	(Maheswara et al. 2006)
FUR	PPh_3 (20 mol%), EtOH,EAA, ammonium acetate, reflux. 5 h,	DHP	94	(Debache et al. 2009)
FUR	Free'' nano-g-Fe_2O_3, EAA, ammonium acetate, 90 °C, 12 min	DHP	89	(Koukabi et al. 2011)
FUR	TiO_2 NPs (10 mol%), EtOH, EAA, NH_4OAc, reflux, 3.75 h	DHP	50	(Tajbakhsh et al. 2012)
FUR	IL–Ni(II)–MNPs, EAA, NH_4OAc, 70 °C, 20 min	DHP	98	(Safari and Zarnegar 2013)
FUR	Fe_3O_4 NPs, EAA, NH_4OAc, 80 °C, 5 min	DHP	94	(Nasr-Esfahani et al. 2014)
FUR	Chitosan NPs, EAA, NH_4OAc,	DHP	95	(Safari et al.

	80 °C, 20 min			2015)
FUR	n-Fe_3O_4@ZrO_2–H_3PO_4, EAA, NH_4OAc, 100 °C, 20 min	DHP	91	(Zolfagharinia et al. 2017)
FUR	MIL-101-SO_3H MOF(1) (20 wt%), EtOH, EAA, NH_4OAc, 60 °C, 8 h	DHP	91	(Devarajan and Suresh 2019)
FUR	AFGONs, EtOH, EAA, NH_4OAc, RT, 3 h	DHP	87	(Choudhury et al. 2020)
FUR	Fe_3O_4-Pec-DSA (1), EtOH, ultrasonic, EAA, NH_4OAc, 40 °C, 30 min	DHP	87	(Bakhtiarian and Khodaei 2021)
FUR	NH_4VO_3, EtOH, EAA, NH_4OAc, reflux, 16 min	DHP	98	(Rahimi et al. 2022)
FUR	$NbCl_5$+$AgClO_4$, EAA, NH_4OAc, RT, 6 h	DHP	88	(Bora et al. 2022)

Abbreviations: AFGONs: amine-functionalized graphene oxide nanosheets.

Numerous heterogeneous and homogeneous catalysts have been reported to improve the yield of the DHPM and DHP via Biginelli and Hantzsch reaction (Table 2.1 and Table 2.2). It comprises of ionic liquids, metal complexes, metal salts, polymer supported catalyst and many others. The reactions have also been researched with and without solvents (Chopda and Dave 2020; Patil et al. 2019). Given the significance of these molecules for medicine, finding green and high producing catalysts is still the scope of research.

2.1.3 Literature review on the synthesis of AcMF

Table 2.3 Direct preparation of AcMF from carbohydrates and biomass

S/N	Feedstock	Reaction condition	Yield (%)	Reference
1	Glucose	EMIM, AcOH, $CrCl_2$, 100 °C, 3 h	5.1	(G.J.M. Gruter 2012)
	Fructose		71.5	
2	D-Fructose	AcOH, Ac_2O, H_2SO_4, 80 °C, 3 h	32	(Hong Yeon-Woo 2013)
	D-Glucose	AcOH, DCE, Ac_2O, 100 °C, 3 h	9	

	1,6-Di-O-acetylfructofuranose	Dowex, THF, reflux, 12 h (step-I); DMAP, Ac_2O, pyridine, RT, 6 h (step-II)	42	
	Pentaacetate fructofuranose	H_2SO_4, dioxane, reflux	19	
3	Crystalline fructose	AcOH, A-15, 110 °C, 3 h	41	(Sanborn and Howard 2009)
4	Commercial cellulose acetate	AcOH, Ac_2O, H_2SO_4, batch reactor, 200 °C, 2 h	36.4	(Gavilà and Esposito 2017)
	Acetylated beech wood		36.6	
	Acetylated glucose	AcOH, Ac_2O, H_2SO_4, continuous flow reactor, 175 °C, 5 min	82	
	Acetylated cellulose		49	
5	Glucose	Sn-Mont, AcOH, 150 °C, 3 h	43	(Shinde et al. 2018)
	Sucrose		51	
	Fructose		55	
6	D-fructose via 1,6-diacetylfructose	Vinyl acetate, lipase cat, 1,4-dioxane, 45 °C, 5 h (step-I); H_2SO_4 (25 mol%), DMSO, 120 °C, 2 h (step-II)	86.6	(Huynh et al. 2019)
	D-fructose via 1,6-diacetylfructose	Vinyl acetate, lipase cat., 1,4-dioxane, 45 °C, 5 h (step-I); A-15, Catalyst/Substrate molar ratio=0.6, 15% DMSO in 1,4 Dioxane, 120 °C, 8 h (step-II)	57.9	
7	Fructose	AcOH (20 mL), 4 eq. $ZnCl_2$, 100 °C, 6 h	75	(Bhat et al. 2023)

Abbreviations: EMIM: 1-ethyl3-methylimidazolium chloride; A-15: Amberlyst-15; DMAP: 4-(dimethylamino)pyridine.

There are many publications on the synthesis of AcMF from platform chemicals like 5-(chloromethyl)furfural (CMF) and HMF with great yields, but there are very few examples in the literature starting from carbohydrates listed in Table 2.3. The researchers continue their attempt to increase the yield of the AcMF by using various catalysts, reaction conditions, and other methods. However, satisfactory yields of AcMF were not obtained from inexpensive feedstock like glucose. Recently, using $ZnCl_2$ as the Lewis acid catalyst and acetic acid as the Brønsted acid catalyst, the effects of reaction temperature, duration, substrate loading, and $ZnCl_2$ dose on AcMF yield were investigated. Fructose and glucose produced AcMF in 80% and 60% isolated yields, respectively, under the ideal conditions of 5 wt% substrate, AcOH, 4 eq $ZnCl_2$, 100 °C, and 6 h. However, creating green, highly efficient catalysts for producing AcMF is still challenging. In this regard, exploring the effect of Brønsted acids as co-catalyst in acetic acid medium is significant.

2.1.4 Literature review on Activated Carbon (AC)

With an emphasis on agricultural waste, researchers are increasingly interested in creating adsorption materials to remove contaminants from air and water. In 2021, Lotfy and Roubík provided a summary of current advancements in the industry and represented an assessment of the various options for using agricultural byproducts to manufacture AC for water filtration (Lotfy and Roubík 2021).

In 2011, AC generated from cashew nut shell (CNS), was used for the methylene blue (MB) adsorption study. The carbon was initially created by carbonizing CNS for 1 h at 700 °C. Following a 1:1 KOH impregnation, the carbon was dried for 24 h at 100 °C. Then the activation was carried out at 850 °C for 2 h. Its maximal MB adsorption was reported to be 68.72 mg/g, and it was discovered to have a BET surface area of 984 m^2/g (Kumar et al. 2011).

Later, Spagnoli et al. used $ZnCl_2$ as the chemical activating agent to synthesize AC starting from CNS. CNS was impregnated with various concentrations of aqueous $ZnCl_2$ for 2 h at 85 °C. It was then dried in an oven for 24 h. The activation was then carried out at 500 °C and maintained there for 2 h. A maximum adsorption capacity of 476 mg/g for MB was achieved at 500 °C (Spagnoli et al. 2017a).

In 2020, AC was prepared using cashew nut husk (CNH) as the feedstock using horizontal tube furnace. Initially CNH was heated for 2.5 h at 600 °C. The resultant char was then ground into powders and combined in ratios of 1:1, 2:1, and 4:1 with various concentrations of KOH. This mixture was magnetically stirred in water for 4 h before being dried at 90 °C for 2 days. The dry solid mixture was heated for 2 h to 850 °C under an argon atmosphere. At a 1:4 (weight basis) CNH and KOH ratio, AC was produced with a large surface area (2742 m^2/g) and pore volume (1.528 cm^3/g). The specific surface area was 1890 m^2/g at 1:2 ratio. To evaluate the supercapacitance, an AC with a particular surface area of 2742 m^2/g was used. It was discovered to have a specific capacitance of 305.2 F/g, and after 4000 cycles of charging and discharging, the capacitance remained at 97% (Cai et al. 2020).

In 2021, a few papers showed the valorization of CNS waste to produce AC. In one of the research articles, the CNS waste was chemically activated and carbonized using 50 wt% of H_2SO_4 after extracting cashew nut shell oil. Using a 2:1 impregnation ratio, the CNS was soaked in H_2SO_4 for 24 h and then dried at 110 °C. Then the carbonization was carried out at 400 °C for 3 h. This AC was employed for the removal of heavy metals such as Cu (II), Pb (II), Cd (II), and Zn (II), and also organic dyes like MB from the aqueous medium. It was found to have a maximum monolayer adsorption capacity of 12.2 mg/g for MB (Nyirenda et al. 2021). AC (specific surface area=884 m^2/g) was obtained by activating CNS with NaOH for 2 h at 800 °C (Wang 2021).

Using H_3PO_4 as the activating agent, AC was prepared from CNS (H_3PO_4:CNS=3.4:1, weight basis) in a horizontal tube furnace by carbonizing and activating at 400 °C for 2 h under an inert atmosphere. The resulting AC was modified by grafting polyethylenimine onto the surface and was investigated for removing Cr (VI) from the aqueous medium. The maximum adsorption capacities of AC were found to be 340 ± 20 mg/g and 320 ± 20 mg/g for unmodified and modified carbons (Geczo et al. 2021). Using H_3PO_4 as the activating agent, AC was prepared from CNS (H_3PO_4:CNS=3.4:1, weight basis) in horizontal tube furnace by carbonizing and activating at 400 °C for 2 h under inert atmosphere. The resulting AC was modified by grafting polyethylenimine onto the surface and were investigated for removing Cr (VI) from aqueous medium. The maximum adsorption capacities of

ACwere found to be 340 ± 20 mg/g and 320 ± 20 mg/g for unmodified and modified carbons (Smith et al. 2021).

Merin et al. used KOH as the chemical activating agent to produce CNS for supercapacitance analysis. After impregnation with KOH in a 1:2 ratio, it was allowed to stir for 3 h, and then dried for 24 h, at 100 °C. Then the carbonization was carried out at 750 °C for 1 h under argon flow. It showed a specific capacitance of 214 F/g with a specific surface area and average pore size of about 900 m^2/g and 2 nm, respectively. Moreover, it retained a capacitance of up to 98% even after 100 cycles of charging and discharging (Merin et al. 2021).

However, there is no literature report on preparing AC from CNH for MB adsorption study. Furthermore, there are no comparative studies in the literature on the physicochemical and adsorption characteristics of AC generated from CNS and CNH.

2.2 SCOPE OF THE WORK

The carbon-carbon bond-forming reactions are at the heart of synthetic organic chemistry. The Morita-Baylis-Hillman (MBH) reaction transforms basic starting materials into highly-functionalized and structurally complex products quickly and efficiently. It is a high-yielding, scalable, and atom-economic carbon–carbon bond forming reaction that has risen from obscurity to high synthetic popularity due to its operational simplicity and the vast applications of Baylis–Hillman products in organic synthesis. The MBH adducts are valuable building blocks for biologically active compounds and natural products. The reaction has many inherent qualities to be branded as a green transformation. For example, the reaction is catalytic, works at ambient temperature and pressure, atom economical, affords product in high yields, uses innocuous solvents (e.g., water), and could even work under solvent-free conditions The substrate scope of the MBH reaction is remarkable as this elegant carbon-carbon bond forming reaction can potentially be extended to any activated alkene attached to a powerful electron withdrawing group and a carbon electrophile (e.g., aldehyde, imine) using a tertiary amine or phosphine as the nucleophilic organocatalyst. Exploring the novel molecules from renewable starting materials like 5-substituted-2-furfuraldehydes and acrylates is crucial to expand the derivative chemistry of furfurals and accessing broader classes of products.

Synthesizing heterocyclic compounds with pharmacological properties has enormous scope in today's world. In this regard, DHPMs and DHPs are well-established classes of heterocyclic compounds with pronounced therapeutic properties. Numerous acid catalysts have been screened for Biginelli and Hantzsch transformations. However, there is still an active search for an efficient, inexpensive, and eco-friendly catalyst that allows the reactions to happen under mild conditions and affords products with desired selectivity and yield. FUR and HMF are often used as representative furanic molecules to demonstrate the diverse substrate scope of various synthetic methodologies, such as the synthesis of heterocycles. However, the systematic study of carbohydrate-derived 5-substituted-2-furaldehydes as substrates for synthesizing various classes of heterocyclic molecules is underexplored. Such systematic studies will assist in unravelling the much-desired reactivity patterns of these biorenewable molecules and expand the horizon of their derivative chemistry. Moreover, the study will pave the pathway for synthesizing hitherto unknown products to explore their properties and potential applications.

In recent years, there has been significant interest in developing a hydrophobic, stable, and non-halogenated functional equivalent of HMF. In this regard, the esters of HMF, such as AcMF, has received immense attention. The targeted functional equivalent of HMF must be accessible directly from carbohydrates in satisfactory yields under economically and environmentally acceptable reaction conditions and must be amenable to participating in all the derivative chemistry of HMF. Numerous publications have been published on synthesizing AcMF from 5-(chloromethyl)furfural (CMF) and HMF. However, the direct synthesis of AcMF from carbohydrates is crucial from an economic standpoint. Therefore, it is important to investigate the straightforward catalytic approach for producing AcMF from carbohydrates.

AC derived from non-renewable sources has been extensively used in wastewater treatment to remove pollutants. However, there are issues with the availability of feedstock and environmental concerns about releasing anthropogenic carbon into the environment. Therefore the method of producing AC from agricultural waste is strongly encouraged due to the economic and environmental advantages. One of the potential feedstocks for manufacturing AC is cashew nut husk (CNH) and

cashew nut shell (CNS) waste. The utilization of CNH and CNS for preparing AC will alleviate their waste management issue and improve the overall cost-effectiveness of the cashew nut processing industry. CNS also possess urushiol, a mixture of polyphenolic organic compounds with potentially allergenic properties. These chemicals can leach up to the outer layer of the cashew nut, making both shell and husk agricultural toxins.

2.3 OBJECTIVES OF THE PRESENT WORK

Based on thorough literature studies, the following objectives were formulated for this thesis.

1. Efficient synthesis of novel acrylates from biomass-derived 5-substituted-2-furaldehydes by Morita-Baylis-Hillman reaction.
2. Reagent-controlled switching between Biginelli and Hantzsch products sourced from biorenewable furfurals using the gluconic acid aqueous solution as the green catalyst.
3. Catalytic synthesis of 5-(acetoxymethyl)furfural directly from fructose in the acetic acid medium using a strong Brønsted acid co-catalyst.
4. Synthesis and characterization of activated carbon from cashew nut husk and shell by chemical activation and application for methylene blue adsorption.

Overall, the present work explores novel strategies to synthesize value-added highly functionalized compounds and heterocycles from biomass-derived platform chemicals. The synthesis of AC and its application in MB removal is studied. The entire thesis comprises seven chapters.

CHAPTER 1 provides a general introduction to biomass and its valorization strategies for a sustainable bioeconomy. The discussion then focuses on converting biomass-derived carbohydrates into furanic chemical platforms by acid catalysis and their downstream synthetic value addition into bioproducts of commercial significance. The conversion of agricultural wastes into sustainable materials, such as activated carbon, is also discussed.

CHAPTER 2 reports the literature study and research gaps associated with MBH reaction of furanics, Biginelli and Hantzsch reaction of furanics to produce DHPMs, and DHPs, production of AcMF directly from fructose, and synthesis of AC from CNS and CNH. The scope and objectives of the present work are listed at the end.

CHAPTER 3 shows twenty three examples of MBH adduct starting from various 5-substituted-2-furaldehydes. Several organic tertiary amines and phosphines were investigated to find an effective organocatalyst for the MBH reaction between 5-substituted-2-furaldehydes and acrylates. The reaction was optimized on the molar ratio between the starting materials and catalyst loading. Attempts were made to produce novel and completely biorenewable MBH adducts using biorenewable 2-furanone as the active olefin.

CHAPTER 4 describes the effective, affordable, and environmentally friendly use of GAAS as a catalyst to synthesize novel DHPMs and DHPs from carbohydrate-derived 5-substituted-2-furaldehydes by employing Biginelli and Hantzsch reaction, respectively. Using ammonium acetate as a nitrogen source produced DHPs in excellent isolated yields, whereas using urea (or thiourea) resulted in good to moderate yield of DHPMs. Furthermore, the effects of various reaction parameters such as temperature, molar ratio of starting materials, and the reaction duration on the selectivity and yield of the targeted product were studied and optimized.

CHAPTER 5 reports the synthesis of AcMF from fructose in the glacial acetic acid medium using strong Bronsted acid co-catalyst, such as MSA, PTSA, A-15, and orthophosphoric acid. The reaction parameters were optimized for each catalyst.

CHAPTER 6 describes the synthesis of AC from CNS and CNH using H_3PO_4 as the chemical activating agent. Two different temperatures (500 °C and 700 °C) were selected for activating AC. The properties of synthesized AC were studied using SEM, FTIR, PXRD, BET, and iodine number. The AC samples were employed as adsorbents to remove methylene blue, an organic dye often found in various industrial effluents, from the aqueous solution.

CHAPTER 7 outlines the summary and conclusions for the present work. It also highlights the scope of future work based on the experimental data discussed in this thesis.

CHAPTER 3

RENEWABLE SYNTHESIS OF NOVEL ACRYLATES FROM BIOMASS-DERIVED 5-SUBSTITUTED-2-FURALDEHYDES BY MORITA-BAYLIS-HILLMAN REACTION

***Abstract**:*

Biomass-derived furfurals are becoming increasingly popular as renewable chemical building blocks for synthesizing specialty chemicals. Morita-Baylis-Hillman (MBH) reaction is a classic carbon-carbon bond-forming transformation between the α-position of an activated alkene and a carbon electrophile (e.g., aldehyde) using a nucleophilic catalyst, such as a tertiary amine or phosphine. The MBH reaction is highly atom economical, affords excellent yields of adducts under mild reaction conditions, introduces substantial molecular complexity, and enjoys broad substrate scope. In this work, several novel MBH adducts have been synthesized starting from biomass-derived 5-substituted-2-furaldehydes and acrylates using 1,4-diazabicyclo[2.2.2]octane (DABCO) as the organocatalyst. This work reports the first systematic study of the MBH reaction of 5-substituted-2-furaldehydes and acrylates. A general synthetic protocol for the high-yielding synthesis of MBH adducts has been developed. The reactions were performed at room temperature under solvent-free conditions, and the spectroscopically pure products were produced in good to excellent isolated yields. Moreover, DABCO was recovered from the reaction mixture and successfully recycled.

Graphical abstract

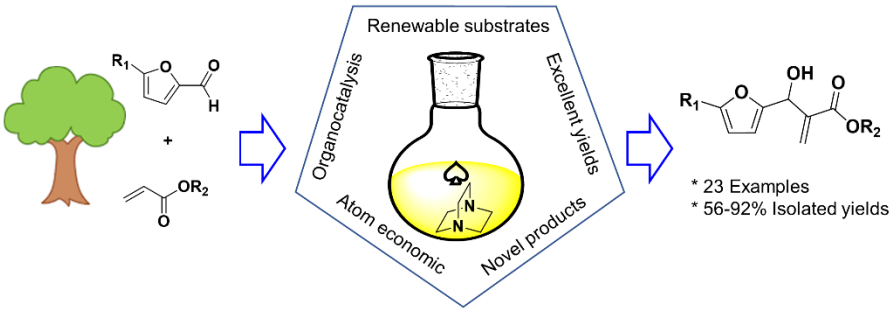

3.1 INTRODUCTION

An overwhelming majority of organic chemicals used in academic and industrial settings originate from exhaustible, anthropogenic carbon sources (e.g., petroleum). The dwindling reserves of economically attainable petroleum combined with its overuse have caused grave economic, sociopolitical, and environmental

consequences (Bardi 2019). In the search for a sustainable and economically viable source of organiccarbon-based feedstock, biomass has garnered considerable attention due to its large-scale availability, inexpensiveness, and carbon-neutral nature (Yadav et al. 2020). In a biorefinery, a handful of chemical intermediates or chemical 'building blocks' could be produced initially and converted into products of targeted molecular characteristics and properties. In this regard, the biomass-derived hexoses (e.g., glucose) and pentoses (e.g., xylose) can be dehydrated into 5-(hydroxymethyl)furfural (HMF) and furfural (FUR), respectively, under acid catalysis (Lee and Wu 2021; Menegazzo et al. 2018). Over the past several years, significant research has been devoted to synthesizing liquid transportation fuels, chemicals, and polymers starting from FUR and HMF (Dulie et al. 2021; Kong et al. 2018). The key to broadening the substrate scope of furaldehydes for synthesizing bulk- and specialty chemicals is to recognize their reactivity patterns and develop sustainable synthetic protocols for their derivative chemistry (Dutta 2023b). For a carbohydrate-based biorefinery to be commercially feasible, it is imperative to expand the chemistry of furfurals and access a broader range of product classes. The wealth of knowledge in organic synthesis and green chemistry must be used in unison to assist in expanding the substrate scope of biorenewable furfurals. The traditional Morita-Baylis-Hillman (MBH) reaction is between an aromatic aldehyde and methyl vinyl ketone catalyzed by triphenylphosphine (Shi and Liu 2006). The substrate scope of the MBH reaction is remarkable as this elegant carbon-carbon bond-forming reaction can be extended to any activated alkene attached to a powerful electron withdrawing group and a carbon electrophile (e.g., aldehyde, imine) using a tertiary amine or phosphine as the nucleophilic organocatalyst (Basavaiah and Tilak Naganaboina 2018). Significant computational studies have also been performed to understand the reaction mechanisms, estimate the effects of various reaction parameters, explain the experimental data, and predict the reactivity of a wide range of substrates toward the MBH reaction (Liu et al. 2017). The MBH reaction significantly increases the molecular complexity and afford densely functionalized product for a wide range of applications or further synthetic alterations. The MBH adducts are valuable building blocks for biologically active compounds and natural products (Haleem et al. 2022).

The reaction has many inherent qualities to be branded as a green transformation. For example, the reaction is catalytic, works at ambient temperature and pressure, atom economical, affords product in high yields, uses innocuous solvents (e.g., water), and could even work under solvent-free conditions (Williams et al. 2020). In addition, the transformations fall under fascinating fields of organic chemistry research, such as C-H activation and organocatalysis (Jangid 2020). The MBH adducts between 5-substituted-2-furaldehydes and acrylates have high synthetic versatility since the substitution can be altered at the 5-position of FUR and the ester functionality in acrylates. The 5-substituted-2-furaldehydes reported in this work were prepared using 5-(chloromethyl)furfural (CMF) as the reactive intermediate using procedures reported earlier (Bhat et al. 2022). Acrylic acid can be synthesized renewably from various biomass components following chemicalcatalytic pathways. For example, the suitable combination of dehydration and oxidation reaction to glycerol leads to acrylic acid (Witsuthammakul and Sooknoi 2012). Catalytic dehydration of glucose-derived lactic acid can also form acrylic acid (Zhang et al. 2016). A biorenewable synthesis of 1,4-diazabicyclo[2.2.2]octane (DABCO) can also be envisioned starting from glucose-derived ethylene glycol and ammonia. Therefore, the DABCO-catalyzed MBH adducts derived from 5-substituted-2-furaldehydes and acrylates may be considered biorenewable in their entirety. Interestingly, the adducts between HMF or FUR with acrylates have been reported to demonstrate the substrate scope during methodology developments of MBH reaction (Ontiveros et al. 2021; Wang et al. 2019a). The MBH adducts of furanics with acrylates have been used as a molecular scaffold to synthesize novel pyran-3(6H)-ones that are present in various bioactive natural products (Guidotti and Coelho 2015). However, the systematic synthesis of the MBH adducts of 5-substituted-2-furaldehydes, renewably prepared from biomass-derived hexose sugars and polymeric carbohydrates, has never been attempted. A systematic study of MBH reactions involving 5-substituted-2- furaldehydes will help better understand their reactivity patterns and expand their derivative chemistry. This work has chosen representative 5-substituted-2-furaldehydes for demonstrating a general synthetic protocol of their MBH adducts with acrylates. Various esters of HMF with aliphatic and aromatic carboxylic acids, such as 5-(acetoxymethyl)furfural

(AcMF) and 5- (benzoyloxymethyl)furfural (BzMF), have been used as substrates (Figure 3.1). In addition, 5-Methylfurfural (5MF) and ethers like 5-(ethoxymethyl)furfural (EMF) have been used to demonstrate the broad substrate scope of the process reported here. Several organic tertiary amines and phosphines have been screened as an organocatalyst for the MBH reaction between 5-substituted-2- furaldehydes and acrylates. The process was optimized on the molar ratio of starting materials and the loading of the catalyst.

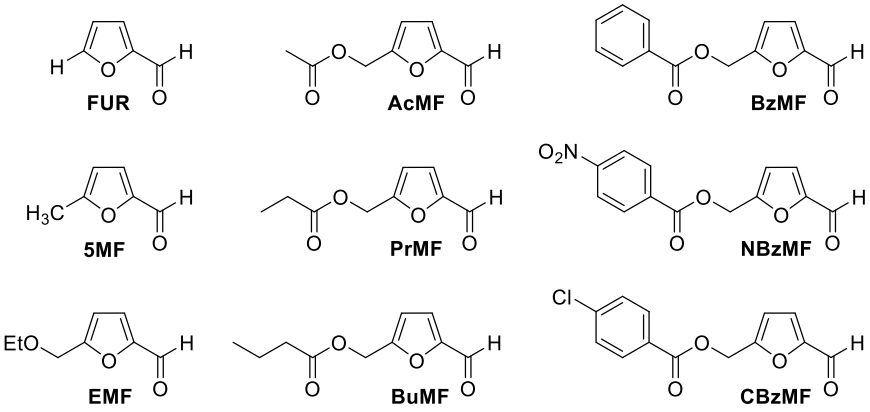

Figure 3.1 Biomass-derived furfural and various 5-substituted furfurals used as substrate in this work for Morita-Baylis-Hillman reaction.

3.2 EXPERIMENTAL SECTION

3.2.1 Materials

Methyl acrylate (99%), ethyl acrylate (99%), furfural (FUR) (99%), and silica gel (60–120 mesh) were purchased from Spectrochem. Butyl acrylate (99%) was purchased from SRL. 1,4-Diazabicyclo[2.2. 2]octane (DABCO) (98%), Sodium bicarbonate (99%), sodium sulfate (anhydrous, 99%), and sodium chloride (99%) were purchased from Loba Chemicals Pvt. Ltd. 5-Methylfurfural (5MF) (99%) was purchased from Sigma. Ethyl acetate (99%) was purchased from Finar. 5-(Ethoxymethyl)furfural (EMF), 5- (acetoxymethyl)furfural (AcMF), 5-(propionyloxymethyl)furfural (PrMF), 5-(butyryloxymethyl)furfural (BuMF), 5-(benzoyloxymethyl)furfural (BzMF), 5-[(4-nitrobenzoyloxy)methyl]furfural (NBzMF), and 5-[(4-chlorobenzoyloxy)methyl]furfural (CBzMF) were prepared following literature processes (Bhat et al. 2022, 2023; Dutta and Mascal 2014; Mascal

and Nikitin 2008; Onkarappa and Dutta 2019). All the chemicals were used as received without using additional purification steps.

3.2.2 Synthetic Procedure

In a 50 mL round-bottomed flask, FUR (0.502 g, 5.225 mmol) and methyl acrylate (0.810 g, 9.409 mmol, 1.8 eq.) were introduced. DABCO (0.586 g, 5.224 mmol, 1 eq.) was added, the flask was stoppered, and the mixture was magnetically stirred at room temperature under solvent-free conditions. The homogeneous reaction mixture was monitored by thin-layer chromatography (TLC) for the disappearance of FUR. Upon completion, the reaction mixture was diluted with ethyl acetate (10 mL) and washed with water, saturated $NaHCO_3$, and finally, with brine solution. The ethyl acetate layer was separated, dried over anhydrous Na_2SO_4, and evaporated under reduced pressure to provide the MBH adduct **1p**. The adduct was purified by filtering through a plug of silica gel (60–120 mesh) using chloroform as the eluent. Evaporation of chloroform in a rotary evaporator under reduced pressure afforded **1p** as a light-yellow oil (0.866 g, 91%). The water layer was decolorized with activated carbon and distilled off to recover DABCO, which was then purified by sublimation and reused for the next reaction. This synthetic procedure was extended to other MBH adducts reported in this work.

3.3 CHARACTERIZATION OF SYNTHESIZED COMPOUNDS

3.3.1 The FTIR, ^{1}H-NMR, and ^{13}C-NMR of Methyl 2-((5-(acetoxymethyl)furan-2-yl)(hydroxy)methyl)acrylate (4p)

Methyl 2-((5-(acetoxymethyl)furan-2-yl)(hydroxy)methyl)acrylate (**4p**): pale yellow liquid (0.278 g, 92%) ^{1}H-NMR ($CDCl_3$, 300 MHz, RT) δ ppm: 6.37 (s, 1H, -CH of $=CH_2$), 6.31 (s, 1H, furly- CH), 6.18 (s, 1H, furyl- CH), 5.96 (s, 1H, -CH of $=CH_2$), 5.55 (s, 1H, -CHOH-), 4.97 (s, 2H, $-OCH_2-$), 3.73 (s, 3H, $-OCH_3$), 2.03 (s, 3H, $-COCH_3$). ^{13}C-NMR ($CDCl_3$, 75 MHz, RT) δ ppm: 170.7, 166.3, 155.0, 149.2, 139.3, 127.0, 111.5, 108.1, 66.9, 58.1, 52.1, 20.8. Elemental Analysis (CHN): Calculated (%): C: 56.69, H: 5.55; Experimental (%): C: 56.55, H: 5.382. FTIR (cm^{-1}): 3475 (-OH stretching), 2853-3127(-CH stretching frequency), 1717 (-COOR), 1635 (C=C stretching frquency).

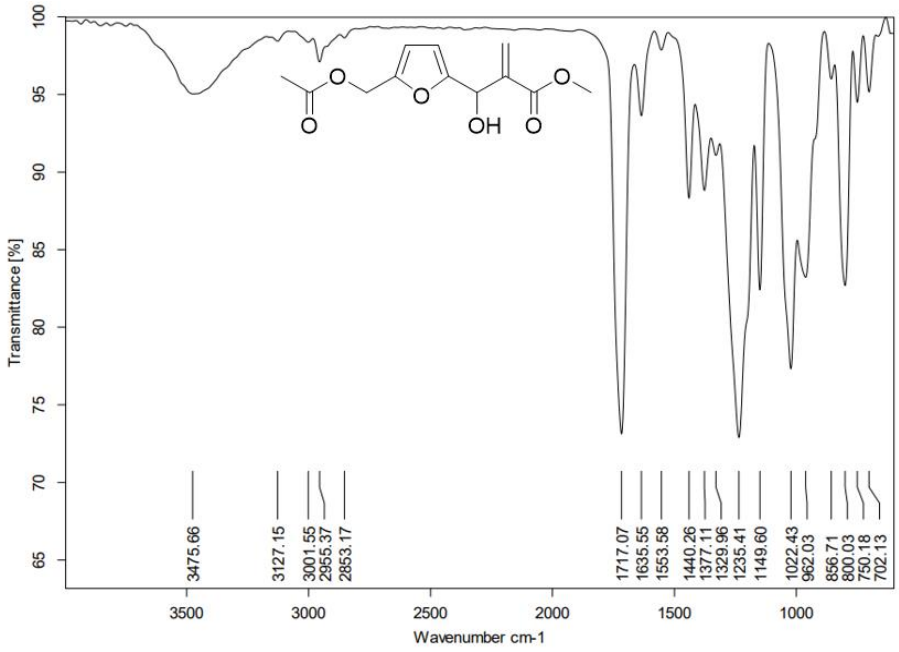

Figure 3.2 The FTIR spectrum of **4p**.

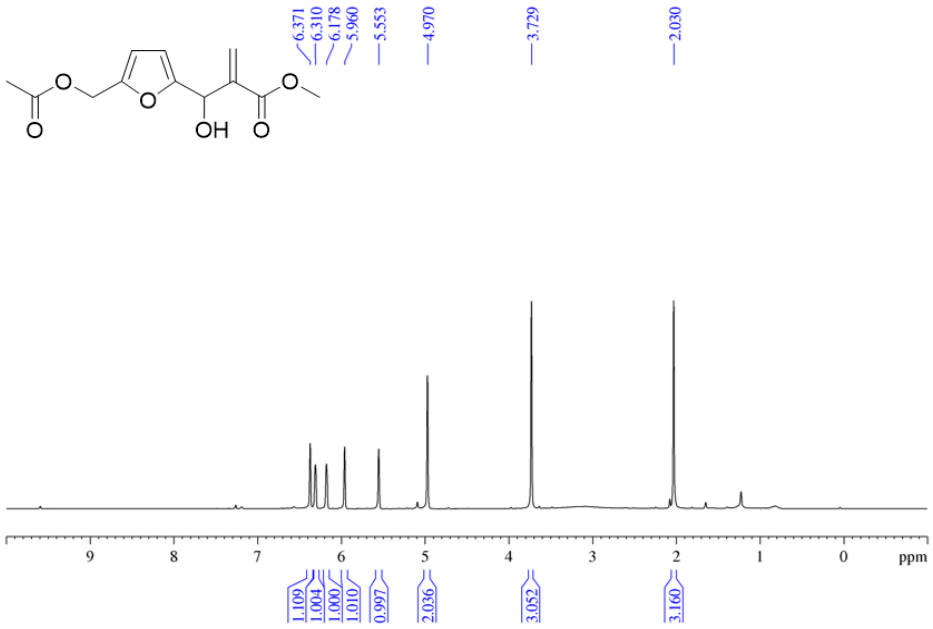

Figure 3.3 The ^{1}H-NMR spectrum of **4p** (solvent-$CDCl_3$).

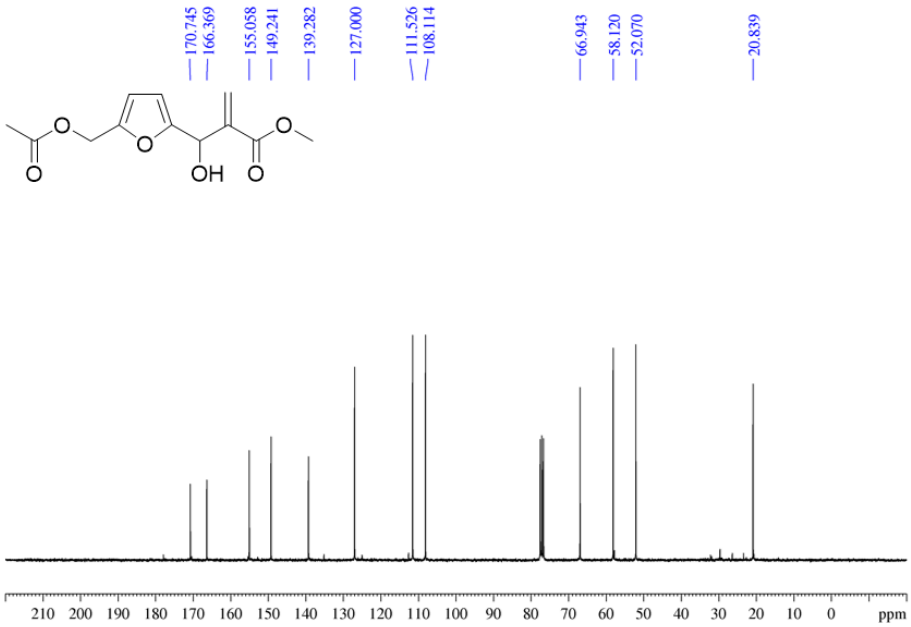

Figure 3.4 The ^{13}C-NMR spectrum of **4p** (solvent-$CDCl_3$).

3.3.2 The FTIR, ^{1}H-NMR, and ^{13}C-NMR of Ethyl 2-((5-(acetoxymethyl)furan-2-yl)(hydroxy)methyl)acrylate (4q)

Ethyl 2-((5-(acetoxymethyl)furan-2-yl)(hydroxy)methyl)acrylate (**4q**): pale yellow liquid (0.287 g, 90%) ^{1}H-NMR ($CDCl_3$, 300 MHz, RT) δ ppm: 6.32 (s, 1H, -CH of $=CH_2$), 6.28 (s, 1H, furyl- CH), 6.15 (s, 1H, furyl-CH), 5.88 (s, 1H, -CH of $=CH_2$), 5.50 (s, 1H, -CHOH), 4.94 (s, 2H, $-OCH_2-$), 4.15 (q, 2H, $-CH_2CH_3$, J = 6.9 Hz), 1.99 (s, 3H, $-COCH_3$), 1.21 (t, 3H, $-CH_2CH_3$, J = 6.9 Hz). ^{13}C-NMR ($CDCl_3$, 75 MHz, RT) δ ppm: 170.7, 165.9, 155.1, 149.2, 139.2, 126.8, 111.5, 108.1, 67.4, 61.1, 58.1, 20.8, 14.1. Elemental Analysis (CHN): Calculated (%): C: 58.20, H: 6.01; Experimental (%): C: 58.15, H: 6.020. FTIR (cm^{-1}): 3472 (-OH stretching), 2928-3135 (-CH stretching frequency), 1718 (-COOR), 1637 (C=C stretching frequency).

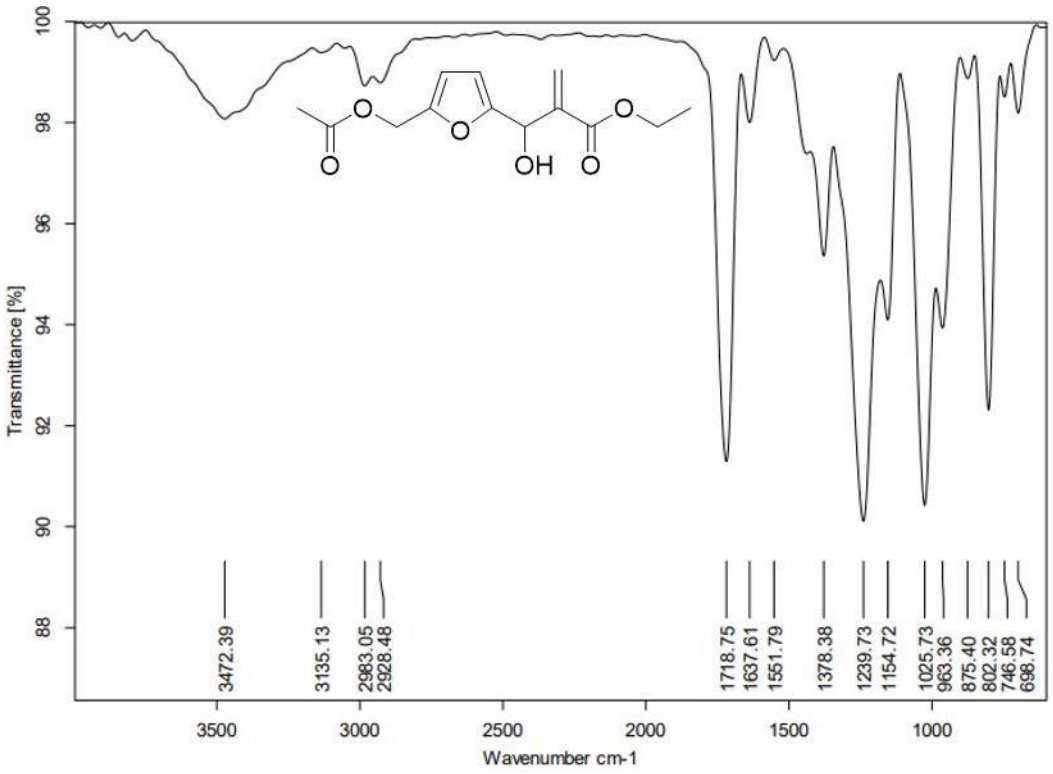

Figure 3.5 The FTIR spectrum of **4q**.

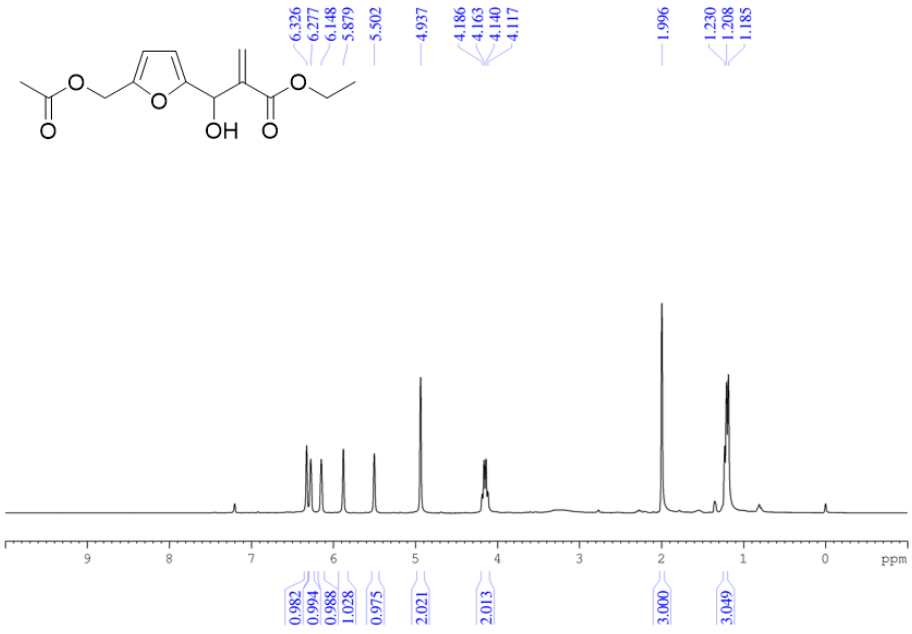

Figure 3.6 The ^{1}H-NMR spectrum of **4q** (solvent-$CDCl_3$).

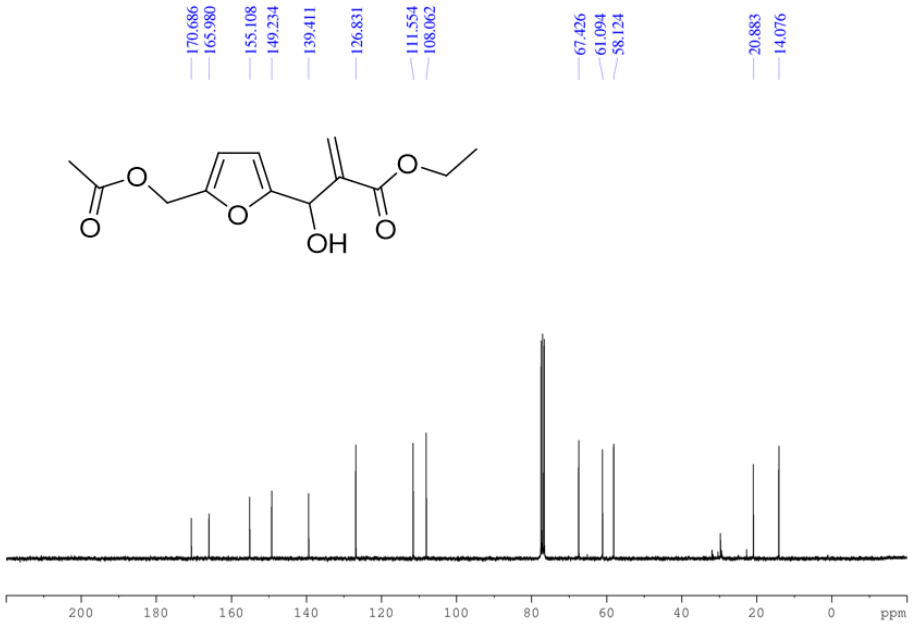

Figure 3.7 The ^{13}C-NMR spectrum of **4q** (solvent-$CDCl_3$).

3.3.3 The FTIR, ^{1}H-NMR, and ^{13}C-NMR of Butyl 2-((5-(acetoxymethyl)furan-2-yl)(hydroxy)methyl)acrylate (4r)

Butyl 2-((5-(acetoxymethyl)furan-2-yl)(hydroxy)methyl)acrylate (**4r**): pale yellow liquid (0.306 g, 87%) ^{1}H-NMR ($CDCl_3$, 300 MHz, RT) δ ppm: 6.38 (s, 1H, -CH of $=CH_2$), 6.33 (s, 1H, furyl- CH), 6.19 (s, 1H, furyl-CH), 5.94 (s, 1 H, -CH of $=CH_2$), 5.55 (s, 1H, -CHOH-), 4.99 (s, 2H, $-OCH_2-$), 4.14 (t, 2H, $-OCH_2CH_2-$, *J* = 6.5 Hz), 2.05 (s, 3H, $-COCH_3$), 1.61 (t, 2H, $-OCH_2CH_2CH_2-$ *J* = 6.5 Hz), 1.35 (m, 2H, $-OCH_2CH_2CH_2CH_3$), 0.90 (t, 3H, $-CH_2CH_3$ *J* = 6.5 Hz). ^{13}C-NMR ($CDCl_3$, 75 MHz, RT) δ ppm: 170.7, 166.0, 155.1, 149.2, 139.4, 126.7, 111.5, 108.0, 67.3, 64.9, 58.1, 30.5, 20.8, 19.1, 13.6. Elemental Analysis (CHN): Calculated (%): C: 60.80, H: 6.80; Experimental (%): C: 60.42, H: 6.535. FTIR (cm^{-1}): 3474 (-OH stretching), 2870-3131 (-CH stretching frequency), 1714 (-COOR), 1636 (C=C stretching frequency).

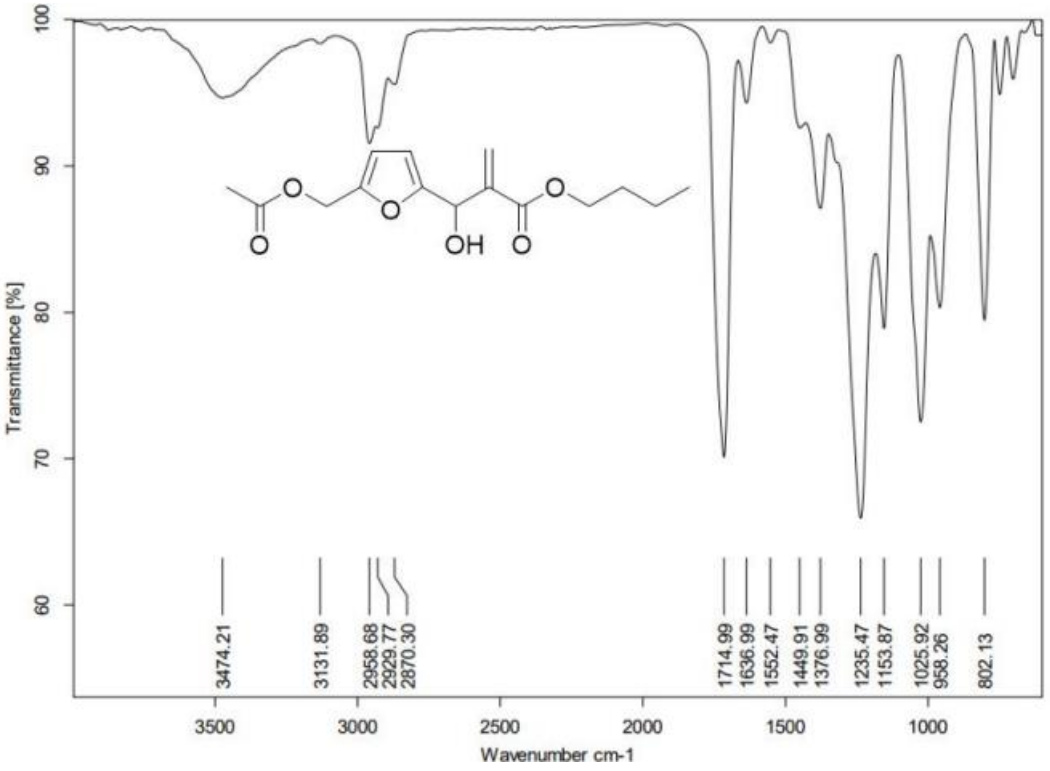

Figure 3.8 The FTIR spectrum of **4r**.

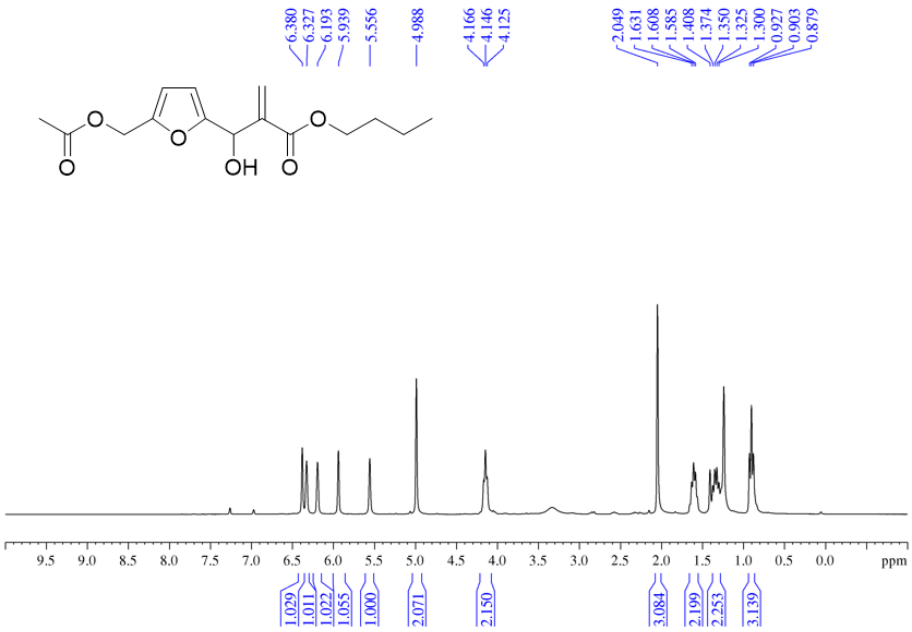

Figure 3.9 The ^{1}H-NMR spectrum of **4r** (solvent-$CDCl_3$).

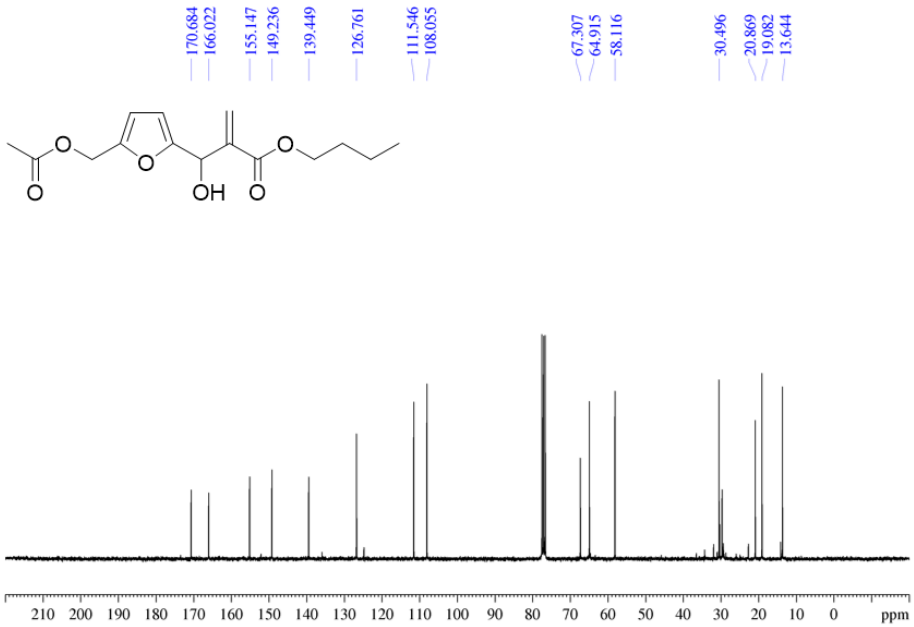

Figure 3.10 The ^{13}C-NMR spectrum of **4r** (solvent-$CDCl_3$).

3.3.4 Characterization data of all synthesized compounds

Methyl 2-(furan-2-yl(hydroxy)methyl)acrylate (**1p**): colorless liquid (91%); ^{1}H-NMR ($CDCl_3$, 300 MHz, RT, δ ppm): 7.29 (s, 1H), 6.30 (s, 1H), 6.24 (s, 1H), 6.17 (s, 1H), 5.88 (s, 1H), 5.51 (s, 1H) , 3.67 (s, 3H); ^{13}C-NMR ($CDCl_3$, 75 MHz, RT, δ ppm): 166.5, 154.2, 142.4, 139.5, 126.8, 110.4, 107.2, 67.0, 52.0; FTIR (cm^{-1}): 3459, 3024-2850, 1714, 1633, 1495, 1279, 1148.

Ethyl 2-(furan-2-yl(hydroxy)methyl)acrylate (**1q**): colorless liquid (87%); ^{1}H-NMR ($CDCl_3$, 300 MHz, RT, δ ppm): 7.30 (s, 1H), 6.32 (s, 1H), 6.26 (s, 1H), 6.17 (s, 1H), 5.91 (s, 1H), 5.54 (s, 1H), 4.14 (d, 2H, *J* = 6.9 Hz), 1.19 (t, 3H, *J* = 6.9 Hz); ^{13}C-NMR ($CDCl_3$, 75 MHz, RT, δ ppm): 165.0, 153.4, 141.2, 138.9, 125.3, 109.3, 106.1, 65.7, 59.9, 12.9; FTIR (cm^{-1}): 3436, 3130-2857, 1711, 1634, 1272, 1151, 1028.

Butyl 2-(furan-2-yl(hydroxy)methyl)acrylate (**1r**): colorless liquid (91%); ^{1}H-NMR ($CDCl_3$, 300 MHz, RT, δ ppm): 7.21 (s, 1H), 6.24 (s, 1H), 6.16 (s, 1H), 6.07 (s, 1H), 5.87 (s, 1H), 5.47 (s, 1H), 3.98 (d, 2H, *J* = 7.2 Hz), 1.46 (t, 2H, *J* = 7.2 Hz), 1.20 (q, 2H, *J* = 7.2 Hz), 0.78 (t, 2H, *J* = 7.2 Hz); ^{13}C-NMR ($CDCl_3$, 75 MHz, RT, δ ppm): 165.9, 154.5, 142.0, 140.1, 125.8, 110.2, 106.9, 66.0, 64.6, 30.4, 18.9, 13.5; FTIR (cm^{-1}): 3438, 3126-2876, 1712, 1635, 1273, 1153, 1041.

Methyl 2-(hydroxy(5-methylfuran-2-yl)methyl)acrylate (**2p**): pale yellow liquid (76%); ^{1}H-NMR ($CDCl_3$, 300 MHz, RT, δ ppm): 6.30 (s, 1H), 6.01 (s, 1H), 5.94 (s, 1H), 5.82 (s, 1H), 5.48 (s, 1H), 3.66 (s, 3H), 2.19 (s, 3H); ^{13}C-NMR ($CDCl_3$, 75 MHz, RT, δ ppm): 166.5, 152.4, 152.1, 139.8, 126.3, 108.1, 106.3, 66.4, 51.9, 13.4; FTIR (cm^{-1}): 3437, 3000-2856, 1718, 1634, 1275, 1030.

Ethyl 2-(hydroxy(5-methylfuran-2-yl)methyl)acrylate (**2q**): pale yellow liquid (72%); ^{1}H-NMR ($CDCl_3$, 300 MHz, RT, δ ppm): 6.36 (s, 1H), 6.09 (s, 1H), 5.93 (s, 1H), 5.89 (s, 1H), 5.53 (s, 1H), 4.20 (q, 2H, *J* = 6.9 Hz), 2.26 (s, 3H), 1.26 (t, 3H, *J* = 6.9 Hz); ^{13}C-NMR ($CDCl_3$, 75 MHz, RT, δ ppm): 166.1, 152.3, 152.2, 139.8, 126.3, 108.0, 106.3, 67.3, 60.9, 14.1, 13.5; FTIR (cm^{-1}): 3465, 3136-2854, 1713, 1635, 1271, 1025.

Butyl 2-(hydroxy(5-methylfuran-2-yl)methyl)acrylate (**2r**): colorless liquid (56%); ^{1}H-NMR ($CDCl_3$, 300 MHz, RT, δ ppm): 6.39 (s, 1H), 6.33 (s, 1H), 6.20 (s, 1H), 5.99 (s, 1H), 5.58 (s, 1H), 5.00 (s, 2H), 3.75 (s, 3H), 3.65 (s, 1H), 2.29 (t, 2H, *J* = 6.9 Hz), 1.64 (q, 2H, *J* = 6.9 Hz), 0.92 (t, 3H, *J* = 6.9 Hz); ^{13}C-NMR ($CDCl_3$, 75 MHz, RT, δ ppm): 166.1, 152.6, 151.9, 140.2, 125.8, 107.9, 106.2, 66.5, 64.6, 30.5, 19.0, 13.5, 13.4; FTIR (cm^{-1}): 3436, 3108-2873, 1711, 1634, 1264, 1020.

Methyl 2-((5-(ethoxymethyl)furan-2-yl)(hydroxy)methyl)acrylate (**3p**): pale yellow liquid (90%); ^{1}H-NMR ($CDCl_3$, 300 MHz, RT, δ ppm): 6.31 (s, 1H), 6.17 (s, 1H), 6.10 (s, 1H), 5.91 (s, 1H), 5.50 (s, 1H), 4.32 (s, 2H), 3.67 (s, 3H), 3.44 (q, 2H, *J* = 6.9 Hz), 1.12 (t, 3H, *J* = 6.9 Hz); ^{13}C-NMR ($CDCl_3$, 75 MHz, RT, δ ppm): 166.4, 154.4, 151.8, 139.4, 126.8, 109.9, 107.8, 66.9, 65.6, 64.5, 52.0, 15.0; Elemental Analysis (CHN): Calculated (%): C: 59.99, H: 6.71. Experimental (%): C: 59.80, H: 6.58; FTIR (cm^{-1}): 3430, 3134-2863, 1719, 1635, 1270, 1087.

Ethyl 2-((5-(ethoxymethyl)furan-2-yl)(hydroxy)methyl)acrylate (**3q**): pale yellow colorless liquid (88%); ^{1}H-NMR ($CDCl_3$, 300 MHz, RT, δ ppm): 6.38 (s, 1H), 6.24 (s, 1H), 6.18 (s, 1H), 5.96 (s, 1H), 5.57 (s, 1H), 4.39 (s, 2H), 4.19 (d, 2H, *J* = 6.9 Hz), 3.51 (d, 2H, *J* = 6.9 Hz), 1.19 (m, 6H); ^{13}C-NMR ($CDCl_3$, 75 MHz, RT, δ ppm): 165.9, 154.6, 151.7, 139.7, 126.5, 109.9, 107.8, 66.9, 65.6, 64.5, 60.9, 15.0, 14.0; Elemental Analysis (CHN): Calculated (%): C: 61.40, H: 7.14. Experimental (%): C: 61.11, H: 6.84; FTIR (cm^{-1}): 3446, 3125-2857, 1713, 1635, 1265, 1025.

Butyl 2-((5-(ethoxymethyl)furan-2-yl)(hydroxy)methyl)acrylate (**3r**): pale yellow liquid (86%); ^{1}H-NMR ($CDCl_3$, 300 MHz, RT, δ ppm): 6.38 (s, 1H), 6.25 (s, 1H), 6.19 (s, 1H), 5.95 (s, 1H), 5.57 (s, 1H), 4.40 (s, 2H), 4.15 (s, 2H), 3.52 (d, 2H, *J* = 7.2 Hz), 1.62 (t, 2H, *J* = 7.2 Hz), 1.35 (q, 2 H, *J* = 7.2 Hz), 1.20 (t, 3H, *J* = 7.2 Hz), 0.92 (t, 3H, *J* = 7.2 Hz). ^{13}C-NMR ($CDCl_3$, 75 MHz, RT, δ ppm): 166.1, 154.5, 151.8, 139.6, 126.6, 109.9, 107.7, 67.2, 65.6, 64.8, 64.5, 30.5, 19.1, 15.1, 13.6. Elemental Analysis (CHN): Calculated (%): C: 63.81, H: 7.85. Experimental (%): C: 63.44, H: 7.73; FTIR (cm^{-1}): 3420, 3127-2872, 1715, 1635, 1263, 1089.

Methyl 2-(hydroxy(5-((propionyloxy)methyl)furan-2-yl)methyl)acrylate (**5p**): colorless liquid (85%); ^{1}H-NMR ($CDCl_3$, 300 MHz, RT, δ ppm): 6.39 (s, 1H), 6.33 (s, 1H), 6.20 (s, 1H), 5.98 (s, 1H), 5.58 (s, 1H), 5.01 (s, 2H), 3.75 (s, 3H), 2.34 (q, 2H, *J* = 6.6 Hz), 1.12 (t, 3H, *J* = 6.6 Hz); ^{13}C-NMR ($CDCl_3$, 75 MHz, RT, δ ppm): 174.2, 166.4, 154.9, 149.4, 139.3, 126.9, 111.4, 108.1, 66.9, 58.0, 52.0, 27.4, 8.9; Elemental Analysis (CHN): Calculated (%): C: 58.20, H: 6.01. Experimental (%): C: 58.11, H: 6.32; FTIR (cm^{-1}): 3461, 3126–2763, 1727, 1634, 1186.

Ethyl 2-(hydroxy(5-((propionyloxy)methyl)furan-2-yl)methyl)acrylate (**5q**): colorless liquid (74%); ^{1}H-NMR ($CDCl_3$, 300 MHz, RT, δ ppm): 6.39 (s, 1 H), 6.34 (s, 1H), 6.21 (s, 1H), 5.96 (s, 1H), 5.58 (s, 1H), 5.01 (s, 2H), 4.21 (q, 2H, *J* = 6.9 Hz), 2.34 (q, 2H, *J* = 7.2 Hz), 1.27 (t, 3H, *J* = 6.9 Hz), 1.13 (t, 3H, *J* = 7.2 Hz); ^{13}C-NMR ($CDCl_3$, 75 MHz, RT, δ ppm): 174.1, 165.9, 155.1, 149.3, 139.5, 126.7, 111.4, 108.0, 67.2, 61.0, 58.0, 27.4, 14.0, 8.9; Elemental Analysis (CHN): Calculated (%): C: 59.57, H: 6.43. Experimental (%): C: 59.39, H: 6.87; FTIR (cm^{-1}): 3470, 3131–2947, 1718, 1637, 1175, 1023.

(5-(1-Hydroxy-2-(methoxycarbonyl)allyl)furan-2-yl)methyl butyrate (**6p**): colorless liquid (89%); ^{1}H-NMR ($CDCl_3$, 300 MHz, RT, δ ppm): 6.39 (s, 1H), 6.33 (s, 1H), 6.20 (s, 1H), 5.99 (s, 1H), 5.58 (s, 1H), 5.01 (s, 2H), 3.75 (s, 3H), 3.65 (s, 1H), 2.29 (t, 2H, *J* = 7.2 Hz), 1.64 (q, 2H, *J* = 7.2 Hz), 0.92 (t, 3H, *J* = 7.2 Hz); ^{13}C-NMR ($CDCl_3$, 75 MHz, RT, δ ppm): 173.3, 166.3, 154.9, 149.4, 139.3, 126.9, 111.3, 108.1, 66.8, 57.9, 52.0, 35.9, 18.3, 13.5; Elemental Analysis (CHN): Calculated (%): C: 59.57, H:

6.43. Experimental (%): C: 59.22, H: 6.55; FTIR (cm^{-1}): 3486, 3127–2882, 1721, 1636, 1265, 1159.

(5-(2-(Ethoxycarbonyl)-1-hydroxyallyl)furan-2-yl)methyl butyrate (**6q**): colorless liquid (72%); ^{1}H-NMR ($CDCl_3$, 300 MHz, RT, δ ppm): 6.39 (s, 1H), 6.34 (d, 1H, *J* = 3.3 Hz), 6.21 (d, 1H, *J* = 3.3 Hz), 5.95 (s, 1H), 5.57 (s, 1H), 5.02 (s, 2H), 4.22 (q, 2H, *J* = 7.2 Hz), 2.29 (t, 2H, *J* = 7.5 Hz), 1.64 (m, 2H), 1.27 (t, 3H, *J* = 7.2 Hz), 0.93 (t, 3H, *J* = 7.5 Hz); ^{13}C-NMR ($CDCl_3$, 75 MHz, RT, δ ppm): 173.3, 165.9, 155.3, 149.4, 139.5, 126.7, 111.3, 108.0, 67.3, 61.0, 57.9, 35.9, 18.3, 14.0, 13.6; Elemental Analysis (CHN): Calculated (%): C: 60.80, H: 6.80. Experimental (%): C: 60.34, H: 6.98; FTIR (cm^{-1}): 3487, 3125–2882, 1718, 1636, 1263, 1168, 1034.

(5-(1-Hydroxy-2-(methoxycarbonyl)allyl)furan-2-yl)methyl benzoate (**7p**): colorless viscous liquid (92%); ^{1}H-NMR ($CDCl_3$, 300 MHz, RT, δ ppm): 8.02 (d, 2H, *J* = 7.2 Hz), 7.53 (d, 1H, *J* = 7.2 Hz), 7.41 (t, 2H, *J* = 7.2 Hz), 6.42 (m, 2H), 6.24 (s, 1H), 5.98 (s, 1H), 5.60 (s, 1H), 5.25 (s, 2H), 3.74 (s, 3H), 3.45 (s, 1H); ^{13}C-NMR ($CDCl_3$, 75 MHz, RT, δ ppm): 166.4, 166.3, 155.0, 149.4, 139.2, 133.1, 129.8, 129.7, 128.3, 127.1, 111.7, 108.2, 67.2, 58.6, 52.1; Elemental Analysis (CHN): Calculated (%): C: 64.55, H: 5.10. Experimental (%): C: 64.06, H: 5.01; FTIR (cm^{-1}): 3483, 3132–2953, 1714, 1633, 1266.

(5-(2-(Ethoxycarbonyl)-1-hydroxyallyl)furan-2-yl)methyl benzoate (**7q**): colorless viscous liquid (91%); ^{1}H-NMR ($CDCl_3$, 300 MHz, RT, δ ppm): 8.01 (d, 2H, *J* = 7.2 Hz), 7.51 (d, 1H, *J* = 7.2 Hz), 7.40 (d, 2H, *J* = 7.2 Hz), 6.40 (d, 2H), 6.23 (s, 1H), 5.98 (s, 1H), 5.61 (s, 1H), 5.24 (s, 2H), 4.17 (q, 2H, *J* = 6.9 Hz), 1.22 (t, 3H, *J* = 6.9 Hz); ^{13}C-NMR ($CDCl_3$, 75 MHz, RT, δ ppm): 166.3, 165.9, 155.3, 149.2, 139.6, 133.1, 129.8, 129.7, 128.3, 126.6, 111.7, 108.1, 66.9, 61.0, 58.6, 14.0; Elemental Analysis (CHN): Calculated (%): C: 65.45, H: 5.49. Experimental (%): C: 65.02, H: 5.62; FTIR (cm^{-1}): 3480, 3132–2874, 1714, 1633, 1267, 1023.

(5-(2-(Butoxycarbonyl)-1-hydroxyallyl)furan-2-yl)methyl benzoate (**7r**): colorless viscous liquid (88%); ^{1}H-NMR ($CDCl_3$, 300 MHz, RT, δ ppm): 8.01 (d, 2H, *J* = 6.6 Hz), 7.52 (d, 1H, *J* = 6.6 Hz), 7.41 (d, 2H, *J* = 6.6 Hz), 6.40 (d, 2H, *J* = 6.6 Hz), 6.22 (s, 1 H), 5.98 (s, 1H), 5.61 (s, 1H), 5.25 (s, 2H), 4.13 (s, 2H), 1.57 (m, 2H), 1.30 (t,

2H, *J* = 6.9 Hz), 0.88 (t, 3H, *J* = 6.9 Hz); ^{13}C-NMR ($CDCl_3$, 75 MHz, RT, δ ppm): 166.3, 166.0, 155.3, 149.2, 139.6, 133.1, 129.8, 129.7, 128.3, 126.6, 111.7, 108.1, 67.0, 64.8, 58.6, 30.4, 19.0, 13.6; Elemental Analysis (CHN): Calculated (%): C: 67.03, H: 6.19. Experimental (%): C: 67.42, H: 6.323; FTIR (cm^{-1}): 3490, 3113–2873, 1715, 1635, 1267.

(5-(1-Hydroxy-2-(methoxycarbonyl)allyl)furan-2-yl)methyl 4-nitrobenzoate (**8p**): light yellow solid (91%); ^{1}H-NMR ($CDCl_3$, 300 MHz, RT, δ ppm): 8.31 (d, 2H, *J* = 6.3 Hz), 8.25 (d, 2H, *J* = 6.3 Hz), 6.48 (s, 1H), 6.42 (s, 1H), 6.27 (s, 1H), 5.99 (s, 1H), 5.60 (s, 1H), 5.32 (s, 2H), 3.78 (s, 3H); ^{13}C-NMR ($CDCl_3$, 75 MHz, RT, δ ppm): 166.4, 164.3, 155.4, 150.6, 148.6, 139.1, 135.4, 130.9, 127.2, 123.5, 112.3, 108.3, 67.4, 59.3, 52.1; Elemental Analysis (CHN): Calculated (%): C: 56.51, H: 4.18; N: 3.88. Experimental (%): C: 56.89, H: 5.16, N: 4.11; FTIR (cm^{-1}): 3492, 3112–2851, 1718, 1633, 1266, 1098.

(5-(2-(Ethoxycarbonyl)-1-hydroxyallyl)furan-2-yl)methyl 4-nitrobenzoate (**8q**): light yellow solid (69%); ^{1}H-NMR ($CDCl_3$, 300 MHz, RT, δ ppm): 8.30 (d, 2H, *J* = 6.6 Hz), 8.23 (d, 2H, *J* = 6.6 Hz), 7.28 (s, 1H), 6.49 (d, 1H, *J* = 2.4 Hz), 6.43 (s, 1H), 6.29 (d, 1H, *J* = 2.4 Hz), 5.96 (s, 1H), 5.61 (s, 1H), 5.34 (s, 2H), 4.25 (q, 2H, *J* = 5.4 Hz), 1.29 (t, 3H, *J* = 5.4 Hz); ^{13}C-NMR ($CDCl_3$, 75 MHz, RT, δ ppm): 165.9, 164.3, 155.5, 150.6, 148.5, 139.3, 135.2, 130.9, 126.9, 123.5, 112.3, 108.2, 67.6, 61.1, 59.3, 14.1; Elemental Analysis (CHN): Calculated (%): C: 57.60, H: 4.57; N: 3.73. Experimental (%): C: 57.75, H: 4.52, N: 3.88; FTIR (cm^{-1}): 3491, 3113–2853, 1716, 1632, 1266, 1041.

(5-(1-Hydroxy-2-(methoxycarbonyl)allyl)furan-2-yl)methyl4-chlorobenzoate (**9p**): white solid (90%); ^{1}H-NMR ($CDCl_3$, 300 MHz, RT, δ ppm): 8.26 (d, 2H, *J* = 8.4 Hz), 8.23 (d, 2H, *J* = 8.4 Hz), 6.47 (s, 1H), 6.41 (s, 1H), 6.27 (s, 1H), 5.97 (s, 1H), 5.59 (s, 1H), 5.31 (s, 2H), 3.77 (s, 3H). ^{13}C-NMR ($CDCl_3$, 75 MHz, RT, δ ppm): 166.4, 164.3, 155.3, 150.6, 148.6, 139.1, 135.2, 130.9, 127.3, 123.5, 112.3, 108.3, 67.5, 59.3, 52.2; Elemental Analysis (CHN): Calculated (%): C: 58.21, H: 4.31. Experimental (%): C: 57.72, H: 4.39; FTIR (cm^{-1}): 3482, 3130-2854, 1714, 1632, 1264, 1091.

(5-(2-(Ethoxycarbonyl)-1-hydroxyallyl)furan-2-yl)methyl 4-chlorobenzoate (**9q**): white solid (88%); ^{1}H-NMR ($CDCl_3$, 300 MHz, RT, δ ppm): 7.96 (d, 2H, *J* = 6.3 Hz), 7.39 (d, 2H, *J* = 6.3 Hz), 6.43 (d, 1H, *J* = 2.4 Hz), 6.39 (s, 1H), 6.25 (d, 1H, *J* = 2.4 Hz), 5.93 (s, 1H), 5.58 (s, 1H), 5.25 (s, 2H), 4.19 (q, 2H, *J* = 5.4 Hz), 1.26 (t, 3H, *J* = 5.4 Hz); ^{13}C-NMR ($CDCl_3$, 75 MHz, RT, δ ppm): 165.9, 165.4, 155.2, 149.1, 139.6, 139.3, 131.1, 128.7, 128.3, 126.8, 111.8, 108.1, 67.6, 61.1, 58.8, 14.0; Elemental Analysis (CHN): Calculated (%): C: 59.27, H: 4.70. Experimental (%): C: 58.94, H: 4.33; FTIR (cm^{-1}): 3483, 3120-2855, 1714, 1633, 1267, 1096.

3.4 RESULTS AND DISCUSSION

The MBH reaction between biomass-derived furaldehydes and acrylates was studied on FUR. The optimized reaction was parameterized on FUR for the best selectivity and yield of the MBH adduct. The optimized process was then extended to various 5-substituted-2-furaldehydes to develop a general synthetic protocol. In this regard, the 5-substituted-2-furaldehydes display markedly different reactivity depending on the substituent present. Therefore, even though developing a general synthetic procedure is challenging, it will be a giant leap toward the sustainable value addition of these biorenewable chemical platforms. DABCO is the most commonly employed catalyst for MBH reaction. The superior catalytic activity of DABCO is often explained by its balanced sterically hindered basicity and nucleophilicity, both of which are crucial from the mechanistic standpoint. The chemical stability, easy availability, low cost, and low toxicity are additional advantages for its widespread use in MBH reactions. However, for specific substrates, other organic amines, such as 4-(dimethylamino)pyridine (DMAP) and triethylamine (TEA), show superior catalytic activity. Various tertiary amines and phosphines were screened to examine their effectiveness as a catalyst in the MBH reaction, and the results are listed in Table 3.1. When TEA was used as the organocatalyst, the reaction did not proceed appreciably at room temperature (RT). Elevating the reaction temperature to 60 °C did not accelerate the reaction rate. In the case of diisopropylethylamine (DIPEA), imidazole, and hexamine as a catalyst, the reaction rate was extremely slow, affording only a trace amount of product even after 30 h of reaction. Using triphenylphosphine or DMAP as the catalyst resulted in a complex mixture. When pyrazine was employed as

the organocatalyst, no reaction was observed even after 24 h at RT and elevated temperatures. The lower basic and nucleophilic strength of pyrazine compared to DABCO may be attributed to such reactivity. The NHC-catalyzed reaction was also tried using thiamine and triethylamine in ethanol, but no reaction was observed. On the contrary, using DABCO as the catalyst afforded a single product, as observed on the TLC, and the reaction was completed in 30 h. The most probable mechanism using DABCO as the catalyst in shown in the scheme 3.1

Table 3.1 Screening of organocatalysts for MBH reaction between FUR and methyl acrylate

S/N	Catalyst	Reaction temperature (°C)	Yield of 1p (%)
1	TEA	RT-60	No reaction
2	DABCO	RT	91
3	Imidazole	RT-60	<10
4	Triphenylphosphine	RT	Mixture
5	DMAP	RT	Mixture
6	DIPEA	RT-60	No reaction
7	Hexamine	RT-60	Trace

Reaction conditions: DABCO (1 eq.), methyl acrylate (2.5 eq.), solvent-free, 24-72 h.

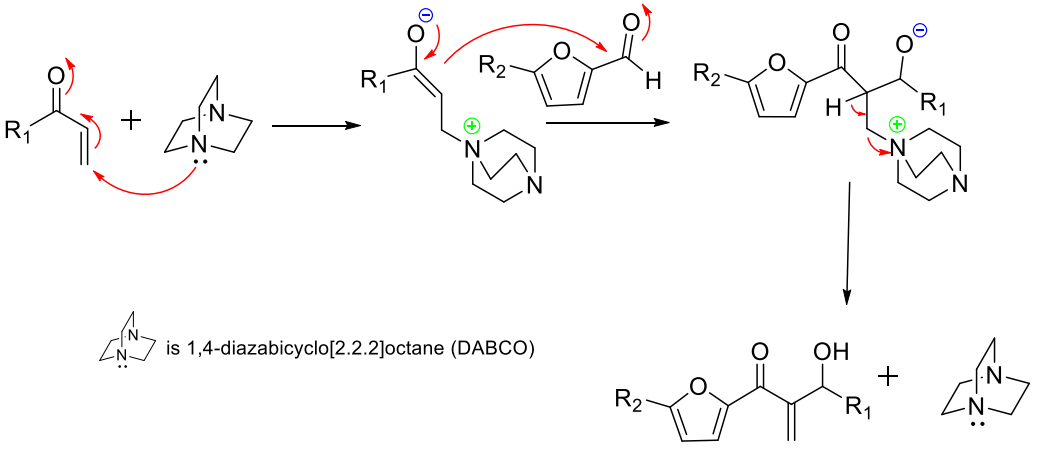

Scheme 3.1 Proposed mechanism of forming Morita Baylis Hillman products from 5-substituted-2- furaldehydes catalyzed by DABCO.

The equivalence of acrylates varied between 1.5 and 2.5 compared to the starting FUR. Using 1.5 eq. or less acrylate led to lower yields of MBH adduct, possibly due to evaporative loss of acrylate and partial decomposition during the reaction. The reaction gave optimum yield using 1.8 eq. of the acrylate reagent. Increasing the acrylate equivalence to 2.5 did not increase the yield of MBH adduct any further. In general, MBH reaction is performed at RT and can take days or even weeks to complete. Polar protic solvents (e.g., ethanol) and weak acids (e.g., acetic acid) accelerate the MBH reaction rate. Therefore, the effects of the reaction solvent and additives were examined next. When the reaction between FUR and methyl acrylate was performed in ethanol, no appreciable change in reaction rate was observed. Moreover, partial decomposition of FUR was observed over time. A catalytic amount of acetic acid accelerated the MBH reaction when 5-MF was used as the substrate. However, the observation was not the same for other substrates. This result justifies the differing reactivity of 5-substituted-2- furaldehydes with changing substituents. Therefore, the reactions were performed under organic solvent-free conditions using DABCO as the catalyst. The non-use of organic solvents and additives simplifies product purification and minimizes waste generation, aligning with green chemistry principles. The MBH reaction of FUR with 1.8 eq. of methyl acrylate at RT using DABCO catalyst under neat condition was then extended to liquid 5-substituted-2-furaldehydes, such as 5MF, EMF, AcMF, 5-(propionyloxymethyl)furfural (PrMF), and 5- (butyryloxymethyl)furfural (BuMF). Solid starting materials such as BzMF, 5-[(4-nitrobenzoyloxy)methyl]furfural (NBzMF), and 5-[(4-chlorobenzoyloxy)methyl]furfural (CBzMF) required slightly more (2.5 eq.) acrylates to ensure uniform mixing and minimize mass transfer limitations. The quantity of DABCO catalyst was optimized next. Lesser catalyst quantities are preferred for lower process costs and simpler product purification. However, other parameters must be factored in, such as the diminished reaction rate and decreased product selectivity, when using lower amounts of the catalyst. When DABCO was used in 0.5 eq. or less (compared to starting FUR), the reaction took >72 h to complete. The reaction slowed down significantly more in some 5-substituted-2-furaldehydes. In addition, partial decomposition of the starting materials was observed

on the TLC plate. Moreover, when the reaction was performed using 0.8 eq. of DABCO, the starting material (i.e., FUR) disappeared within 30 h at RT, signifying the completeness of the reaction. Increasing the amount of DABCO to 1 eq. did not change the reaction rate appreciably but marginally improved the yield of the MBH adduct. The result may be because of the faster rate of MBH reaction, minimizing other side reactions involving FUR. The amount of DABCO was kept at 1 eq. to compensate for partial sublimation of DABCO during the reaction, especially when using solid 5-substituted-2-furaldehydes. When higher equivalents of solid DABCO were added, the reaction became heterogeneous, and the reaction rate got slowed down due to insufficient mass transfer. Methyl-, ethyl-, and butyl acrylate were used as an activated alkene, and various 5-substituted-2-furaldehydes such 5MF, EMF, AcMF, PrMF, BuMF, BzMF, NBzMF, and CBzMF were used as the electrophiles. Therefore, structural diversity in the MBH adducts has been introduced in the acrylate and the furaldehyde moiety. The reactions were carried out at RT using DABCO as the catalyst under organic solvent-free conditions. The chemical structure and yield data of the synthesized MBH adducts are tabulated in Table 3.2. When FUR was reacted with methyl-, ethyl, and butyl acrylates, the reactions were completed after 30 h, resulting in excellent yields of the corresponding MBH adduct. In the case of 5-MF, the MBH reaction was noticeably slow, and the reaction stopped evolving any further after 96 h (observed by TLC). The yield of MBH adduct was marginally low since 5-MF was not completely consumed. A hydrogen-bonding catalyst or an acidic additive is known to accelerate the DABCO-catalysed MBH reaction. When a catalytic amount of acetic acid was introduced as a promoter, the reaction accelerated in the beginning. However, the rate slowed as the reaction progressed, and a similar yield of the corresponding MBH adduct was obtained. The reaction between 5-substituted-2-furaldehydes (i.e., AcMF, EMF, BzMF, BuMF, PrMF, NBzMF, and CBzMF) and acrylates (i.e., methyl-, ethyl-, and butyl) produced novel MBH adducts in good to excellent isolated yields. The alkyl group in acrylate moiety did not influence the reaction rate or product yield significantly in most cases. However, methyl acrylates afforded marginally higher yields of the MBH adducts, possibly due to less sterical hindrance. After the stipulated time, the reaction mixture was diluted in

water, and the product was extracted in an organic solvent. DABCO was successfully recovered from the aqueous fraction and recycled. All the synthesized compounds were characterized by FTIR, ^{1}H-NMR, ^{13}C-NMR, and elemental analysis. The characterization data of **1(p–r)** and **2(p–r)** matched with published literature (Fort et al. 1992a; Guidotti and Coelho 2015; Wang et al. 2019a). Finally, the reaction between FUR and 2-furanone was tried using catalysts such as DABCO, TEA, imidazole, triphenylphosphine, DMAP, DIPEA, and hexamine at RT. All the reactions resulted in a complex mixture. The reactions were also investigated by slow addition of DABCO and changing the sequence of addition of the reactants and catalyst. Furthermore, solvents like water, water-dioxane mixture(1/1:v/v), chloroform, THF, ethanol, and acids (e.g., acetic acid) were used to improve selectivity using DABCO as the catalyst. Interestingly, the above solvents and additives did not improve the reaction selectivity to any noticeable extent. All the reactions led to the sticky reaction mixture with complex TLC spots.

Table 3.2 Synthesis of the MBH adducts of various 5-substituted-2-furaldehydes and methyl acrylate using DABCO as the catalyst.

Entry	**Starting material**	**Product**	**Yield (%)[d]**	**Yield (%)[e]**	**Yield (%)[f]**
1[a]	FUR	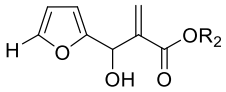 R_2= Me, **1p**; Et, **1q**; Bu, **1r**	91	87	88
2[b]	5-MF	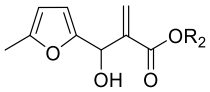 R_2= Me, **2p**; Et, **2q**; Bu, **2r**	76	72	56
3[a]	EMF	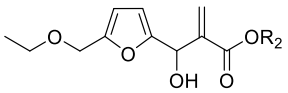 R_2= Me, **3p**; Et, **3q**; Bu, **3r**	90	88	86

4[a]	AcMF	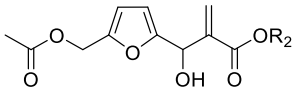 R_2= Me, **4p**; Et, **4q**; Bu, **4r**	92	90	87
5[a]	PrMF	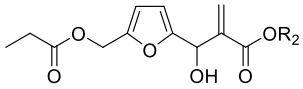 R_2= Me, **5p**; Et, **5q**	85	74	-
6[a]	BuMF	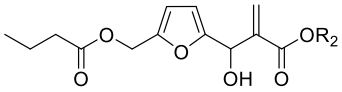 R_2= Me, **6p**; Et, **6q**	89	72	-
7[c]	BzMF	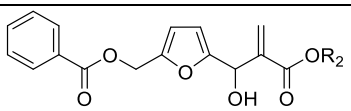 R_2= Me, **7p**; Et, **7q**; Bu, **7r**	92	91	88
8[c]	NBzMF	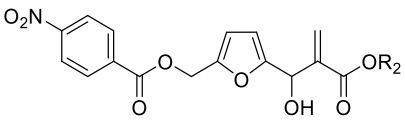 R_2= Me, **8p**; Et, **8q**	91	69	-
9[c]	CBzMF	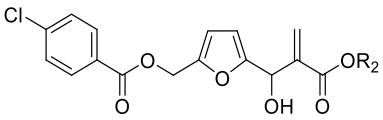 R_2= Me, **9p**; Et, **9q**	90	88	-

Reaction conditions: [a] DABCO (1 eq.), acrylate reagent (1.8 eq.), RT, 30 h, [b]96 h; [c] DABCO (1 eq.), acrylate reagent (2.5 eq.), RT, 30 h, [d] methyl acrylate, [e] ethyl acrylate, [f] butyl acrylate.

3.5 CONCLUSION

A general synthetic protocol was developed for the straightforward and high-yielding synthesis of twenty-three MBH adducts starting from biomass-derived 5-substituted-2-furaldehydes and acrylates. DABCO was found to be the most efficient organocatalyst among the various tertiary amines and phosphines examined. The

MBH adducts were synthesized by performing the reactions at RT under solvent-free conditions using an equivalent amount of DABCO catalyst and a slight excess of acrylate. The reactions were completed within a reasonable time (ca. 30 h) at RT, which is advantageous from the process development standpoint. The DABCO catalyst was successfully recovered from the aqueous extract. Future research will explore using biorenewable α,β-unsaturated lactones, and ketones as the active olefins.

CHAPTER 4

REAGENT-CONTROLLED SWITCHING BETWEEN BIGINELLI AND HANTZSCH PRODUCTS SOURCED FROM BIORENEWABLE FURFURALS USING GLUCONIC ACID AQUEOUS SOLUTION (GAAS) AS THE GREEN CATALYST

Abstract:

Biginelli reaction provides 3,4-dihydropyrimidin-2(1H)-ones (DHPMs), whereas Hantzsch reaction leads to 1,4-dihydropyridines (DHPs) by the one-pot, multicomponent, and operationally simple transformations starting from readily available starting materials. DHPMs and DHPs are well-established heterocyclic moieties in the synthetic organic chemistry literature and have pronounced pharmacological activities. This work reports the synthesis of novel DHPMs and DHPs from carbohydrate-derived 5-substituted-2-furaldehydes by employing gluconic acid aqueous solution (GAAS) as the efficient, inexpensive, and eco-friendly catalyst. The use of urea (or thiourea) as the reagent led to DHPMs, whereas ammonium acetate produced DHPs, selectively, keeping the other two starting materials (i.e., furfurals and ethyl acetoacetate) and the reaction parameters unaltered. Using the general synthetic protocol under optimized reaction conditions (60 °C, 6 h, 25 mol% GAAS cat.), all the DHPM and DHP derivatives were obtained in good to excellent isolated yields.

Graphical abstract*:*

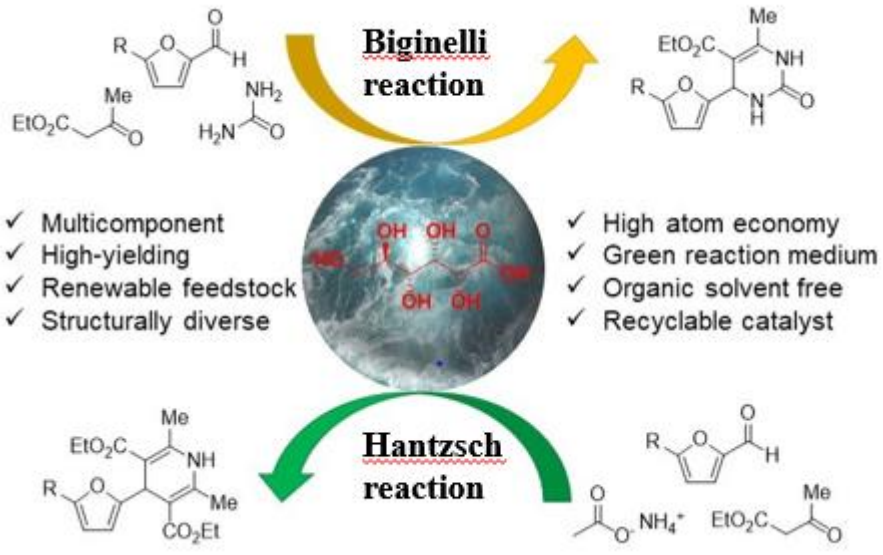

4.1 INTRODUCTION

Carbohydrates have received significant attention over the past three decades as a commercially viable source of biogenic carbon for sustainably synthesizing value-added organic chemicals that are otherwise sourced from exhaustible feedstock like petroleum (Sheldon 2018). The catalytic value addition of carbohydrates has received particular interest since the processes are fast, selective, scalable, eco-friendly, and can be integrated seamlessly into the petrorefinery infrastructure (Mika et al. 2018). For chemical products that do not necessitate preserving the native structure of sugars, a two-step synthetic strategy is adopted. Carbohydrates are initially converted into a handful of functionalized small molecules that act as chemical building units. In the second step, the reactive intermediates are synthetically transformed into products of desired structural features (Anchan et al. 2022). In this regard, the acid-catalyzed dehydration of pentoses (e.g., xylose) leads to furfural (FUR), whereas the dehydration of hexoses (e.g., glucose) forms 5-(hydroxymethyl)furfural (HMF) (Lee and Wu 2021; Zhao et al. 2021). The processes typically use an acid catalyst and produce water as an innocuous byproduct. The production and derivative chemistry of FUR and HMF have been explored scrupulously over the past decades (Li et al. 2016; Wang et al. 2022).In this regard, the synthesis and study of heterocycles is one of the cornerstones of synthetic organic chemistry primarily due to the remarkable properties and fascinating pharmacological activities of the heterocyclic molecules (Qadir et al. 2022). Significant importance has been given to designing green synthetic protocols for various heterocyclic moieties. FUR and HMF are often used as representative furanic molecules to demonstrate the diverse substrate scope of various synthetic methodologies, such as the synthesis of heterocycles (Phan et al. 2022). However, the systematic study of carbohydrate-derived 5-substituted-2-furaldehydes as substrates for synthesizing various classes of heterocyclic molecules is underexplored. Such systematic studies will assist in unraveling the much-desired reactivity patterns of these biorenewable molecules and expand the horizon of their derivative chemistry. Moreover, the study will pave the pathway for synthesizing hitherto unknown products to explore their properties and potential applications. Some of the commonly encountered biorenewable 5-substituited-2-furaldehydes apart from HMF include 5-methylfurfural (5MF), 5-

(acetoxymethyl)furfural (AcMF), and 5-(ethoxymethyl)furfural (EMF). 5MF is a potential biofuel and a renewable chemical intermediate that can be produced by reducing HMF or directly from carbohydrates (Xu et al. 2021). EMF is a potential fuel oxygenate obtained by acid-catalyzed ethanolysis of sugars and polymeric carbohydrates (Bai et al. 2018). AcMF has recently received significant attention as a hydrophobic congener of HMF with several markets (Bhat et al. 2023). These five compounds (i.e., FUR, HMF, 5MF, EMF, and AcMF) have been used as representative examples of biorenewable furaldehydes for developing a general synthetic protocol of the Biginelli and Hantzsch reactions.

In this regard, 3,4-dihydropyrimidin-2(1*H*)-ones (DHPMs) and 1,4-dihydropyridines (DHPs) are well-established classes of heterocyclic compounds with pronounced therapeutic properties (Majellaro et al. 2021; Parthiban and Makam 2022). DHPMs are produced by the Biginelli reaction protocol involving a multicomponent reaction (MCR) between an aromatic aldehyde, esters of acetoacetic acid, and urea (or thiourea) (de Fátima et al. 2015). The acid-catalyzed process typically affords products in excellent isolated yield, possesses excellent atom economy, and forms water as the only byproduct. Similarly, DHPs are produced by the Hantzsch reaction between an aromatic aldehyde, esters of acetoacetic acid, and an ammonium salt (Wang et al. 2019c). MCRs are where more than two reactants with complementary reactive functionalities combine sequentially and produce the product in high selectivity and excellent atom economy. MCRs allow the introduction of significant structural complexity in the product molecule starting from inexpensive and readily available starting materials in a one-pot reaction, predominantly following catalytic steps, decreasing the number of synthetic steps, and minimizing waste formation. Therefore, MCRs are an important part of sustainability in synthetic organic chemistry, and there have been continuing attempts to identify such transformations and use them coherently to design molecules of desired structural features and properties (John et al. 2021). Biginelli and Hantzsch transformations are well-documented MCRs, and their products have remarkable pharmacological properties. Even though FUR has been used as the substrate for these transformations to demonstrate the substrate scope of the catalyst systems, the systematic study involving the 5-substituted-2-furaldehydes is virtually unexplored in the literature.

Numerous homogeneous and heterogeneous acid catalysts have been screened for Biginelli and Hantzsch transformations. Metal-free organocatalysts have shown promising activities for these transformations. A SciFinder search on the Biginelli product of MF 1b as a model 5- substituted-2-furaldehyde revealed that heterogeneous catalysts, such as sulfated zirconia, Zn^{2+}-modified MCM-41, silica-supported sulfonic acid, preyssler heteropolyacids, and titanium silicate had been used that afforded acceptable yields of **4b** under moderate reaction conditions (Ninan et al. 2022). However, there is still an active search for an efficient, inexpensive, and eco-friendly catalyst that allows the reactions to happen under mild conditions and affords products with desired selectivity and yield (Patil et al. 2019). Gluconic acid aqueous solution (GAAS) has received much interest as an acid−based organocatalyst and a green reaction medium for various organic transformations (Lim and Dolzhenko 2021; Zhou et al. 2011). Gluconic acid has roughly 10 times stronger Brønsted acidity (pKa = 3.86) than acetic acid (pKa = 4.76) and is nontoxic, nonvolatile, noncorrosive, and biodegradable. GAAS can be conveniently produced from glucose via catalytic or enzymatic oxidation in water (Kornecki et al. 2020; Zhang et al. 2021a).

This work reports the organic solvent-free synthesis of novel DHPMs and DHPs starting from carbohydrate-derived 5-substituted-2-furaldehydes using GAAS as an efficient but inexpensive catalyst. When the combination of a suitable 5-substituted-2-furaldehyde, urea (or thiourea), and ethyl acetoacetate was heated using GAAS as the catalyst, the resulting Biginelli transformation formed DHPMs. When urea (or thiourea) was replaced with an ammonium salt (e.g., ammonium acetate), the Hantzsch reaction formed DHPs. The substitution pattern at the 5-position of carbohydrate-derived 2-furaldehydes has noticeably different reactivity. Therefore, a general synthetic protocol for synthesizing a specific class of product from these biorenewable chemicals is challenging but rewarding. In this study, a general synthetic protocol for DHPMs and DHPs has been developed that works on all the 5-substituted-2-furaldehydes and produces the desired products selectively by reagent control (Scheme 4.1).

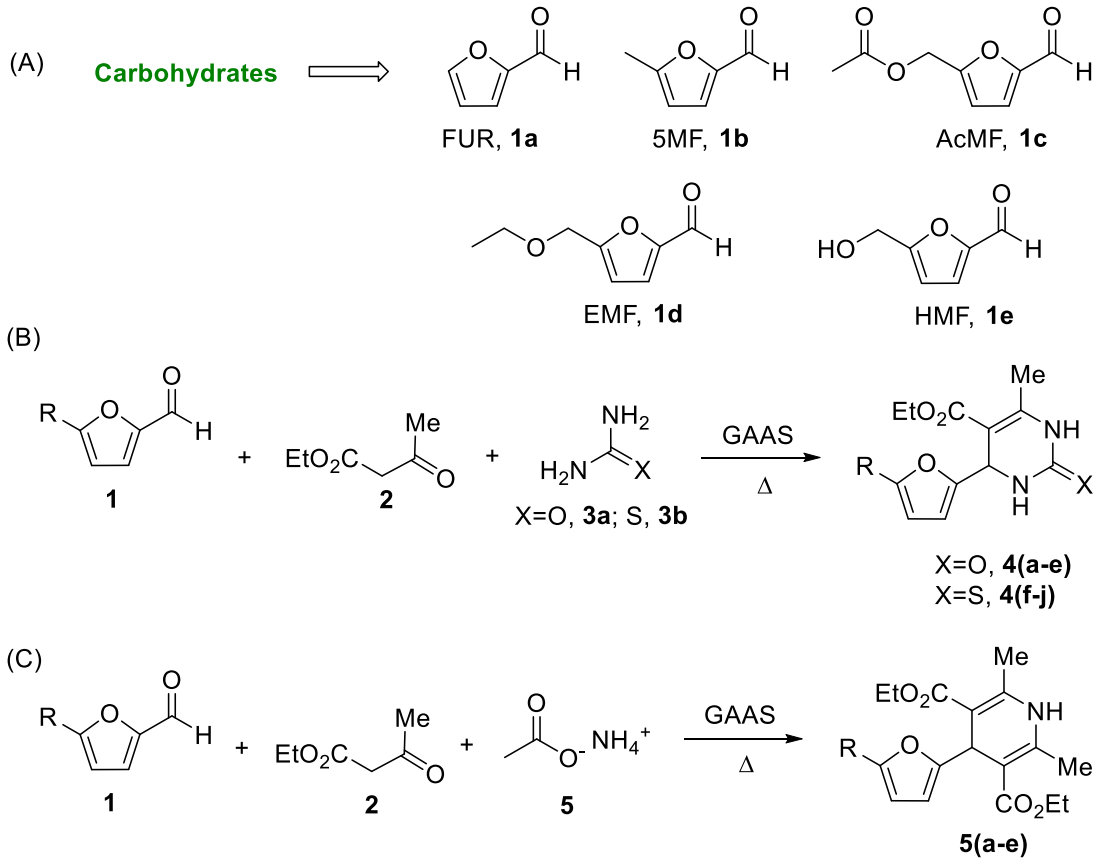

Scheme 4.1 (A) Structures of various 5-substituted-2-furladyhdes obtained from carbohydrate, (B) synthesis of the novel 3,4-dihydropyrimidin-2(1H)-ones, and (C) synthesis of 1,4-dihydropyridines from biorenewable furfurals.

4.2 EXPERIMENTAL SECTION

4.2.1 Materials

Furfural (FUR) (99%), ethyl acetoacetate (99%), urea (99.5%), formic acid (98%) and thiourea (98%) were purchased from Spectrochem. 5-Methylfurfural (5MF) (99%) was purchased from Sigma Aldrich. Deionized (DI) water, oxalic acid dihydrate (99%), succinic acid (99%), glacial acetic acid (99%), petroleum ether, ethyl acetate (99.5%) were purchased from Loba Chemie Pvt. Ltd. Gluconic acid aqueous solution (GAAS, 50%) and lactic acid (85%, aq) were purchased from TCl chemicals. Ethanol (99.9%) was purchased from CSS China. 5-(Acetoxymethyl)furfural (AcMF), 5-(hydroxymethyl)furfural (HMF), 5-

(chloromethyl)furfural (CMF), and 5-(ethoxymethyl)furfural (EMF) were synthesized and purified using literature process (Bhat et al. 2022, 2023).

4.2.2 Synthetic Procedure

4.2.2.1 Synthesis of 3,4-dihydropyrimidin-2(1H)-ones (DHPMs) from furfurals

A mixture of FUR, 1a (0.502 g, 5.22 mmol), ethyl acetoacetate (0.689 g, 5.22 mmol), urea (0.470 g, 7.83 mmol), and GAAS (0.50 g, 25 mol%) was stirred at 60 °C. The progress of the reaction was monitored by using thin-layer chromatography (TLC). After the completion of the reaction (6 h), the reaction mixture was cooled down to RT and poured into crushed ice. The solid was filtered using vacuum filtration, dried in a hot-air oven (60 °C, 12 h), and recrystallized using absolute ethanol to get pure **4a** (1.15 g, 90%).

A similar synthetic strategy was applied for synthesizing **4b-4e**. The synthesized compounds were confirmed by FTIR, NMR, and elemental analysis.

4.2.2.2 Synthesis of 3,4-dihydropyrimid-2-(*1H*)-thiones using Biginelli condensation

FUR, 1a (0.502 g, 5.22 mmol), ethyl acetoacetate (0.679 g, 5.22 mmol), thiourea (1.59 g, 20.89 mmol), GAAS (1.10 g, 50 mol%) were charged in a round-bottomed flask fitted with a reflux condenser and magnetically stirred in a pre-heated oil bath at 80 °C for 12 h. After the reaction, the mixture was cooled to RT and poured into crushed ice. The solid product is filtered under vacuum, dried in a hot-air oven (60 °C, 12 h), and recrystallized using absolute ethanol to get pure **4f** (1.17 g, 86%).

A similar synthetic strategy was applied for the synthesis of **4g-4j**. The synthesized compounds were confirmed by FTIR, NMR, and elemental analysis.

4.2.2.3 Synthesis of 1,4-dihydropyridines (DHPs) using Hantzsch condensation

FUR, 1a (0.502 g, 5.22 mmol), ethyl acetoacetate (1.37 g, 10.44 mmol), ammonium acetate (0.604 g, 7.83 mmol), and GAAS (0.50 g, 25 mol%) were charged in a round-bottomed flask fitted with a reflux condenser and magnetically stirred in a pre-heated (60 °C) oil bath for 3 h. After the reaction, the mixture was cooled to RT and poured into crushed ice. The solid product is filtered under vacuum, dried, and recrystallized using ethanol to get pure **5a** (1.61 g, 97%).

A similar synthetic strategy was applied for the synthesis of **5b**-**5e**. The synthesized compounds were confirmed by FTIR, NMR, and elemental analysis.

4.3 CHARACTERIZATION OF THE SYNTHESIZED COMPOUNDS

4.3.1 The FTIR, ^{1}H-NMR, and ^{13}C-NMR spectra of ethyl 4-(furan-2-yl)-6-methyl-2-oxo-1,2,3,4-tetrahydropyrimidine-5-carboxylate (4a)

Ethyl 4-(furan-2-yl)-6-methyl-2-oxo-1,2,3,4-tetrahydropyrimidine-5-carboxylate (**4a**): Light yellow solid; 1.180 g, 90%; Melting point: 200-202 °C; ^{1}H-NMR (DMSO-d_6, 400 MHz, RT) δ (ppm): 9.25 (s, 1H, NH), 7.76 (s, 1H, NH), 7.55 (d, 1H, furyl-CH), 6.35 (t, 1H, furyl-CH), 6.08 (d, 1H, furyl-CH), 5.209 (s, 1H, CH), 4.02 (q, 2H, -OCH_2CH_3, J = 6.8 Hz), 2.23 (s, 3H, -CH_3), 1.13 (s, 3H, -OCH_2CH_3, J = 6.8 Hz); ^{13}C-NMR (DMSO-d_6, 100 MHz, RT) δ (ppm): 165.2, 156.1, 152.6, 149.6, 142.3, 110.5, 105.5, 96.9, 59.4, 47.9, 17.9, 14.3; FTIR (cm^{-1}): 3242 (-NH stretching frequency), 3117 (furanic –CH stretch), 2918 (-CH stretches), 1729 (-$COOCH_2CH_3$), 1706 (CO stretching frequency of -NHCONH-), 1653 (C=C stretches), 1231(C-O stretching frequency). Elemental analysis (CHN): Calculated (%): C: 57.59, H: 5.64, N: 11.19; Experimental (%): C: 57.14, H: 5.46, N: 10.93.

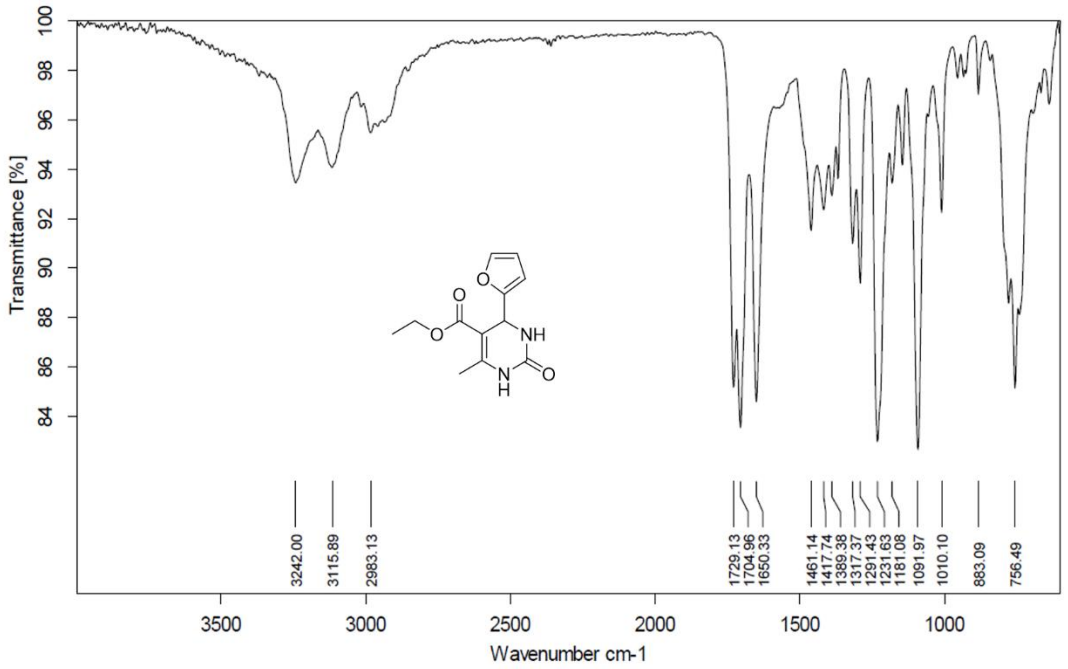

Figure 4.1 The FTIR spectrum of **4a**.

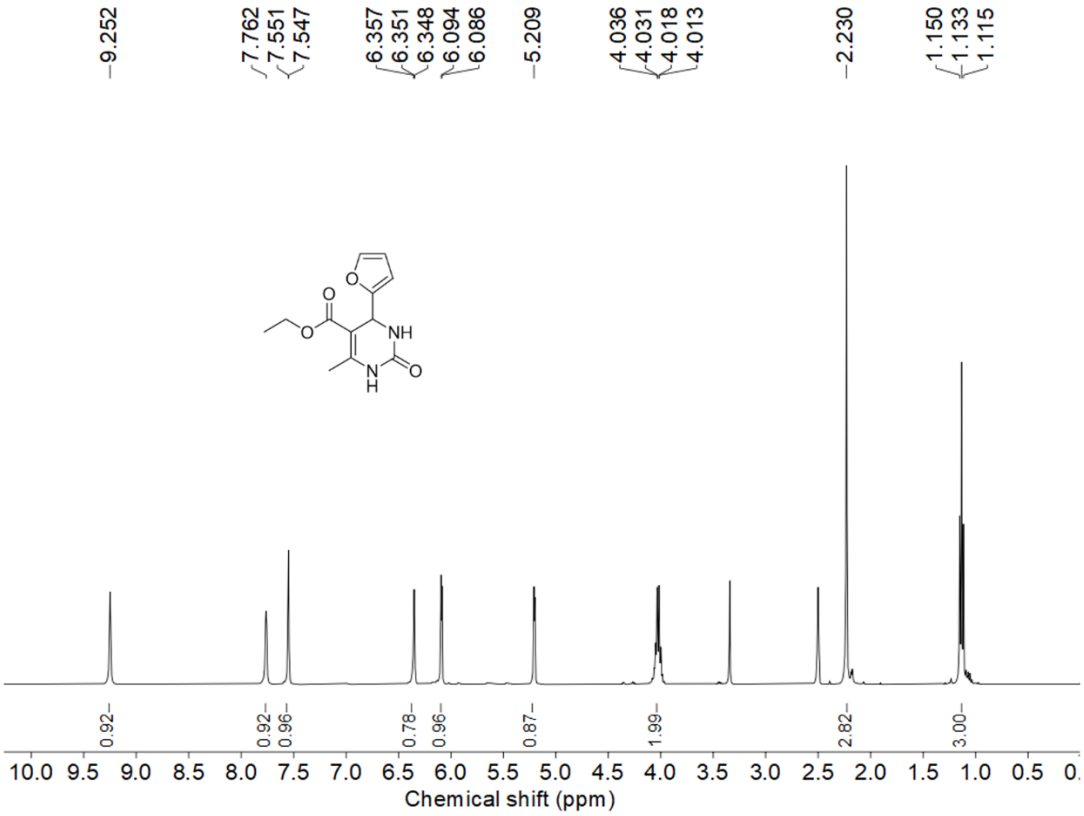

Figure 4.2 The ^{1}H-NMR spectrum of **4a** (solvent: DMSO-d_6).

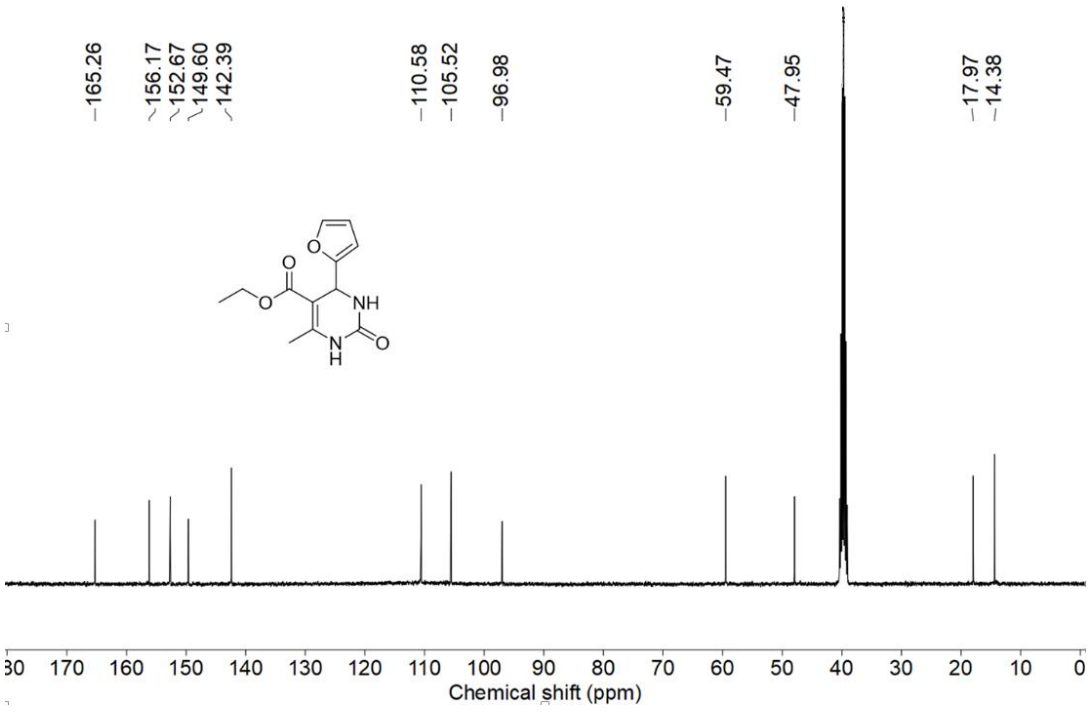

Figure 4.3 The ^{13}C-NMR spectrum of **4a** (solvent: DMSO-d_6).

4.3.2 The FTIR, ^{1}H-NMR, and ^{13}C-NMR spectra of diethyl 4-(furan-2-yl)-2,6-dimethyl-1,4-dihydropyridine-3,5-dicarboxylate (5a)

Diethyl 4-(furan-2-yl)-2,6-dimethyl-1,4-dihydropyridine-3,5-dicarboxylate (**5a**): Light yellow solid; 1.618 g, 97%; Melting point: 166-168 °C; ^{1}H-NMR (DMSO-d_6, 400 MHz, RT) δ (ppm): 8.91 (s, 1H), 7.38 (s, 1H), 6.24 (d, 1H), 5.83 (d, 1H), 5.04 (s, 1H), 4.06 (q, 4H, J = 7.2 Hz), 2.25 (s, 6H), 1.16 (t, 3H, J = 7.2 Hz); ^{13}C-NMR (DMSO-d_6, 100 MHz, RT) δ (ppm): 166.9, 159.0, 146.6, 141.2, 110.3, 104.1, 98.7, 59.2, 32.9, 18.4, 14.4; FTIR (cm^{-1}): 3345 (-NH stretching frequency), 3118 (furanic –CH stretch), 2983-2850 (-CH stretches), 1732-1706 (C=O stretching frequency of -$COOCH_2CH_3$), 1656 (C=C stretching frequency), 1235 (C-O stretching frequency). Elemental analysis (CHN): Calculated (%): C: 63.94, H: 6.63, N: 4.39; Experimental (%): C: 63.77, H: 6.618, N: 5.03.

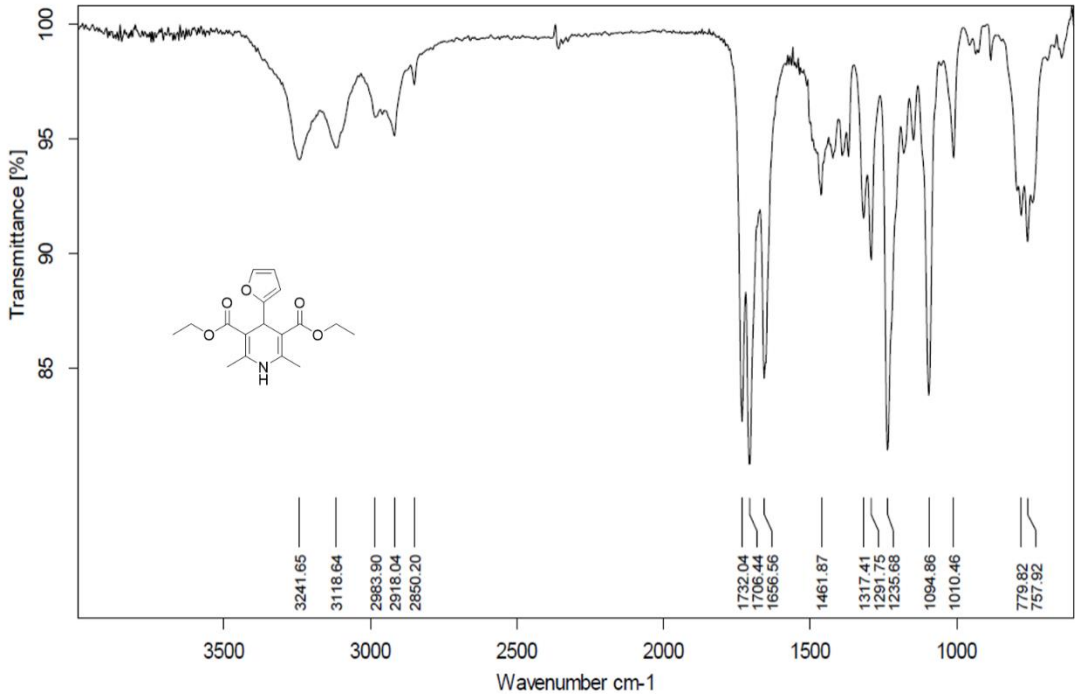

Figure 4.4 The FTIR spectrum of **5a**.

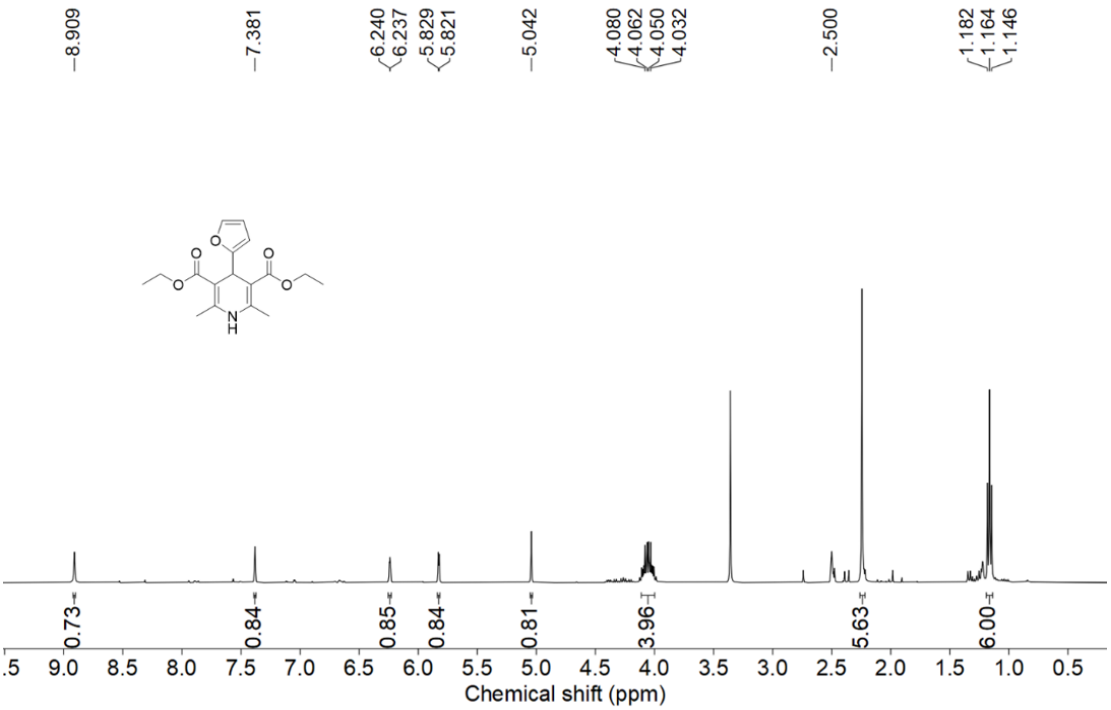

Figure 4.5 The ^{1}H-NMR spectrum of **5a** (solvent: DMSO-d_6).

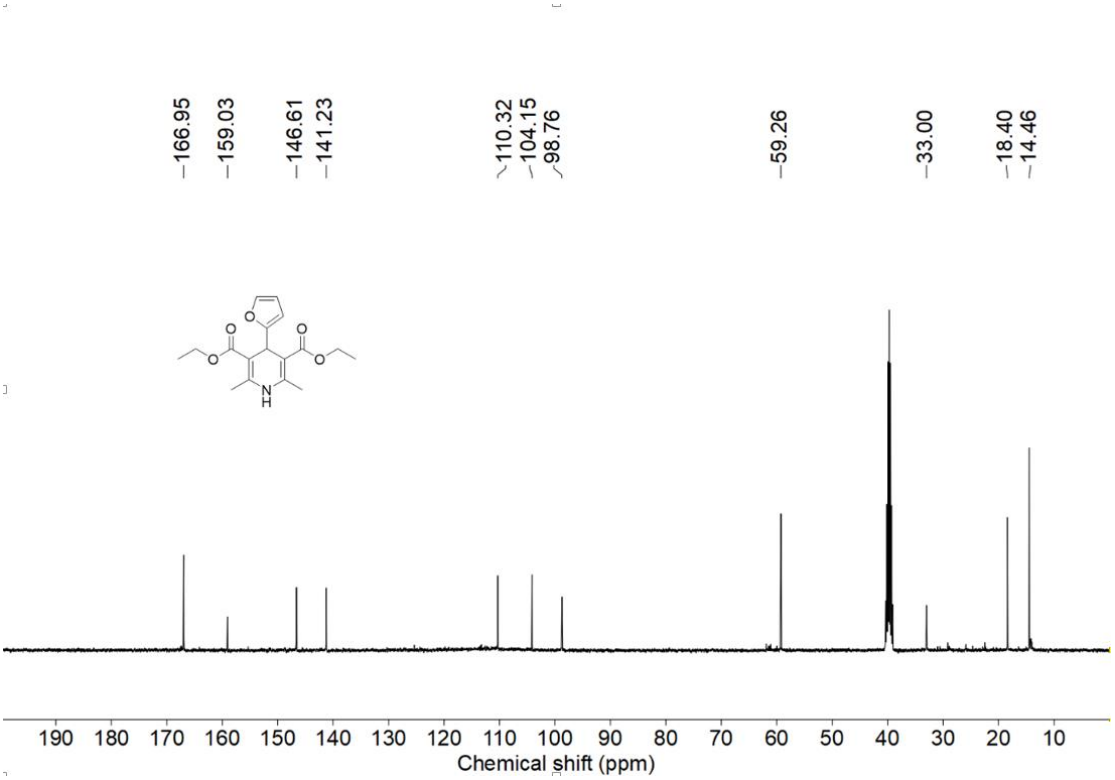

Figure 4.6 The ^{13}C-NMR spectrum of **5a** (solvent: DMSO-d_6).

4.3.3 Characterization data of all the synthesized compounds

Ethyl 6-methyl-4-(5-methylfuran-2-yl)-2-oxo-1,2,3,4-tetrahydropyrimidine-5 carboxylate (**4b**): Light yellow solid; 0.903 g, 75%; Melting point: 218-220 °C; ^{1}H-NMR (DMSO-d_6, 300 MHz, RT) δ (ppm): 9.18 (s, 1H), 7.70 (s, 1H), 5.93 (s, 2H), 5.13 (s, 1H, CH), 4.02 (q, 2H, J = 6.6 Hz), 2.21 (s, 6H), 1.13 (t, 3H, J = 6.9 Hz); ^{13}C-NMR (DMSO-d_6, 75 MHz, RT) δ (ppm): 165.1, 154.2, 152,4, 150.7, 149.2, 106.3, 106.0, 96.8, 59.2, 47.7, 17.7, 14.2, 13,4; FTIR (cm^{-1}): 3232, 3107, 2918, 1706, 1653, 1089. Elemental analysis (CHN): Calculated (%): C: 59.08, H: 6.10, N: 10.60; Experimental (%): C: 58.89, H: 6.30, N: 10.30.

Ethyl 4-(5-(acetoxymethyl)furan-2-yl)-6-methyl-2-oxo-1,2,3,4-tetrahydropyrimidine-5- carboxylate (**4c**): Light brown solid; 0.677 g, 70%; Melting point: 154-158 °C; ^{1}H-NMR (DMSO-d_6, 400 MHz, RT) δ (ppm): 9.25 (s, 1H), 7.81 (d, 1H), 6.41 (d, 1H, J = 3.2 Hz), 6.07 (d, 1H, J = 3.2 Hz), 5.18 (d, 1H, J = 3.6 Hz), 4.96 (s, 2H,), 4.03 (q, 2H J = 6.8 Hz), 2.23 (s, 3H), 2.02 (s, 3H), 1.13 (t, 3H, J = 6.8 Hz); ^{13}C-NMR (DMSO-d_6, 100 MHz, RT) δ (ppm): 169.9, 164.9, 156.8, 152.2, 149.6, 148.4, 111.6, 106.2, 96.5, 59.2, 57.6, 47.7, 20.5, 17.7, 14.1; FTIR (cm^{-1}): 3244, 3124, 2920, 1739, 1701, 1645, 1092. Elemental analysis (CHN): Calculated (%): C: 55.90, H: 5.63, N: 8.69; Experimental (%): C: 56.35, H: 5.80, N: 8.26.

Ethyl 4-(5-(ethoxymethyl)furan-2-yl)-6-methyl-2-oxo-1,2,3,4-tetrahydropyrimidine-5- carboxylate (**4d**): Light yellow solid; 0.606 g, 60%; Melting point: 130-134 °C; ^{1}H-NMR (DMSO-d_6, 400 MHz, RT) δ (ppm): 9.23 (s, 1H), 7.79 (s, 1H), 6.28 (d, 1H, J = 3.2 Hz), 6.02 (d, 1H, J = 3.2 Hz), 5.18 (d, 1H, J = 3.6 Hz), 4.30 (s, 2H), 4.03 (q, 2H, J = 6.8 Hz), 3.43 (q, 2H, J = 6.8 Hz), 2.23 (s, 3H), 1.13 (t, 3H, J = 6.8 Hz), 1.10 (t, 3H, J = 6.8 Hz); ^{13}C-NMR (DMSO-d_6, 100 MHz, RT) δ (ppm): 164.9, 155.9, 152.3, 151.2, 149.4, 109.8, 105.9, 96.6, 64.7, 63.6, 59.2, 47.7, 17.7, 14.9, 14.1; FTIR (cm^{-1}): 3243, 3121, 2975, 1702, 1644, 1090, 1016; Elemental analysis (CHN): Calculated (%): C: 58.43, H: 6.54, N: 9.09; Experimental (%): C: 57.99, H: 6.568, N: 9.09.

Ethyl 4-(5-(hydroxymethyl)furan-2-yl)-6-methyl-2-oxo-1,2,3,4-tetrahydropyrimidine-5- carboxylate (**4e**): Light yellow solid; 0.670 g, 60%; ^{1}H-NMR (DMSO-d_6, 300 MHz) δ (ppm): 9.20 (s, 1H), 7.75 (s, 1H), 6.15 (s, 1H), 6.00 (t, 2H), 5.17 (s, 1H), 4.31 (s, 2H), 2.23 (s, 3H), 1.16 (t, 3H); ^{13}C-NMR (DMSO-d_6, 75 MHz, RT) δ (ppm):

165.0, 155.1, 154.7, 152.3, 149.4, 107.6, 105.9, 96.6, 59.2, 55.7, 47.7, 17.7, 14.1; FTIR (cm^{-1}): 3330, 2919, 2854, 1733, 1685, 1211, 1018.

Ethyl 4-(furan-2-yl)-6-methyl-2-thioxo-1,2,3,4-tetrahydropyrimidine-5-carboxylate (**4f**): Light brown solid; 1.182 g, 85%; Melting point: 222-224 °C; ^{1}H-NMR (DMSO-d_6, 400 MHz, RT) δ (ppm): 10.39 (s, 1H), 9.63 (s, 1H), 7.58 (s, 1H) 6.37 (s, 1H), 6.14 (d, 1H, J = 3.2 Hz), 5.22 (d, 1H, J = 4.0 Hz), 4.03 (q, 2H, J = 7.2 Hz), 2.27 (s, 3H), 1.13 (t, 3H, J = 7.2 Hz); ^{13}C-NMR (DMSO-d_6, 100 MHz, RT) δ (ppm): 174.8, 164.7, 154.5, 145.9, 142.6, 110.4, 106.2, 98.1, 59.5, 49.7, 17.0, 14.0; FTIR (cm^{-1}): 3308, 3177, 2919, 1709, 1693, 1660, 1181. Elemental analysis (CHN): Calculated (%): C: 54.12, H: 5.30, N: 10.52, S: 12.04; Experimental (%): C: 54.72, H: 5.192, N: 10.54, S: 11.546.

Ethyl 6-methyl-4-(5-methylfuran-2-yl)-2-thioxo-1,2,3,4-tetrahydropyrimidine-5-carboxylate (**4g**): Light yellow solid; 0.894 g, 70%; Melting point: 153-155 °C; ^{1}H-NMR (DMSO-d_6, 300 MHz, RT) δ (ppm): 10.35 (s, 1H), 9.61 (s,1H), 5.98 (s, 2H), 5.16 (s, 1H), 4.04 (q, 2H, J = 3.6 Hz), 2.27 (s, 3H), 2.21 (s, 3H), 1.14 (t, 3H, J = 3.6 Hz); ^{13}C-NMR (DMSO-d_6, 75 MHz, RT) δ (ppm): 174.7, 164.8, 152.8, 151.2, 145.9, 107.0, 106.5, 98.2, 59.5, 47.6, 17.1, 14.0, 13.4; FTIR (cm^{-1}): 3190, 2982, 2925, 1706, 1621, 1094, 1020. Elemental analysis (CHN): Calculated (%): C: 55.70, H: 5.75, N: 9.99, S: 11.44; Experimental (%): C: 55.761, H: 6.692, N: 9.916, S: 11.474.

Ethyl 4-(5-(acetoxymethyl)furan-2-yl)-6-methyl-2-thioxo-1,2,3,4-tetrahydropyrimidine -5-carboxylate (**4h**): Light yellow solid; 0.676 g, 67%; Melting point: 130-132 °C; ^{1}H-NMR (DMSO-d_6, 300 MHz, RT) δ (ppm): 10.41 (s, 1H), 9.69 (s, 1H), 6.43 (s, 1H), 6.11 (s, 1H), 5.21 (s, 1H), 4.97 (s, 2H), 4.04 (q, 2H), 2.28 (s, 3H), 2.02 (s, 3H), 1.13 (t, 3H); ^{13}C-NMR (DMSO-d_6, 75 MHz, RT) δ (ppm): 174.8, 169.9, 164.7, 155.4, 148.9, 146.2, 111.7, 107.2, 97.9, 59.6, 57.5, 47.7, 20.5, 17.1, 14.0; FTIR (cm^{-1}): 3192, 3015, 2956, 2853, 1738, 1709, 1652, 1099, 1021. Elemental analysis(CHN): Calculated (%): C: 53.24, H: 5.36, N: 8.28, S: 9.47; Experimental (%): C: 53.59, H: 5.491, N: 8.20, S: 9.480.

Ethyl 4-(5-(ethoxymethyl)furan-2-yl)-6-methyl-2-thioxo-1,2,3,4-tetrahydropyrimidine-5- carboxylate (**4i**): Light yellow solid; 0.678 g, 64%; Melting

point: 134-136 °C; ^{1}H-NMR (DMSO-d_6, 300 MHz, RT) δ (ppm): 10.39 (s, 1H), 9.67 (s, 1H), 6.30 (s, 1H), 6.07 (s, 1H), 5.20 (s, 1H), 4.31 (s, 2H), 4.04 (q, 2H), 3.43 (q, 2H), 2.28 (s, 3H), 1.09 (t, 6H); ^{13}C-NMR (DMSO-d_6, 75 MHz, RT) δ (ppm): 174.8, 164.7, 154.6, 151.6, 146.1, 109.9, 106.9, 98.0, 64.7, 63.6, 59.6, 47.7, 17.1, 14.9, 14.0; FTIR (cm^{-1}): 3188, 2920, 2855, 1702, 1653, 1562, 1178, 1016. Elemental analysis (CHN): Calculated (%): C: 55.54, H: 6.21, N: 8.64, S: 9.88; Experimental (%): C: 55.59, H: 6.04, N: 8.86, S: 9.89.

Ethyl 4-(5-(hydroxymethyl)furan-2-yl)-6-methyl-2-thioxo-1,2,3,4-tetrahydropyrimidine-5- carboxylate (**4j**): Light brown solid; 0.708 g, 60%; ^{1}H-NMR (DMSO-d_6, 300 MHz, RT) δ (ppm): 10.36 (s, 1H), 9.65 (s, 1H), 6.18 (s, 1H), 6.04 (s, 1H), 5.20 (s, 1H), 4.32 (s, 2H), 4.04 (q, 2H), 2.28 (s, 3H), 1.13 (t, 3H); ^{13}C-NMR (DMSO-d_6, 75 MHz, RT) δ (ppm): 174.7, 164.8, 155.1, 153.8, 146.1, 107.7, 106.9, 98.1, 59.6, 55.7, 47.8, 17.2, 14.1; FTIR (cm^{-1}): 3331, 2920, 1697, 1653, 1182, 1015.

Diethyl 2,6-dimethyl-(5-methylfuran-2-yl)-1,4-dihydropyridine-3,5-dicarboxylate (**5b**): Light yellow solid; 1.292 g, 85%; Melting point: 142-144 °C; ^{1}H-NMR (DMSO-d_6, 300 MHz, RT) δ (ppm): 8.85 (s, 1H), 5.82 (s, 1H), 5.64 (s, 1H), 4.96 (s, 1H), 4.07 (q, 4H, J = 7.2 Hz), 2.23 (s, 6H), 2.12 (s, 3H), 1.16 (t, 3H, J = 7.2 Hz); ^{13}C-NMR (DMSO-d_6, 75 MHz, RT) δ (ppm): 166.8, 157.2, 149.4, 146.2, 106.1, 104.7, 98.7, 59.0, 32.7, 18.2, 14.3, 13.5; FTIR (cm^{-1}): 3337, 2979, 2920, 1678, 1623, 1019. Elemental analysis (CHN): Calculated (%): C: 64.85, H: 6.95, N: 4.20; Experimental (%): C: 64.30, H: 6.970, N: 4.28.

Diethyl 4-(5-(acetoxymethyl)furan-2-yl)-2,6-dimethyl-1,4-dihydropyridine-3,5-dicarboxylate (**5c**): Light yellow solid; 1.051 g, 90%; Melting point: 94-98 °C; ^{1}H-NMR (DMSO-d_6, 300 MHz, RT) δ (ppm): 8.92 (s, 1H), 6.29 (d, 1H, J = 2.7 Hz), 5.79 (d, 1H, J = 2.7 Hz), 5.01 (s, 1H), 4.89 (s, 2H), 4.04 (q, 4H, J = 7.2 Hz), 2.24 (s, 6H), 2.00 (s, 3H), 1.17 (t, 6H, J = 7.2 Hz); ^{13}C-NMR (DMSO-d_6, 75 MHz, RT) δ (ppm): 169.9, 166.6, 160.0, 147.2, 146.5, 111.4, 105.1, 98.3, 59.08, 57.7, 32.9, 20.5, 18.1, 14.2; FTIR (cm^{-1}): 3339, 2981, 2931, 1740, 1680, 1624, 1094. Elemental analysis (CHN): Calculated (%): C: 61.37, H: 6.44, N: 3.58; Experimental (%): C: 62.40, H: 6.821, N: 3.97.

Diethyl 4-(5-(ethoxymethyl)furan-2-yl)-2,6-dimethyl-1,4-dihydropyridine-3,5-dicarboxylate (**5d**): Yellow solid; 1.093 g, 89%; Melting point: 69-71 °C; ^{1}H-NMR (DMSO-d_6, 300 MHz, RT) δ (ppm): 8.90 (s, 1H), 6.16 (s, 1H), 5.74 (s, 1H), 5.00 (s, 1H), 4.22 (s, 2H), 4.06 (m, 4H), 2.24 (s, 6H), 1.16 (s, 6H), 1.06 (t, 3H); ^{13}C-NMR (DMSO-d_6, 75 MHz, RT) δ (ppm): 166.7, 159.1, 150.1, 146.4, 109.7, 104.7, 98.5, 64.5, 63.8, 59.1, 32.9, 18.2, 14.9, 14.2; FTIR (cm^{-1}): 3335, 2976, 2851, 1696, 1625, 1097. Elemental analysis (CHN): Calculated (%): C: 63.65, H: 7.21, N: 3.71; Experimental (%): C: 63.33, H: 7.341, N: 3.56.

Diethyl 4-(5-(hydroxymethyl)furan-2-yl)-2,6-dimethyl-1,4-dihydropyridine-3,5 dicarboxylate (**5e**): Yellow solid; 1.168 g, 84%; ^{1}H-NMR (DMSO-d_6, 300 MHz, RT) δ (ppm): 8.88 (s, 1H), 6.05 (s, 1H), 5.72 (s, 1H), 5.01 (s, 1H), 4.26 (s, 2H), 4.06 (q, 4H), 2.23 (s, 6H), 1.17 (t, 6H); ^{13}C-NMR (DMSO-d_6, 75 MHz, RT) δ (ppm): 166.8, 158.2, 153.5, 146.3, 107.6, 104.7, 98.5, 59.1, 55.8, 32.8, 18.2, 14.3; FTIR (cm^{-1}): 3331, 3094, 2919, 2854, 1733, 1685, 1211, 1018.

4.4 RESULTS AND DISCUSSION

Initially, the catalytic efficiency of some commonly encountered water-soluble biogenic carboxylic acids were explored toward the Biginelli reaction of FUR (1a) with ethyl acetoacetate (2) and urea (3a) forming DHPM **4a**. Table 4.1 shows the results obtained by performing the Biginelli reaction of 1a with 2 and 3a in the presence of various aqueous carboxylic acids as innocuous catalysts under organic solvent-free conditions.

Table 4. 1 Synthesis of DHPM (**4a**) from FUR (1a) using an aqueous solution of biogenic carboxylic acids as an efficient and innocuous catalyst.

Entry	Catalyst	Yield of **4a** (%)[a]
1	Formic acid	74
2	Acetic acid	65
3	Lactic acid	82
4	GAAS	88
5[b]	Oxalic acid	46(51)
6	Succinic acid	58

[a]Reaction conditions: FUR 1a (0.502 g, 5.225 mmol), ethyl acetoacetate (0.680 g, 5.225 mmol), urea (0.470 g, 7.837 mmol), catalyst (50% aq., 25 mol%), 60 °C, 6 h. [b]Yield in parentheses used oxalic acid amount assuming it as a monobasic acid.

When a 25 mol % loading of an aqueous solution (50%) of formic acid (pKa = 3.75) was employed as the catalyst, the reaction completed within 6 h at 60 °C and DHPM 4a was obtained in a 74% isolated yield (entry 1, Table 4.1). The reaction progress was monitored by TLC for the disappearance of 1a or until the reaction mixture stopped evolving any further. The reaction mixture was quenched in ice-cold water to precipitate 4a. The reported yields of 4a were obtained after purifying the crude product via column chromatography. When acetic acid (50%, aq) was used as the catalyst, a 65% yield of **4a** was observed (entry 2, Table 4.1). The low yield can be attributed to the lower acidity of acetic acid (pKa = 4.76). Lactic acid and GAAS afforded excellent isolated yields of **4a** (>80%) under the reaction conditions employed (entries 3 and 4, Table 4.1). Interestingly, oxalic acid and succinic acid provided only moderate yields of **4a** (entries 5 and 6, Table 4.1). The result was attributed to the partial decomposition of 1a during the reaction. Evidently, GAAS showed the highest efficiency in terms of selectivity for synthesizing **4a** under the reaction conditions explored. Therefore, the process optimization of the Biginelli reaction using GAAS as a catalyst was studied next using 1a, 2, and 3a as model substrates/reagents. The mixture was heated in an oil bath and magnetically stirred during the reaction. When the reaction was carried out without adding any catalyst, the product was not formed, even at elevated temperatures. Initially, the reaction was carried out using excess GAAS starting from a 1:1:1.5 molar ratio of 1a, 2, and 3a at room temperature (Figure 4.7).

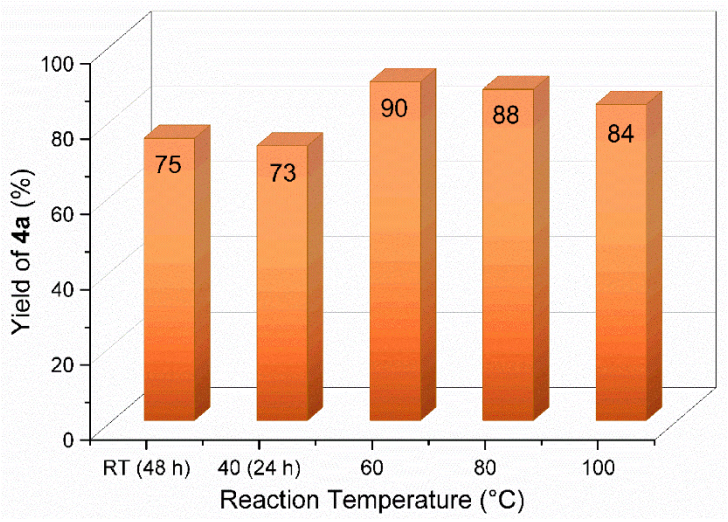

Figure 4.7 The effect of reaction temperature on yield **4a**.

Reaction Conditions:1a (0.502 g, 5.22 mmol), ethyl acetoacetate (0.689 g, 5.22 mmol), urea (0.470 g, 7.83 mmol), GAAS (0.50 g, 25 mol%), 6 h.

Even after a prolonged reaction time of 24 h, the reaction did not complete, and only a 65% isolated yield of **4a** was obtained. When a catalytic amount of GAAS (25 mol % of 1a) was employed and the reaction was allowed to run for 48 h, the yield of 4a reached 75%. When the reaction temperature was increased slightly to 40 °C, the isolated yield of **4a** reached 73% within 24 h. The mass balance of the reaction was the unreacted starting materials. When the reaction temperature was elevated to 60 °C, the reaction was completed in 6 h, affording a 90% isolated yield of **4a**. Further increase of the reaction temperature to 80−100 °C for faster kinetics and shorter duration marginally lowered the yield of **4a**, possibly due to diminished selectivity. The effect of reaction duration was studied by varying reaction time from 4 to 8 h (Figure 4.8).

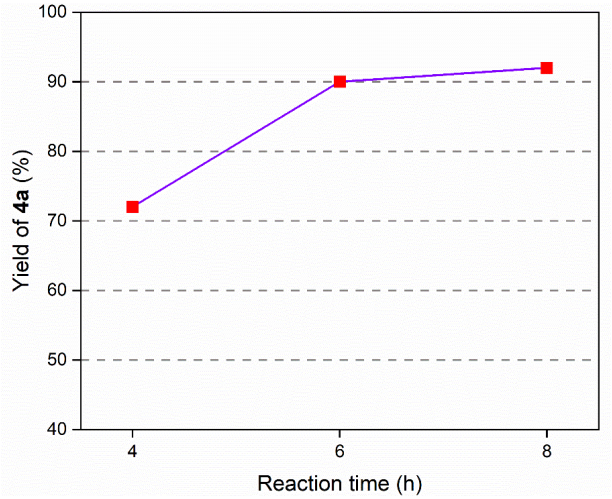

Figure 4.8 The effect of reaction time on the yield of **4a**.

Reaction Condtions:1a (0.502 g, 5.22 mmol), ethyl acetoacetate (0.689 g, 5.22 mmol), urea (0.470 g, 7.83 mmol), GAAS (0.50 g, 25 mol%), 60 °C.

When the reaction was carried out for 4 h, the isolated yield of 4a was only 72% at 60 °C using 25 mol% of GAAS as a catalyst. In comparison, the reaction conducted for 6 h gave 90% 4a under similar reaction conditions. Increasing the reaction duration to 8 h gave only a marginal increase in the amount of **4a** (ca. 92%). Therefore, a reaction temperature of 60 °C and a duration of 6 h were taken as optimized parameters for synthesizing 4a from biomass derived 1a using GAAS (25 mol%) as the catalyst.

The amount of GAAS catalyst was varied between 10 and 30 mol% to check the catalytic activity during the formation of 4a. When only a 10 mol% loading of the GAAS catalyst was employed, **4a** was obtained in a 72% isolated yield (60 °C, 6 h), and the mass balance was predominantly the unreacted starting materials. Increasing the loading of GAAS to 30 mol% did not show any observable change in the yield of **4a**. Therefore, a 25 mol% loading of GAAS was considered optimum for the reaction. The molar ratio of the starting materials was studied next to improve the process economy and minimize waste formation. It was found that urea needed to be used more than the equivalent amount due to its instability during the reaction, especially at elevated temperatures. A 1:1:1.5 molar ratio between 1a, 2, and 3a was found to be most suitable for the Biginelli reaction affording a satisfactory yield of 4a.

After optimization of the reaction conditions, the synthetic protocol was applied for the synthesis of novel DHPMs from representative 5-substituted-2-furaldehyses, such as MF (1b), AcMF (1c), EMF (1d), and HMF (1e). Interestingly, the reaction kinetics was slower for 5-substituted-2-furaldehydes than 1a. Under the optimized conditions (60 °C, 6 h), 1b, 1c, 1d, and 1e gave 75, 70, 60, and 60% of their corresponding DHPM, respectively (Figure 4.9).

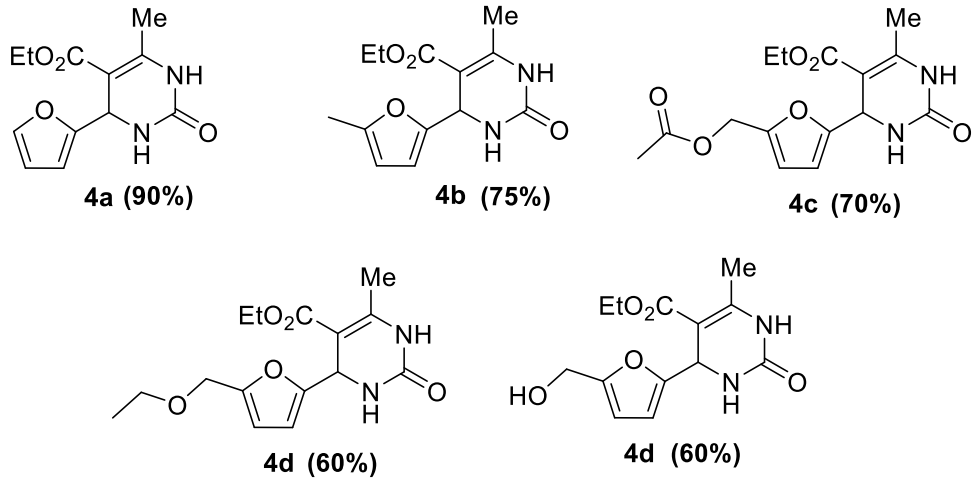

Figure 4.9 The synthesis of 3,4-dihydropyrimidin-2(*1H*)-ones from biorenewable furfurals.

Reaction Conitions: substituted furaldehyde (0.502 g), ethyl acetoacetate (1 eq.), urea (1.5 eq.), GAAS (25 mol%), 60 °C, 6 h.

The synthesis of 3,4-dihydropyrimidin-2(1H)-thiones from 5-substituted-2-furaldehydes was attempted next by replacing urea with thiourea (Table 4.2).

Table 4.2 The synthesis of 3,4-dihydropyrimidin-2(*1H*)-thiones from biorenewable furfurals.

Entry	Starting material	Product structure and code	Yield (%)
1	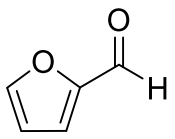 **1a**	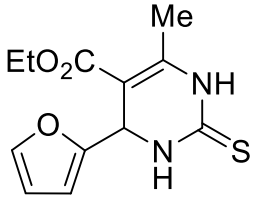 **4f**	85

2	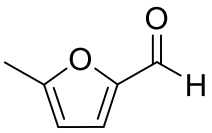 **1b**	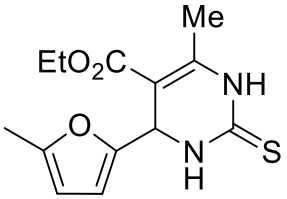 **4g**	70
3	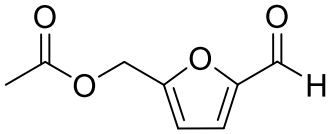 **1c**	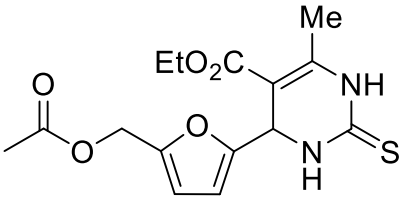 **4h**	67
4	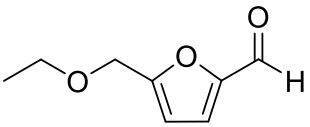 **1d**	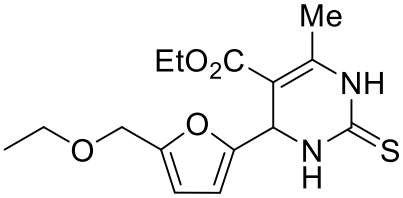 **4i**	64
5	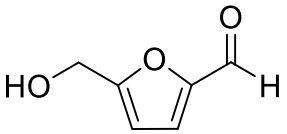 **1e**	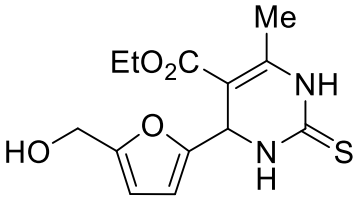 **4j**	60

Reaction conditions: furfuraldehyde (0.502 g), ethyl acetoacetate (1 eq.), thiourea (4 eq.), GAAS (50 mol%), 80 °C, 12 h.

However, only a 30% yield of 4f was obtained under the previously optimized molar ratio or reagents due to the faster decomposition of thiourea under the reaction conditions. Excess thiourea (4 equiv) had to be used to compensate for the decomposition of thiourea during the reaction, but less yield of 4f was observed (~30%) under identical conditions (60 °C, 6 h, 25 mol% GAAS) due to slower kinetics. The use of a 1:1:4 molar ratio between furfural(s), ethyl acetoacetate 2, and thiourea 3b gave 85, 70, 67, 64, and 60% yields of **4f, 4g, 4h, 4i,** and **4j** from 1a, 1b, 1c, 1d, and 1e, respectively, by performing the reaction for 12 h at 80 °C using 50 mol % GAAS as the catalyst. The proposed mechanistic pathway is shown in scheme 4.2.

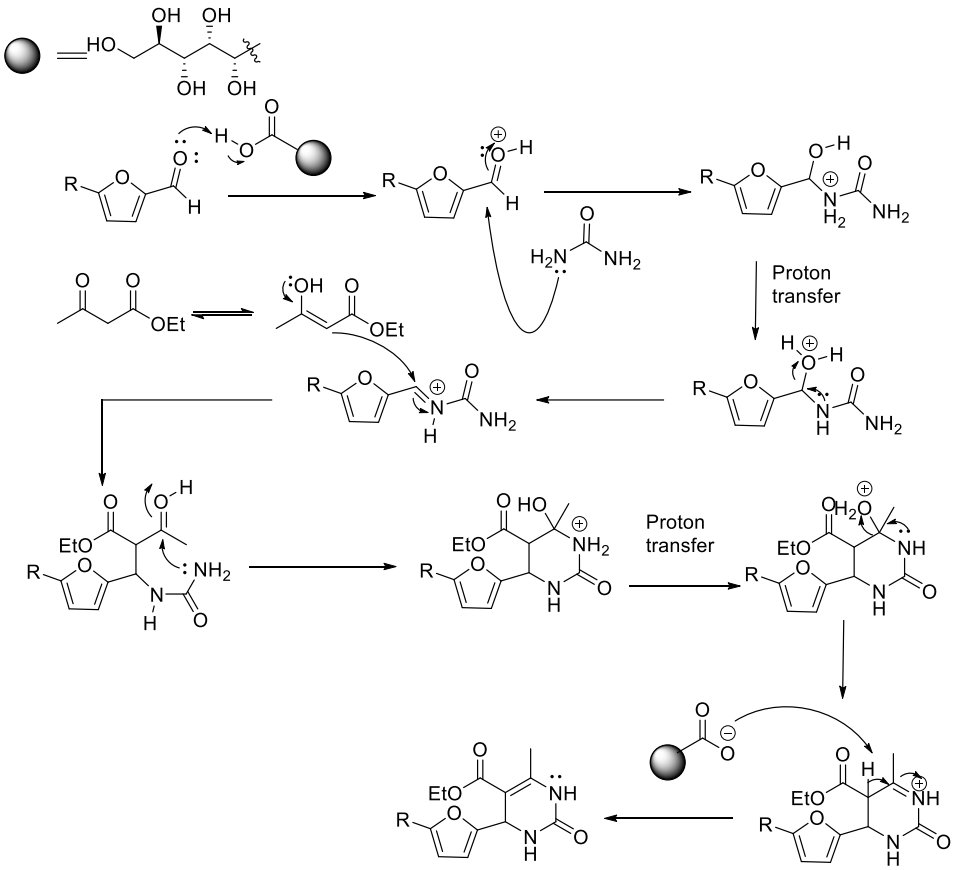

Scheme 4.2 Proposed mechanism of forming Biginelli products from 5-substituted-2-furaldehydes catalyzed by gluconic acid aqueous solution.

A similar catalyst system was used for synthesizing 1,4- dihydropyridines using the Hantzsch condensation protocol (Figure 4.10). When a 1:2:1.5 molar ratio of 1a, ethyl acetoacetate 2, and ammonium acetate 5 was used, the reaction was completed within 3 h at 60 °C and 97% of **5a** was isolated. Using similar reaction conditions, 85, 90, 89, and 84% of **5b, 5c, 5d**, and **5e** were isolated from 1b, 1c, 1d, and 1e, respectively. The proposed mechanistic pathway is shown in scheme 4.3

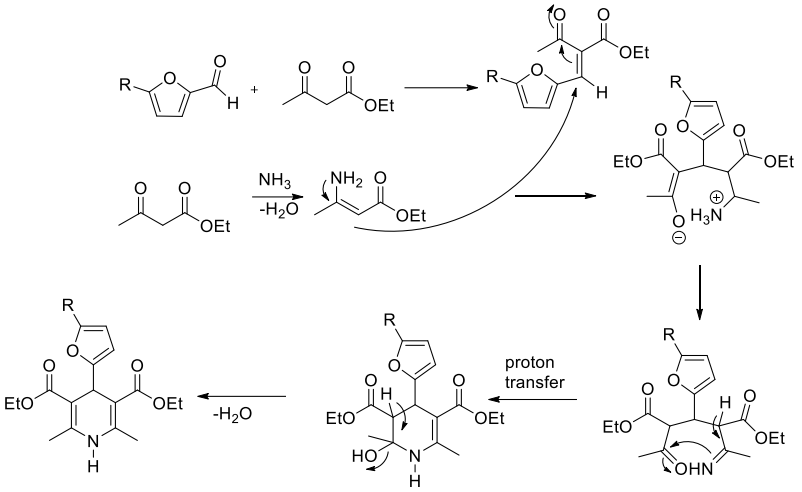

Scheme 4.3 Proposed mechanism for Hantzsch product formation starting from 5-substituted-2-furaldehydes using gluconic acid aqueous solution as the catalyst.

We envisaged that using the ammonium salt of gluconic acid would improve the atom economy of the process. When using ammonium acetate as the reagent, the incorporation of ammonia in the Hatzsch product leaves an acetic acid impurity in GAAS, whereas the use of aqueous ammonia keeps gluconic acid unadulterated. However, when ammonium gluconate was used as the reagent to prepare **5a**, the reaction did not proceed appreciably even after 6 h at 60 °C. However, performing the reaction at 90 °C for 12 h afforded a 70% yield of **5a**. The observation may be justified by the high stability of ammonium gluconate. Finally, the recyclability of the GAAS catalyst for the synthesis of the Biginelli product **4a** was also studied using optimized reaction conditions. The reaction was performed with a 1:1:1.5 molar ratio of 1a, 2, and 3a. After the reaction, the reaction mixture was quenched in ice water, and precipitated **4a** was recovered by vacuum filtration. The minor organic-soluble impurities in the aqueous layer were removed by extracting with chloroform. The water layer was then evaporated to dryness under a controlled vacuum to get gluconic acid as a white solid. The concentration was finally adjusted to 50% by adding the required amount of deionized water and used for the next catalytic cycle. The isolated yield of **4a** with the fresh GAAS catalyst was 88%. The yield of **4a** dropped to 77% after the first cycle, which may be responsible for organic contamination during the recovery. Interestingly, the yield of **4a** remained 72−74% until the fourth recycle.

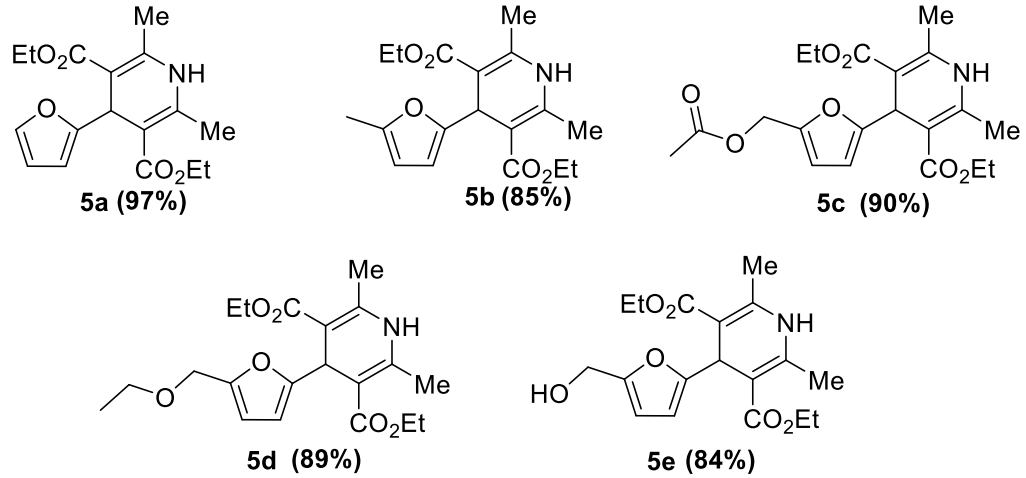

Figure 4.10 Synthesis of 1,4-dihydropyrimidines from biorenewable furfurals.
Reaction Condtions: 5-substituted-2-furfuraldehyde (0.502 g), ethyl acetoacetate (2 eq.), ammonium acetate (1.5 eq.), GAAS (25 mol%), 60 °C, 3 h.

4.5 CONCLUSION

In summary, novel 3,4-dihydropyrimidin-2(1H)-ones, 3,4- dihydropyrimidin-2(1H)-thiones, and 1,4-dihydropyridines have been synthesized from carbohydrate-derived 5-substituted-2-furaldehydes in good to excellent isolated yields following the Biginelli and Hantzsch reaction protocols, respectively. The gluconic acid aqueous solution proved to be an excellent catalyst and reaction medium that is renewable, nontoxic, inexpensive, and recyclable. The reactions were completed within 6 h at 60 °C using equivalent or only slight excess of the reagents. The optimized conditions were then applied on 10 g of furfural to demonstrate the scalability of the general synthetic protocol developed for both Biginelli and Hantzsch products. The gluconic acid aqueous solution catalyst was also successfully recycled and showed only a marginal dip in activity.

CHAPTER 5

CATALYTIC SYNTHESIS OF 5-(ACETOXYMETHYL)FURFURAL FROM FRUCTOSE IN ACETIC ACID MEDIUM USING A STRONG BRONSTED ACID CO-CATALYST

Abstract

5-(Acetoxymethyl)furfural (AcMF) has received significant attention as a hydrophobic, stable, and halogen-free congener of 5-(hydroxymethyl)furfural (HMF) for synthesizing various value-added chemicals. In this work, AcMF has been synthesized directly from fructose using strong Brønsted acid co-catalysts such as methanesulfonic acid (MSA), p-toluenesulfonic acid (PTSA), amberlyst-15 (A-15) and orthophosphoric acid (H_3PO_4) in conjugation with glacial acetic acid. The process was optimized for each catalyst to find the optimum reaction conditions for affording satisfactory yields of AcMF. The effect of reaction temperature, duration, loading of the substrate, and catalyst loading on the yield of AcMF were explored. Fructose provided a 51% isolated yield of AcMF at 100 °C and 45 minutes using MSA as a co-catalyst.

Graphical Abstract:

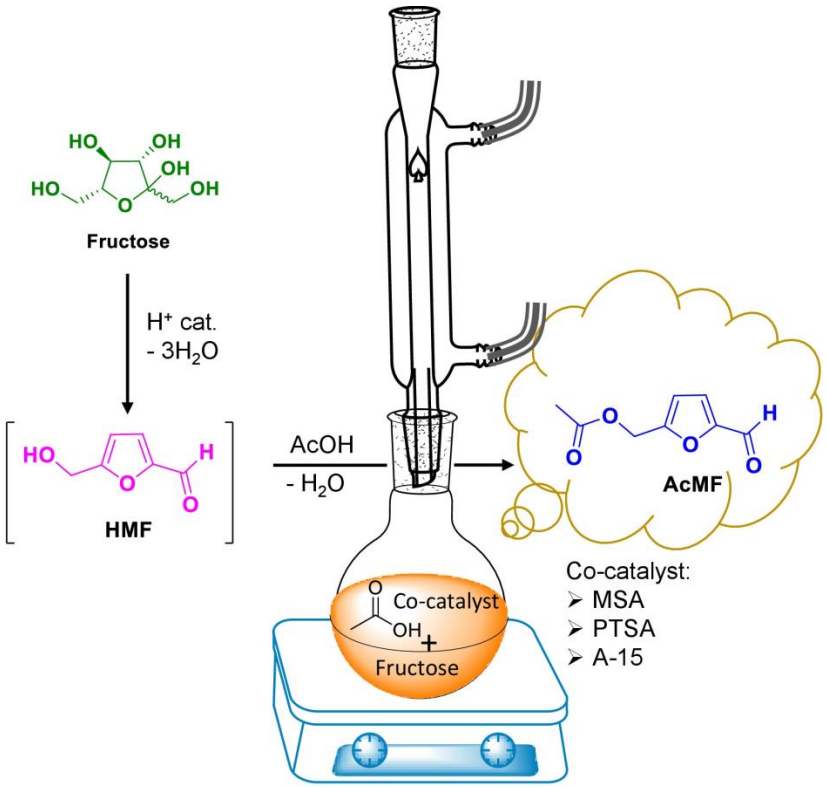

5.1 INTRODUCTION

5-(Hydroxymethyl)furfural (HMF), produced by the catalytic hydrolysis and dehydration of hexoses (e.g., glucose), is at the forefront of biorefinery research. HMF has been used as a platform chemical to synthesize renewable fuels, fuel

oxygenates, chemicals, and polymers. An acid catalyst of some sort is routinely used in the aqueous or polar reaction media to assist in the hydrolysis (in the case of polysaccharide starting material) and dehydration reactions. Decades of dedicated research on the production and derivative chemistry of HMF have produced extensive data that can be used for the commercial adoption of HMF in a carbohydrate-based biorefinery. However, some inherent properties of HMF continue to plague the scalability of its production and process economics. HMF is hydrophilic, unstable in aqueous acid, and thermally labile. This creates a paradoxical issue of maximizing the yield of HMF in the aqueous acid where it is unstable. The hydrophilic character makes it challenging to extract it into an organic solvent to phase-separate it from the aqueous acid and slow its decomposition. Regardless, HMF is typically formed in good to excellent yields from sugars like fructose using a special reaction medium like DMSO and an extracting organic solvent. Producing HMF in satisfactory yields from inexpensive feedstock like cellulose under economically and environmentally acceptable conditions remains challenging. Isolating HMF from the reaction medium as a hydrophobic, more stable congener is one technique to resolve this issue. As the hydrophobic congeners of HMF, the halogenated analogs such as 5-(Chloromethyl)furfural (CMF) and 5-(Bromomethyl)furfural (BMF) have demonstrated excellent potential. CMF and BMF, on the other hand, are produced using concentrated mineral acids and have halogen atoms in their moiety. Since the hydrophobic compounds formed by esterifying HMF with carboxylic acids do not contain any halogen atoms in their moiety and have greater hydrolytic stability than HMF, 5-(acyloxymethyl)furfurals (AMFs) are of special interest in this regard. Among AMFs, 5-(acetoxymethyl)furfural (AcMF) has received particular interest because the acetic acid required for its synthesis is stable, inexpensive, biogenic, and available on the bulk scale. With a suitable recycling strategy for acetic acid, the production of AcMF is expected to be economically competitive. Further, with high-energy content (8.7 KWh L^{-1}), which is nearly the same as gasoline (8.8 KWh L^{-1}) and significantly more than ethanol (6.1 KWh L^{-1}), AcMF could be a novel fuel additive (Krystof et al. 2013). AcMF was employed in synthesizing cartorimine, one of the medicines used to improve blood circulation, and is used as a component for the synthesis of therapeutic agents for osteoporosis. AcMF can virtually participate in

all major derivative chemistry of HMF. AcMF can be converted into various furanic derivatives such as 2,5-furandicarboxylic acid, 2,5-dimethylfuran, 2,5-dihydroxymethylfuran, 5-hydroxymethyl-2-furoic acid, and 5-formyl-2-furancarboxylic acid (Kang et al. 2015). AcMF performed better than HMF in Friedel-crafts reaction with mesitylene, xylene, and toluene in making novel diesel additives. Though there are several reports on the preparation of AcMF from HMF and CMF, there is no specific economic advantage (Kang et al. 2015). Direct preparation of AcMF from biomass-derived carbohydrates is important from an economic standpoint. In recent years, there has been significant development in the preparation of AcMF from monosaccharides and polysaccharides. In 2005, the dehydration of D-fructose in supercritical acetic acid was reported with 38% selectivity toward AcMF (Bicker et al. 2005). In a later report, stannic ion supported on montmorillonite clay (Sn-Mont) with both Lewis and Brønsted acidic sites as a heterogeneous catalyst resulted in 55% AcMF at 150 °C in 3 hours (Shinde et al. 2018). Very recently, a one-pot synthesis of AcMF preparation using anhydrous $ZnCl_2$ as a Lewis acid catalyst gave 80% yield from fructose in 6 h at 100 °C (Bhat et al. 2023). Nevertheless, there is still a need for active research in this field to investigate effective catalysts in conjunction with Brønsted acid (acetic acid) to generate AcMF in high yield and on a large scale for commercialization. Acetic acid with pKa value of 4.76 cannot alone catalyze the dehydration of fructose at a significant rate. In this regard, adding a strong Brønsted acid co-catalyst can accelerate the dehydration process. Therefore, acetic acid mostly assumes the role of a reaction medium and reagent, whereas the non-nucleophilic strong Brønsted acidplays the role of an acid catalyst.

In this study, the effects of various strong Brønsted acid co-catalysts (homogeneous and heterogeneous) on the yield of AcMF from fructose were studied in the glacial acetic acid medium. Strong Brønsted acid co-catalysts used in this study includemethanesulfonic acid (MSA), p-toluenesulfonic acid (PTSA), amberlyst-15 (A-15), and orthophosphoric acid (H_3PO_4). Other than these, choline chloride (ChCl) was also employed as a biorenewable ionic liquid to investigate its effect on the yield of AcMF. The reaction was optimized for each co-catalyst by varying parameters such as reaction temperature, duration, and loading of the catalyst.

5.2 EXPERIMENTAL SECTION

5.2.1 Materials

D-Fructose (98%) and silica gel (60-120 mesh) were purchased from Spectrochem. Sodium sulfate anhydrous (99%), sodium hydrogen carbonate, chloroform (99%), glacial acetic acid (99.5%), and ethyl acetate (99%) were purchased from Finar. All the reagents and solvents were used as received without additional purification.

5.2.2 Synthetic procedures

The round bottom flask was charged with D-fructose, acetic acid, and co-catalyst in an appropriate ratio and stirred magnetically in a pre-heated oil bath at the desired temperature. The reaction was conducted at reflux condition with the condenser connected to a round-bottomed flask. After the reaction, the round bottom flask was cooled to room temperature and diluted slightly with the chloroform. This diluted mixture was added dropwise to the saturated sodium bicarbonate solution. The chloroform layer was then separated from the aqueous layer and evaporated under pressure to produce crude AcMF. The crude sample was then passed through a small plug of silica to obtain the pure AcMF. Alternatively, the solution was distilled under a vacuum to remove acetic acid and water. Then, the reaction was diluted with water and extracted with chloroform.

5.3 CHARACTERIZATION OF SYNTHESIZED AcMF

5.3.1 The FTIR, ^{1}H-NMR, and ^{13}C-NMR of AcMF

^{1}H-NMR ($CDCl_3$, 300 MHz, RT) δ (ppm): 9.58 (s, 1H, -CHO), 7.17 (d, 1H, furyl-CH), 6.55 (d, 1H, furyl-CH), 5.07 (s, 2H, -OCH_2-), 2.05 (s, 3H, -$COCH_3$); ^{13}C-NMR ($CDCl_3$, 75 MHz, RT) δ (ppm): 177.8, 170.3, 155.4, 152.8, 121.8, 112.6, 57.8, 20.6; FTIR (ATR, cm^{-1}): 3124 (furanic –CH stretching frequency), 2923-2847 (-CH stretching frequency), 1744 (-$COOCH_3$), 1679 (-CHO), 1224 (C-O stretching frequency).

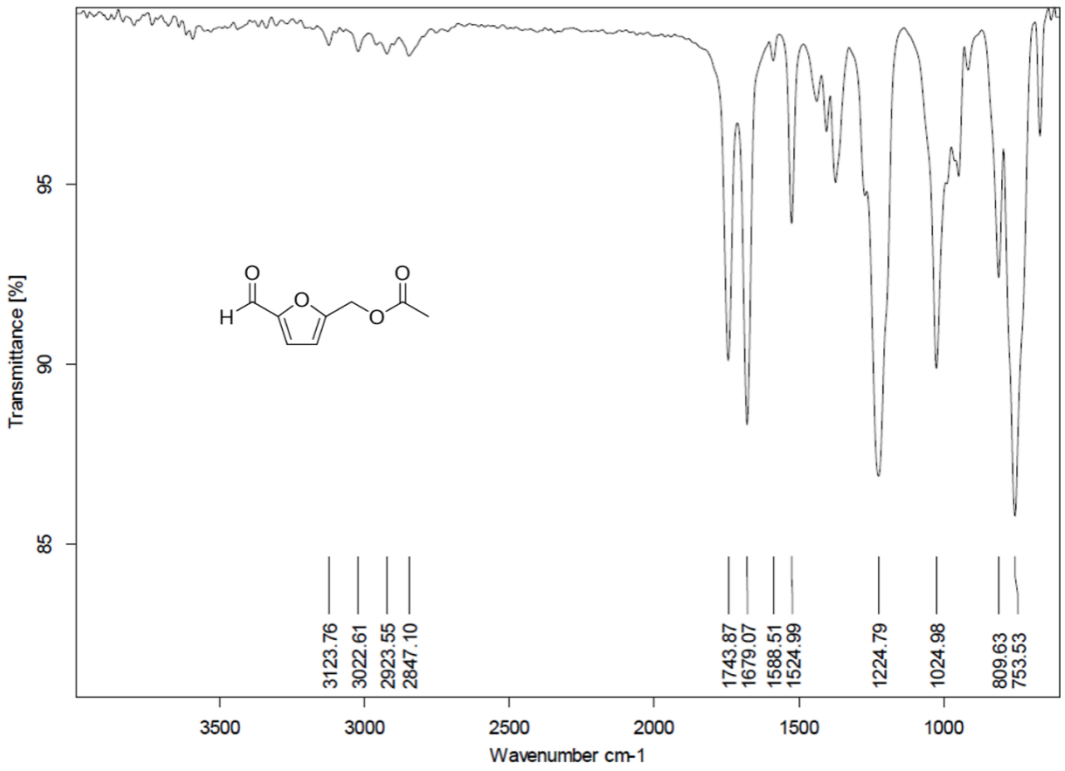

Figure 5.1 The FTIR spectrum of AcMF.

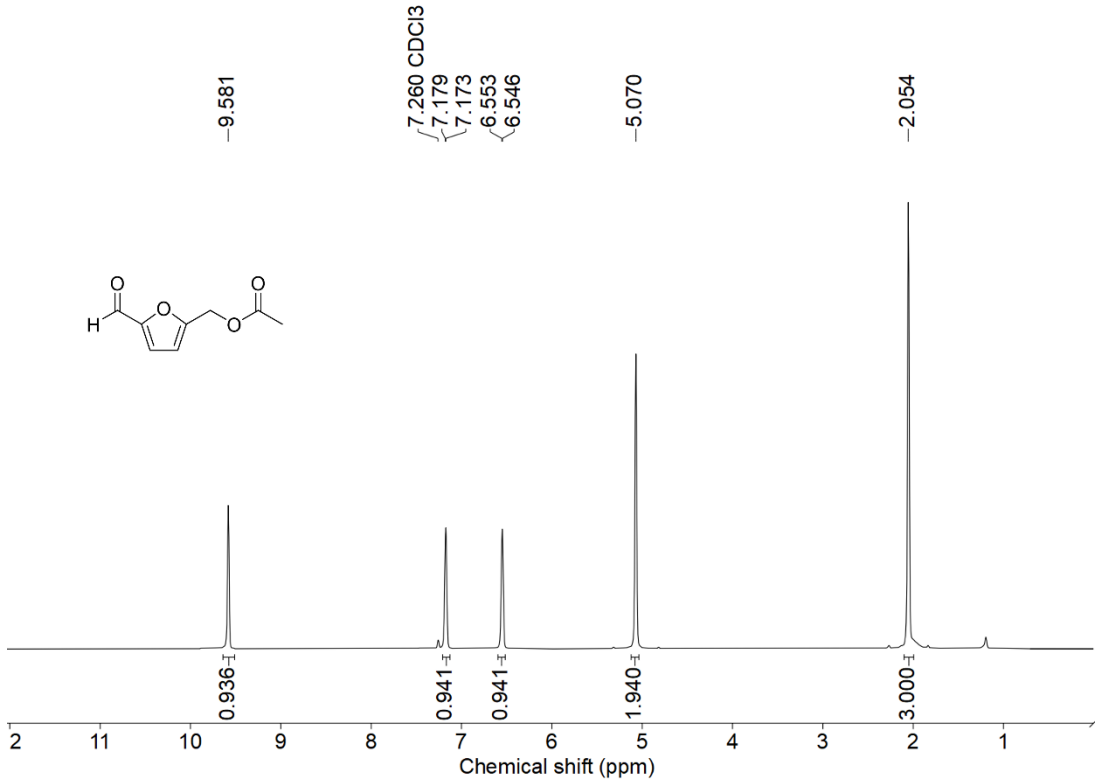

Figure 5.2 The ^{1}H-NMR spectrum of AcMF (solvent: $CDCl_3$).

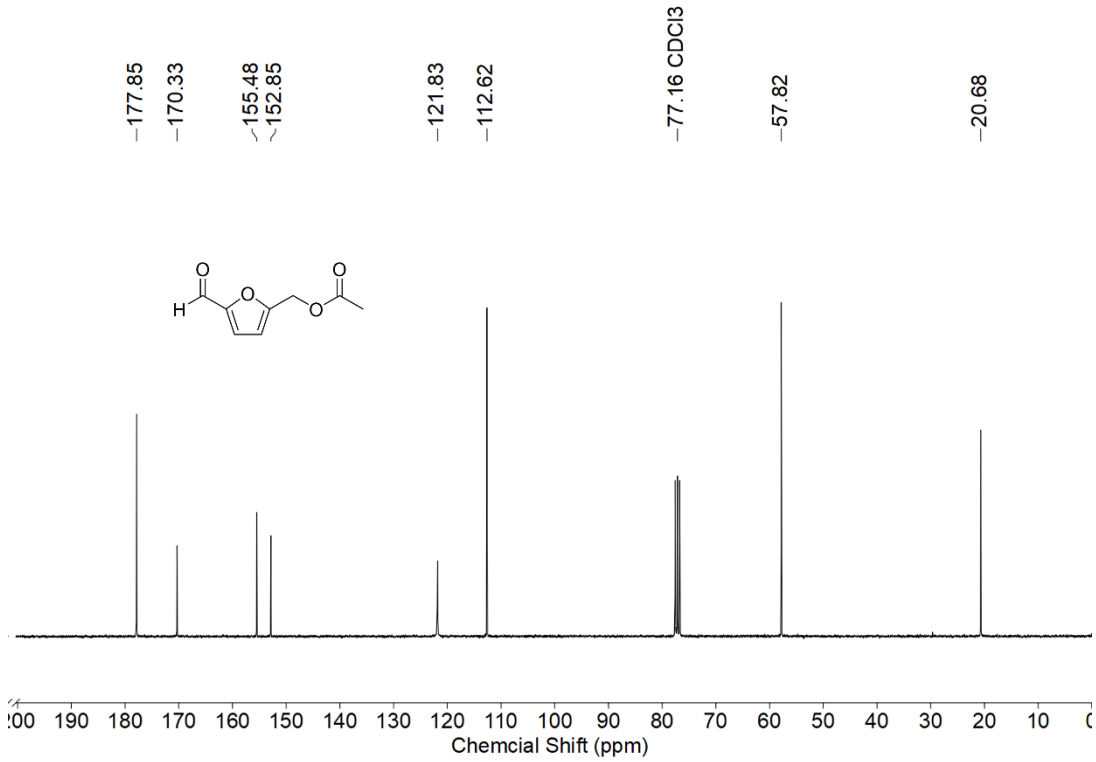

Figure 5.3 The ^{13}C-NMR spectrum of AcMF (solvent: $CDCl_3$).

5.4 RESULTS AND DISCUSSION

The dehydration of fructose has been investigated to improve the yield of AcMF using different Brønsted acid co-catalysts such as MSA, PTSA, A-15, and H_3PO_4. The results are depicted in the bar graphs. The control reaction in the presence of glacial acetic acid gave only a 10 % yield of AcMF when the reaction was carried out at 100 °C for 6 h. The reaction was first optimized for MSA. The initial reaction was performed at 100 °C for 6 h using MSA as a co-catalyst in the glacial acetic acid medium gave only an 8% yield. A significant amount of humin formation was apparent. Therefore, the reaction duration was periodically decreased for process optimization (Figure 5.4). When the reaction was performed for only 45 min, a 51% yield of AcMF was ensured. The effect of reaction temperature on the yield of AcMF has been shown in Figure 5.5. The maximum yield of AcMF was obtained at 100 °C with a duration of 45 min. Further, the temperature scan was done for 1.5 h, as shown in Figure 5.6, but the yields of AcMF were unsatisfactory (<40%). Therefore, under optimized reaction conditions (100 °C, 45 min), a 51% yield of AcMF was achieved. Interestingly, an increase in the co-catalyst loading and acetic acid amount did not increase the yield of AcMF to any noticeable extent. When a 90% acetic acid aqueous

solution was employed instead of glacial acetic acid, the yield of AcMF drastically reduced to 32%. This result may be explained by the hydrolysis of AcMF into HMF or poor esterification of HMF into AcMF.

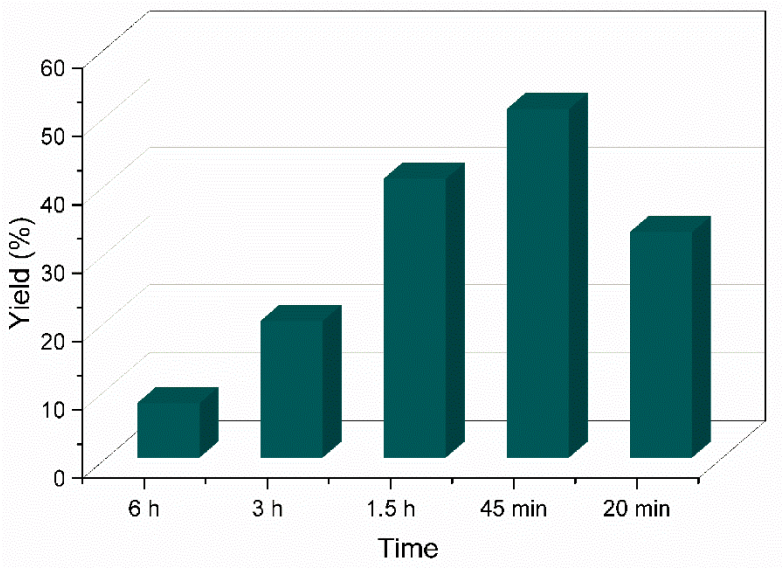

Figure 5.4 Synthesis of AcMF using MSA at different time interval at 100 °C.
Reaction Conditions: Fructose (1 g), MSA (1 mL), acetic acid (10 mL), 100 °C.

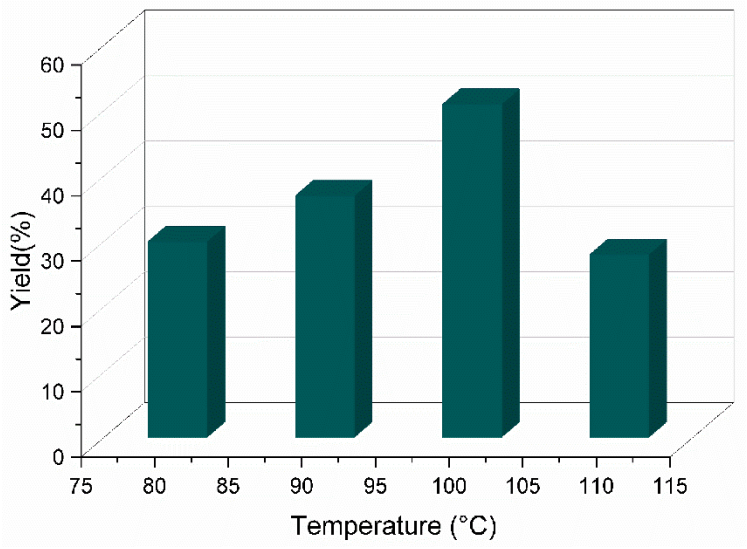

Figure 5.5 Synthesis of AcMF using MSA at different temperature at 45 min.
Reaction Conditions: Fructose (1 g), MSA (1 mL), acetic acid (10 mL), 45 min.

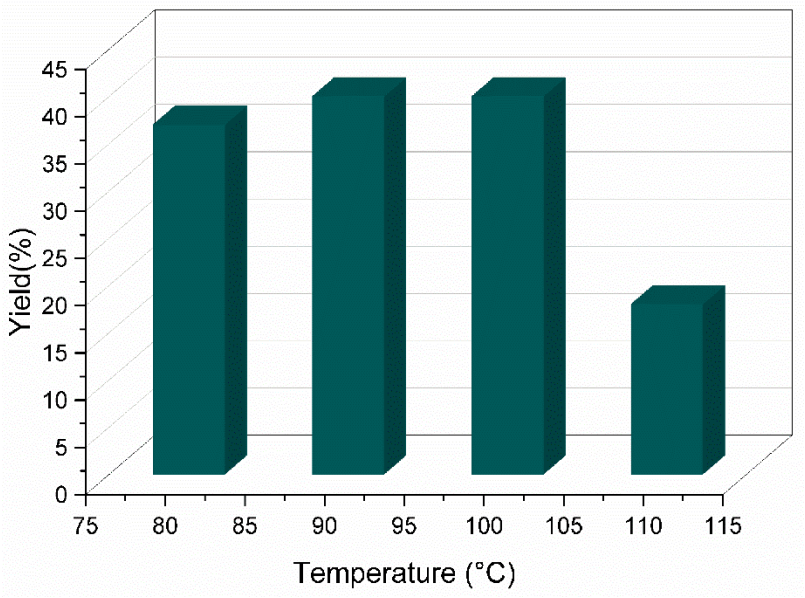

Figure 5.6 Synthesis of AcMF using MSA at different temperature at 1.5 h.

Reaction Conditions: Fructose (1 g), MSA (1 mL), acetic acid (10 mL), 1.5 h.

The lower yield at lower temperatures was attributed to the incomplete conversion of the fructose. At very high temperatures, the yield of AcMF decreased due to increased humin production. Next, PTSA was used as the co-catalyst to investigate its influence on the yield thoroughly.

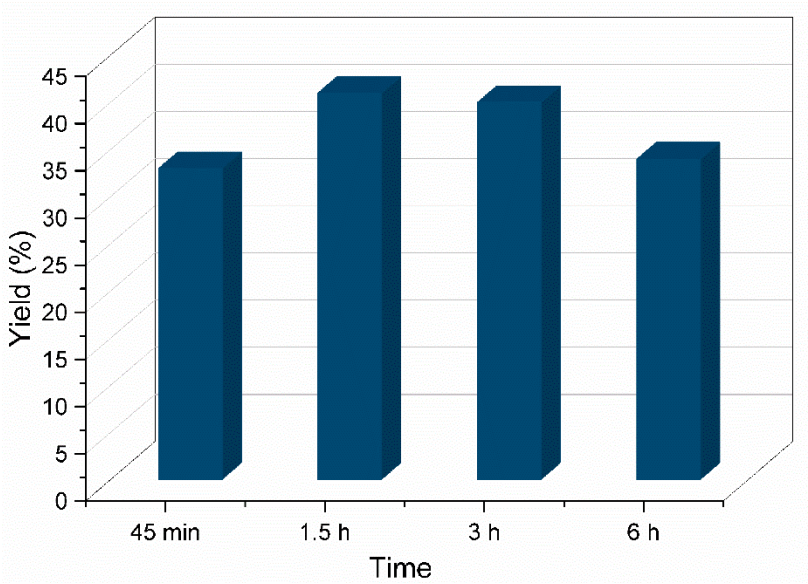

Figure 5.7 Synthesis of AcMF at different time intervals using PTSA at 100 °C.

Reaction Conditions: Fructose (1 g), PTSA (0.25 g), acetic acid (10 mL), 100 °C.

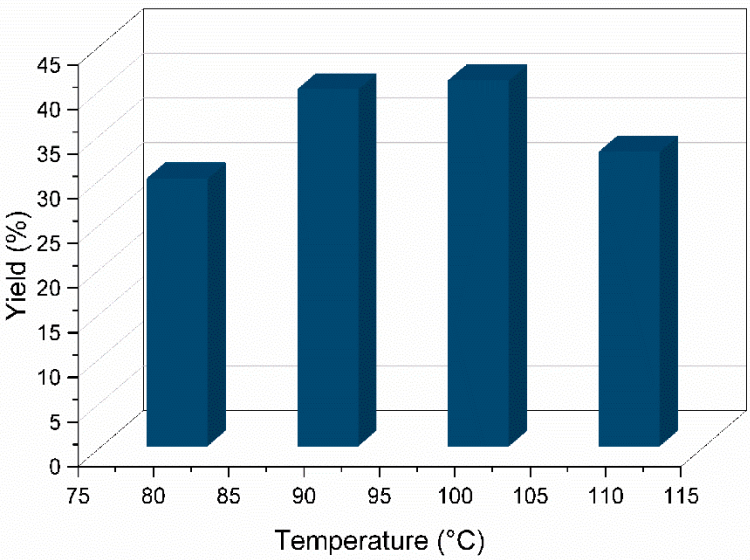

Figure 5.8 Synthesis of AcMF at different temperatures using PTSA as the co-catalyst and the reaction duration fixed at 1.5 h.

Reaction Conditions: Fructose (1 g), PTSA (0.25 g), acetic acid (10 mL), 1.5 h.

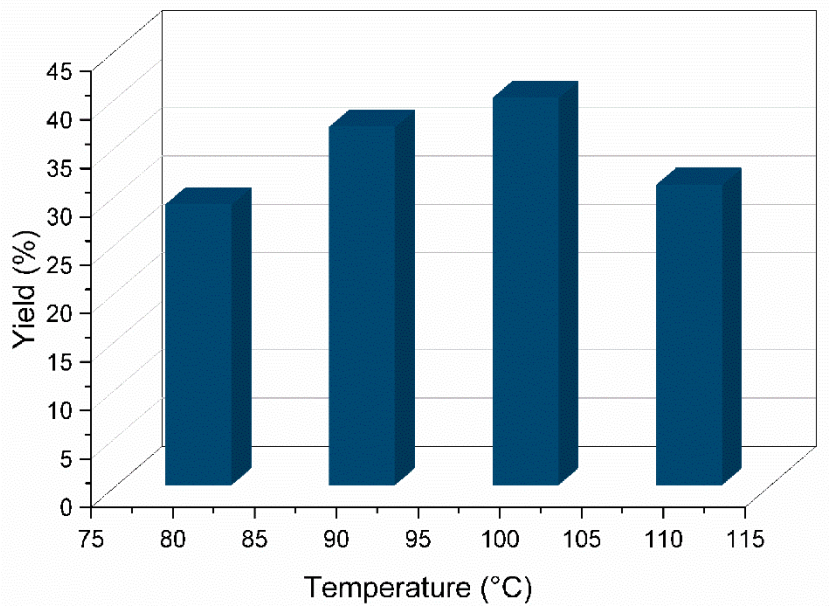

Figure 5.9 Synthesis of AcMF at different temperatures using PTSA as the catalyst and 3 h duration.

Reaction Conditions: Fructose (1 g), PTSA (0.25 g), acetic acid (10 mL), 3 h.

At 100 °C, PTSA gave 33%, 41%, 40%, and 34 % yield of AcMF at 45 min, 1.5 h, 3 h, and 6 h, respectively (Figure 5.7). Therefore 1.5 h and 3 h were chosen as optimum times, and the reaction temperature was varied to find the optimum one. At 1.5 h, a 41% yield was obtained at 100 °C (Figure 5.8). Increasing or decreasing the

temperature led to a decrease in the yield. At 3 h, a maximum 40% yield was obtained again at 100 °C, and an increase or decrease in the temperature resulted in lower yields (Figure 5.9). Under optimized conditions (100 °C, 1.5 h), PTSA acted as an efficient co-catalyst and afforded a 41% yield of AcMF. PTSA (pKa: -2.8) is roughly ten times stronger acid than MSA (pKa: -1.86). However, the yield of AcMF using MSA is greater than that using PTSA. This is because, in the case of PTSA, a significant amount of humin formation was observed, leading to a decreased yield of AcMF. Other Brønsted co-catalysts such as H_3PO_4 and A-15 have also been tried. On optimization, fructose gave 30% yield using H_3PO_4, as co-catalyst (fructose (1 g), H_3PO_4 (1 g), acetic acid (10 mL), 110 °C, 3 h). Using A-15 as co-catalyst, 36% yield was obtained from fructose under optimized reaction conditions (fructose (1 g), A-15 (1 g), acetic acid (10 mL), 120 °C). The cocatalysts can be recycled after the reaction. On completion of the reaction, acetic acid was removed from the reaction mixture by vacuum distillation. The product was then extracted into an organic solvent, and the cocatalyst was extracted into the aqueous layer. The evaporation of water gives cocatalysts that can be used in a consecutive cycle.

Next, the AcMF yield using ChCl as a co-catalyst was investigated in glacial acetic acid. The initial reaction was carried out at 120 °C for 6 h and gave a 39% yield; therefore, the reaction time was extended to 10 h, which gave a 36% yield. Decreasing the time to 3 h gave a 30% yield (Figure 5.10). The effect of reactiontemperature on the yield of AcMF with a fixed duration of 6 h is shown in Figure 5.11. When ChCl was used as the co-catalyst (not a Brønsted acid), the yield of AcMF reached 39% after 6 h reaction at 120 °C.

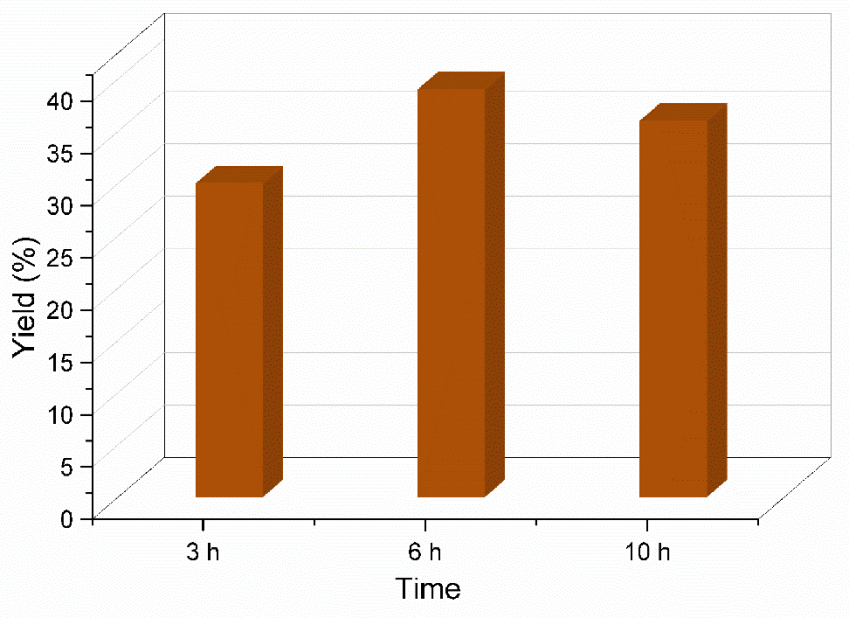

Figure 5.10 Synthesis of AcMF using ChCl at 120 °C at different time intervals.

Reaction Conditions: Fructose (1 g), ChCl (1 g), acetic acid (10 mL), 120 °C.

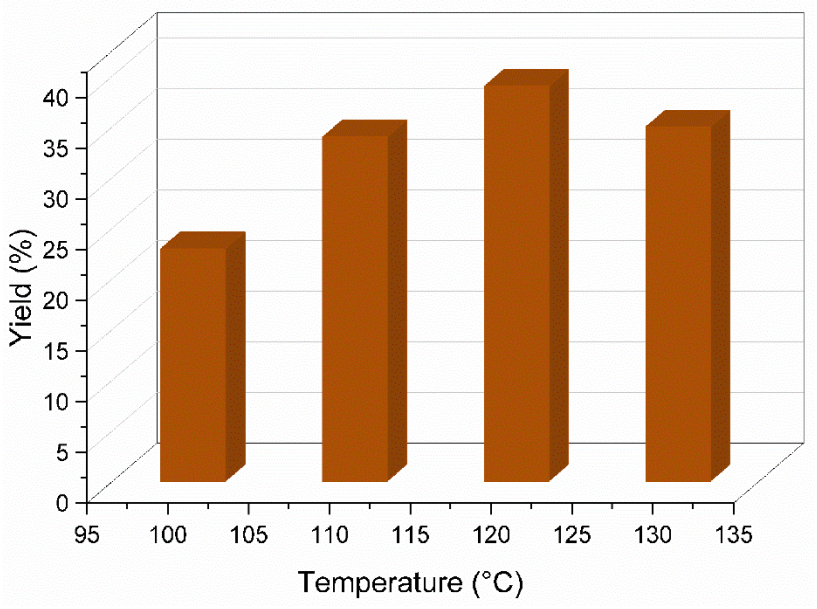

Figure 5.11 Synthesis of AcMF using ChCl at 6 h using a range of reaction temperatures.

Reaction Conditions: Fructose (1 g), ChCl (1 g), acetic acid (10 mL), 6 h.

5.5 CONCLUSION

Various Bronsted acid co-catalysts, both homogeneous and heterogeneous, have been screened for producing AcMF from fructose using glacial acetic acid as the reaction medium. MSA showed the best results compared to all other Brønsted co-

catalystsstudied and up to a 51% isolated yield of AcMF under optimized reaction conditions. Homogeneous acid co-catalysts, such as MSA and PTSA, required nearly 90-100 °C to get acceptable yields of AcMF. Heterogeneous acid catalysts, such as A-15, required elevated reaction temperature for faster kinetics. Choline chloride also promoted the dehydration reaction and made AcMF faster than the control reaction (glacial acetic acid alone), but the yield of AcMF remained low.

CHAPTER 6

ACTIVATED CARBON FROM CASHEW NUT HUSK AND CASHEW NUT SHELL WASTES: SYNTHESIS, CHARACTERIZATION, AND ADSORPTION STUDIES

Abstract

Activated carbon (AC) is a key material in numerous industrial applications, including wastewater treatment, catalysis, personal care products, and the pharmaceutical industry. Producing AC from waste biomass is of much interest since the environmental footprint is low and the economics are favorable for most applications. Cashew nut husk (CNH) and cashew nut shell (CNS) are typically considered wastes in the cashew nut processing industry. Synthesis of AC from CHN and CNS allows value addition of these materials and improves the economic prospects of the cashew nut processing industry. Herein, we report the production of AC by carbonization of CNH and CNS using orthophosphoric acid as the activating agent. The results showed that 700 °C is a suitable activation temperature for CNH, whereas 500 °C was enough for activating CNS. The AC samples were extensively characterized by FTIR, PXRD, BET, and FESEM-EDX analysis. The AC produced from CNH at 700 °C (H-700) exhibited very high specific surface area and iodine number of 1511.09 m^2/g and 961 mg/g, respectively. Therefore, H-700 was used for adsorbing methylene blue from water as a model for wastewater treatment. The H-700 sample showed an adsorption capacity of 520 mg/g with good recyclability up to five cycles.

Graphical abstract:

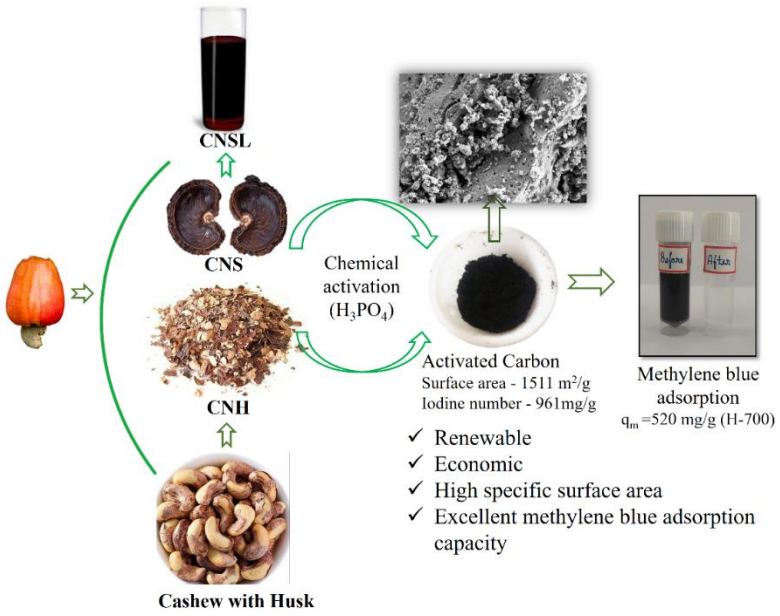

6.1 INTRODUCTION

The past several years have seen dedicated research for converting biomass wastes (e.g., agricultural residues) into sustainable fuels, chemicals, and materials (Rathore and Singh 2022). The advantage of this strategy is threefold: (1) mitigating the waste management issues, such as negative environmental impacts arising out of enormous quantities of biomass wastes, (2) reducing dependency on fossilized sources for sustainability, and (3) improving the economic feasibility of the industries that generated the biomass waste (Ubando et al. 2020). In this regard, India is the second-largest producer of cashew nuts in the world and one of the largest importers for its downstream processing (D'Silva 2021). As a cash crop and a food crop, cultivating cashew trees (*Anacardium occidentale*) is a major source of income in several low- to middle-income countries (Catarino et al. 2015). Technical grade cashew nut shell liquid, isolated from cashew nut shells (CNS), is a cardanol-rich non-food oil typically used as fuel, renewable chemical feedstock, and also for phenolic polymers (Kumar et al. 2018b; Lubi and Thachil 2000; Roy et al. 2022). Cashew nut husk (CNH), i.e., the tough outer cover of the cashew kernel and the de-oiled CNS, are treated as wastes and have only limited markets (Zafeer and Bhat 2023). Proximate analysis of CNS shows around 91% dry mass and 9% moisture. The dry mass contains crude protein (19.52%), crude fiber (18.82%), cellulose (28.08%), hemicellulose (16.94%), ether extract (2.33%), and ash (8.5%) (Bamgbola et al. 2020). CNH was found to contain interesting natural products, such as (+)-catechin, (-)-epicatechin, β-carotene, lutein, α-tocopherol, zeaxanthin, γ-topopherol, stearic acid, linoleic acid, and thiamine (Trox et al. 2011). Effective utilization of CNS and CNH will help cashew processing and related industries to be economically and environmentally more sustainable. The cost of AC derived from CNS has been projected to be lower than other crops, such as bamboo or coconut shells (Khang et al. 2020). Not surprisingly, several publications in recent years have attempted to convert CNS into activated carbon (AC) for high-value applications (Cai et al. 2020; Kumar et al. 2011; Spagnoli et al. 2017a). AC is an amorphous material with a highly developed porous structure, large specific surface area, chemical inertness, and good mechanical stability. It is a commonly used component for formulating and compounding various commodity chemicals and materials (Jiang et al. 2019; Sanchez

et al. 2020). The high adsorptive power of AC makes it desirable in wastewater treatment, air purification, energy storage, cosmetics, catalysis, and chemicals manufacturing industries (El maguana et al. 2020; Moral-Rodríguez et al. 2019). The chemical properties of AC depend on the residual surface functional groups originally present in the feedstock or developed during the carbonization and activation process (Vottero et al. 2022). more expensive, commercially available ACs Various chemical activating agents, such as $ZnCl_2$, H_3PO_4, K_2CO_3, and KOH, have been employed to synthesize AC of different porosities (Heidarinejad et al. 2020). AC is classified based on the average pore diameter (micro<2 nm, meso~2-50 nm, macro>50 nm (Khamkeaw et al. 2020). The physicochemical characteristics and adsorption strength of the synthesized AC samples depend on the type of precursor used, activating agents, the temperature of activation, and various other reaction parameters (Wan Daud et al. 2003). Carbonization induces primary porosity with fixed carbon content and reduction in volatile content while the activation process helps in the enhancement of specific surface area by creating new pores, expanding existing pores, and unlocking previously unreachable pores, resulting in AC as a highly porous solid material (Gao et al. 2020; Heidarinejad et al. 2020). A major application of AC is as an inexpensive solid adsorbent for removing organic contaminants (e.g., dyes) from industrial effluents (Khan et al. 2022). Methylene blue (MB), a cationic dye containing fused aromatic heterocycles, is used for staining cells, organic synthesis, and as medication for various health conditions (Patel et al. 2021). MB in textile wastewater is a serious health and environmental concern; therefore, it is routinely selected as the standard dye for developing processes for wastewater treatment (Khan et al. 2022; Mulushewa et al. 2021). AC derived from CNS has already been used for MB adsorption and has shown promising results (Kumar et al. 2011).

However, to our knowledge, there is no literature report on preparing AC from CNH for MB adsorption. Moreover, the literature lacks comparative studies on the physicochemical and adsorption properties of AC derived from CNS and CNH. This study shows the preparation of AC from de-oiled CNS and CNH using H_3PO_4 as the chemical activating agent and compares their physicochemical characteristics and performance on MB adsorption from an aqueous solution. Four AC samples were prepared, two each from CNS and CNH, by choosing 500 °C and 700 °C as the

activating temperature. The AC samples were characterized by FTIR, PXRD, BET, FESEM, EDX, and Iodine number. The equilibrium adsorption capacity of the synthesized AC samples was determined using the Langmuir and Freundlich isotherm models. Structural features, such as pore size and volume, surface morphology, and elemental composition, were investigated to better understand the MB adsorption process.

6.2 EXPERIMENTAL SECTION

6.2.1 Materials

The CNH sample was procured from Kalbavi cashews, Karnataka, India. The de-oiled CNS was supplied by Mahalasa Impex, Manipal, Karnataka, Orthophosphoric acid (H_3PO_4, 85%), deionized (DI) water, and methylene blue (99%) were purchased from Loba Chemie Pvt. Ltd. Methanol (99.5%) was purchased from Finar chemical company. Iodine (sublimed) was purchased from Spectrochem. The carbonization and activation of CNH and CNS samples were carried out in a temperature-programmable muffle furnace. The chemicals were used as received without any further purification.

6.2.2 Preparation of AC from CNH and CNS

In a typical synthetic strategy, CNS or CNH (2.00 g) was intimately mixed with H_3PO_4 (85%, 4 g), i.e., 1:2 mass ratio (w/w), in a mortar and pestle and kept aside for soaking (2 h, RT) (Figure 6.1). The mixture was then transferred to a silica crucible and carbonized at 200 °C in the muffle furnace under flowing N_2 for 2 h. The carbonized sample was ground to a fine powder and was heated at the activation temperature (i.e., 500 or 700 °C) for 2 h under a nitrogen atmosphere in the muffle furnace. The crucible was cooled to RT, and the carbon sample was suspended in DI water (50 mL). The suspension was ultrasonicated for 1 h and filtered through a Whatman filter paper (grade 1) under reduced pressure. The ultrasonication and washing cycles were repeated until the pH of the filtrate increased to 7. The sample was dried at 80 °C in a hot-air oven for 24 h and then sonicated in methanol (20 mL) for 30 min for uniform dispersion. Methanol was then evaporated under reduced pressure, and the solid was dried at 150 °C in a muffle furnace for 24 h. The AC samples obtained by this process were then characterized. The AC samples were labeled based on the starting feedstock and activation temperature. AC samples

obtained from CNH and activated at 500 °C and 700 °C were named H-500 and H-700, respectively. Similarly, AC samples obtained from CNS were activated at 500 °C and 700 °C were named S-500 and S-700, respectively.

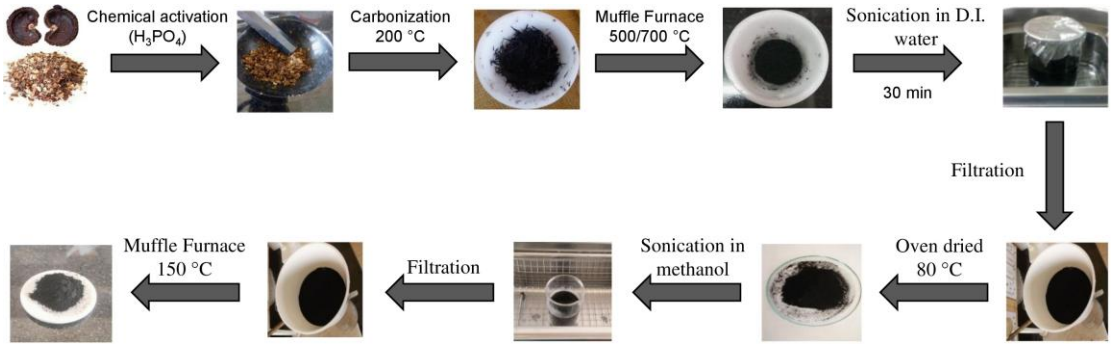

Figure 6.1 Synthesis of AC from CNS and CNH.

6.3 CHARACTERIZATION METHODS

Fourier-transform infrared spectroscopy (FTIR) spectra of the ACs were recorded on a Bruker Alpha 400 FTIR spectrometer using the KBr pellet technique in the 500-4000 cm^{-1} range with a scan rate of 4 scans/s. Powder X-ray diffraction (PXRD) patterns were recorded on RigakuMiniFlex 600 (Japan) X-ray Powder Diffractometer using Cu Kα radiation as the source. The surface morphology of the samples was investigated using field emission scanning electron microscopy (FESEM), Gemini 300, Carl Zeiss, operating at an accelerating voltage of 15 kV. Brunauer-Emmett-Teller (BET) surface area of the samples was measured using Autosorb IQ-XR-XR, Anton Paar, employing N_2 adsorption at 77 K. The pore size distribution of the samples was determined from nitrogen desorption isotherms using the Barrett-Joyner-Halenda (BJH) method. The absorbance of methylene blue was found using a UV-Visible spectrophotometer (model 2080) by Analytical Technologies Ltd.

6.4 RESULTS AND DISCUSSION

6.4.1 Physicochemical characterization

The AC samples named H-500, H-700, S-500, and S-700 were characterized by FTIR, PXRD, FESEM, and BET. Moreover, the quality (e.g., adsorption capacity) of the synthesized AC samples was estimated by measuring their iodine number (IN). As a widely used technique, IN is defined as the amount of iodine (in mg) adsorbed

per gram of a carbon sample. The IN of the synthesized ACs was determined according to ASTM D 4607-94 standards (ASTM-D4607-14R21 Standard test method for determination of iodine number of activated carbon, ASTM International, West Conshohocken, PA, 2021). The IN values of H-500, H-700, S-500, and S-700 were found to be 629 mg/g, 961 mg/g, 827 mg/g, and 738 mg/g, respectively. A high IN indicates a high surface area containing a micro- and mesoporous structure.

The FTIR spectrum showed a broad absorption band around 3449 cm^{-1}, characteristics of the stretching vibration band of the hydroxyl group from the surface bonded water (Figure 6.2). Small peaks at 2913 cm^{-1} and 2854 cm^{-1} are ascribed to asymmetric and symmetric C–H stretching vibrations. The peak at 1630 cm^{-1} is due to the O-H bending (scissoring) vibrations, and the peak around 1593 cm^{-1} corresponds to C=C stretching vibrations. The 1389 cm^{-1} absorption peak can be assigned to C–H bending vibrations.

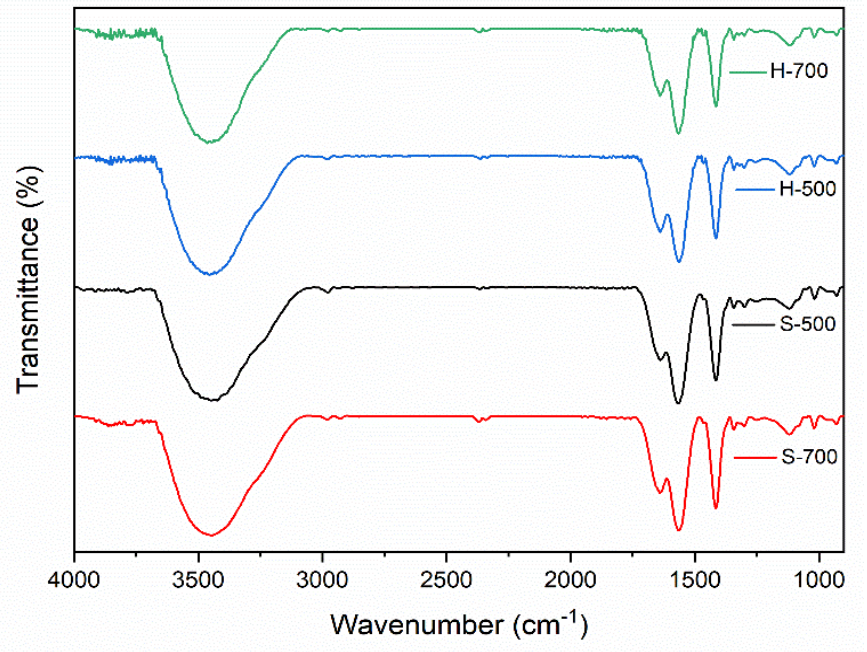

Figure 6.2 The FTIR spectrum of the synthesized AC.

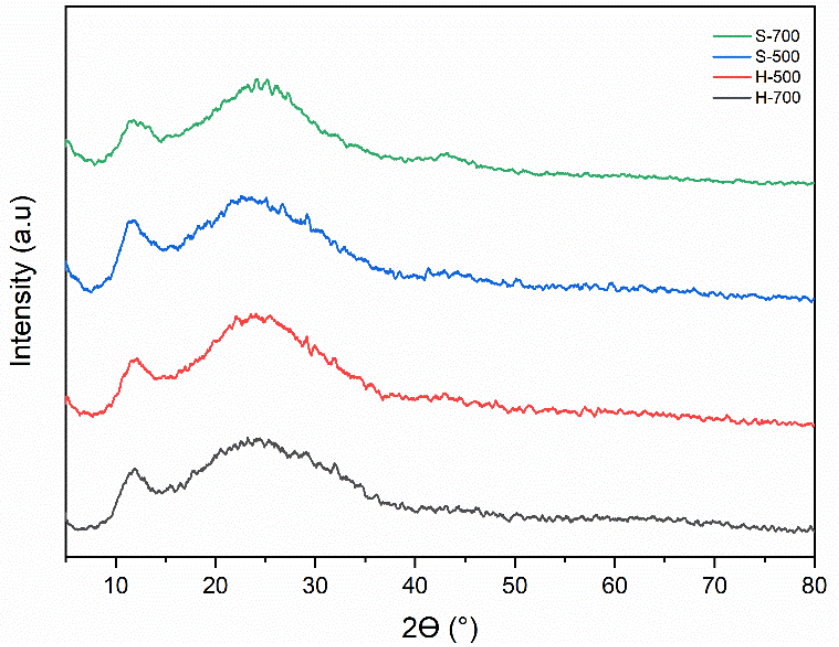

Figure 6.3 The PXRD patterns of AC from CNS and CNH.

PXRD is a technique used in materials science to determine the crystallographic structure of a material. The PXRD patterns of the ACs are shown in Figure 6.3. The broad diffraction peak at 2θ = 15-30° and 2θ = 40-50° can be attributed to the (002) plane and (101) plane reflecting the amorphous carbon nature (ICDD No. 41-1487) (Merin et al. 2021).

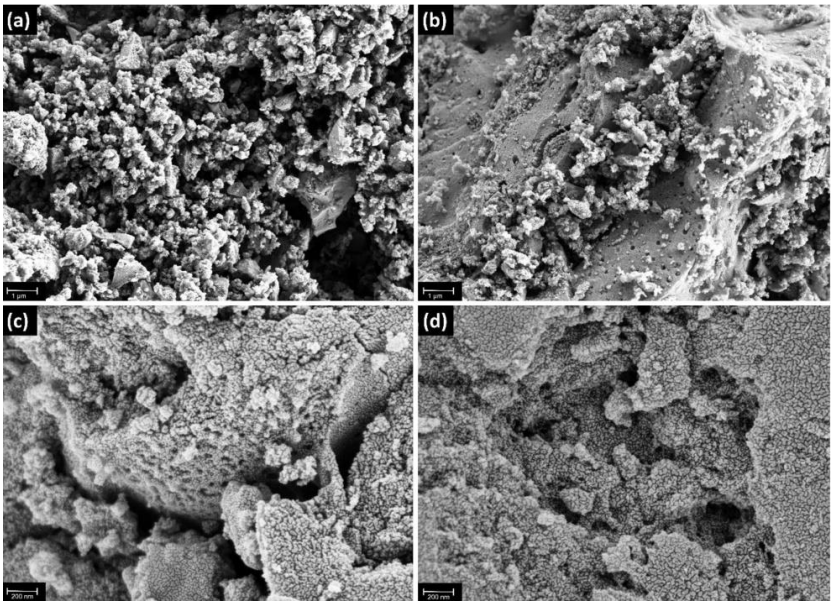

Figure 6.4 The FESEM images of (a) H-500, (b) H-700, (c) S-500, and (d) S-700

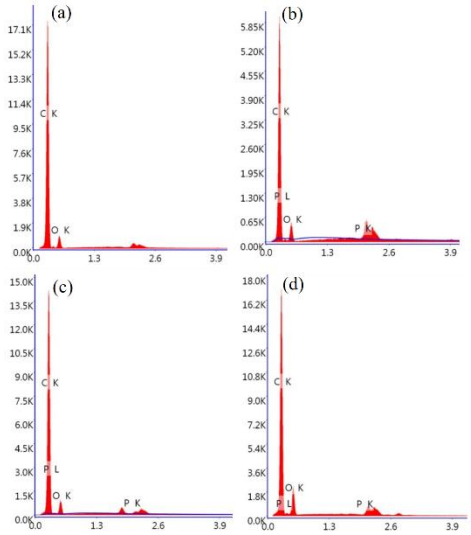

Figure 6.5 EDAX pattern of (a) H-500, (b) H-700, (c) S-500, and (d) S-700.

The surface morphology of the ACs was determined using FESEM analysis, as shown in Figure 6.4. The surface of the synthesized ACs was found to have a well-developed pore structure with an irregular surface. The elemental composition in the AC samples was confirmed by energy-dispersive X-ray analysis (EDX). The presence of a trace percentage of phosphorous was due to the incomplete washing of H_3PO_4 (Figure 6.5).

The porous structure and surface area of the synthesized ACs were characterized by nitrogen adsorption/desorption. The BET surface area of H-500, H-700, S-500, and S-700 was calculated to be 1100 m^2/g, 1511.089 m^2/g, 1432.47 m^2/g and 1323.22 m^2/g, respectively. All the samples show type IV adsorption isotherm (Figure 6.6), with hysteresis loop showing monolayer-multilayer adsorption with capillary condensation, characteristic of mesoporous materials according to the classification established by IUPAC (Sing 1985). From the BJH pore size distribution curves, the pore size ranged between 15 Å and 40 Å, and a distinct peak at 18.9 Å confirms that the materials are micro-mesoporous with pores of irregular shape and broad size distribution (Figure 6.7). The pore structure parameters are summarized in Table 6.1.

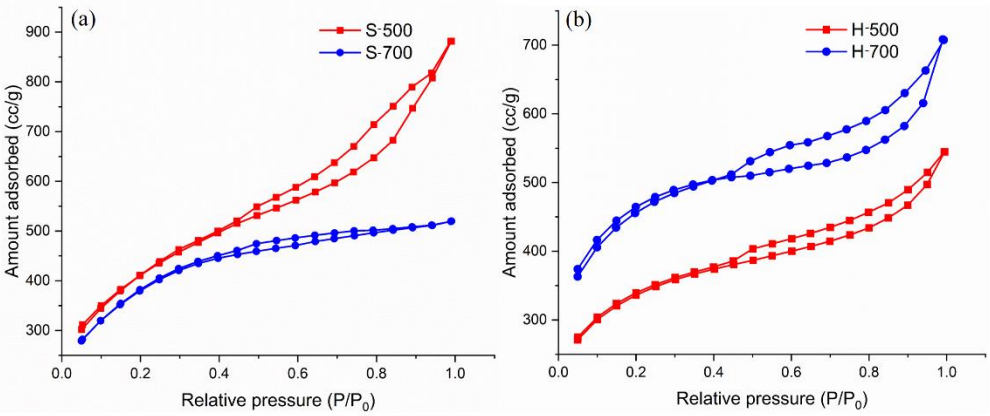

Figure 6.6 The N_2 adsorption isotherms of (a) S-500, S-700, and (b) H-500, H-700, samples of AC.

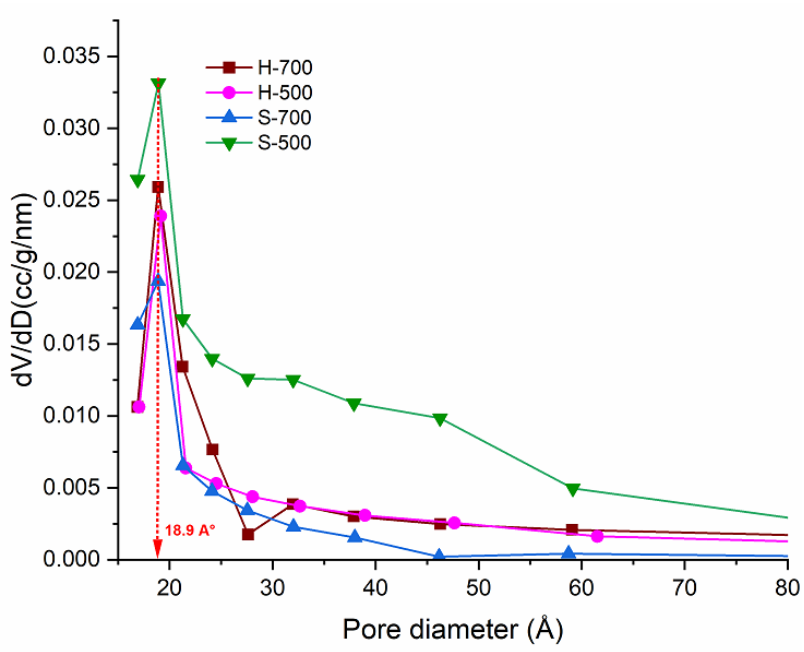

Figure 6.7 BJH pore size distribution curves of ACs.

Table 6.1 Pore structure parameters of ACs.

Sample	Iodine Number (mg/g)	S_{BET} (m^2/g)	V_{total} (cc/g)
H-500	629	1100	0.349
H-700	961	1511	0.421
S-500	827	1432	0.806
S-700	738	1323	0.175

6.4.2 Methylene blue adsorption study

Adsorption experiments were performed on different initial concentrations of aqueous solution of MB, ranging from 250-600 ppm. In a typical experiment, H-700 (0.1 g) was suspended in a 100 mL solution of MB of desired initial concentration taken in an Erlenmeyer flask. The suspension was stirred magnetically (300 rpm) for 24 h at RT. After 24 h, the H-700 sample was removed by filtration, and the final concentration of MB in the filtrate was determined by absorption in a UV-Vis spectrophotometer. The photographs of MB solutions of various initial concentrations (before and after adsorption by H-700) are depicted in Figure 6.8. The amount adsorbed at equilibrium was calculated using the formula shown below.

$$q_e = \frac{(C_o - C_e)V}{m}$$

Where C_o and C_e (mg/L) are the initial and equilibrium concentration of MB solution before and after adsorption. Volume (*V)* of the solution (in Liter) and *m* is the mass of the H-700 sample used (in grams).

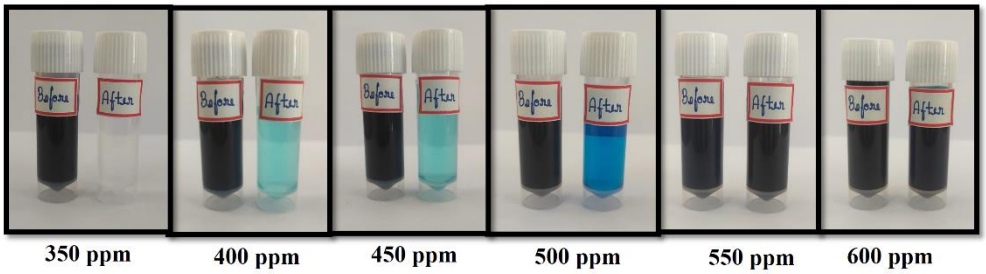

Figure 6.8 The MB solutions before and after adsorption using H-700 at different initial concentrations (350-600 ppm).

The percentage (%) removal of MB is calculated using the following expression:

$$\%\, removal\ of\ MB = \frac{(C_o - C_e)100}{C_o}$$

The H-700 sample was chosen for the MB adsorption study due to its high iodine number and specific surface area. Langmuir and Freundlich isotherm models were used to study the adsorption isotherm, and the isotherm parameters are listed in Table 6.2. Langmuir adsorption model depicts the adsorbate's monolayer adsorption

onto the adsorbent's surface with all the binding sites possessing the same affinity for adsorption and no molecular interaction between the adsorbed molecules.The linear form of the Langmuir isotherm equation is represented as:

$$\frac{C_e}{q_e} = \frac{1}{K_L q_m} + \frac{C_e}{q_m}$$

Where q_e is the quantity of MB adsorbed at equilibrium (mg/g), C_e is the equilibrium concentration of MB (mg/L), q_m and K_L are Langmuir constants related to maximum monolayer adsorption capacity and energy of adsorption, respectively. When C_e/q_e is plotted against C_e, a straight line with slope $1/q_m$ and intercept $1/K_L q_m$ was obtained (Figure 6.9), which showed that the adsorption of MB fits well with the Langmuir isotherm model. The values of q_m and K_L were calculated from the intercept and slope of the linear plot. The value of q_m, which represents the maximum monolayer adsorption capacity of H-700, was found to be 520 mg/g. The dimensionless equilibrium parameter R_L was calculated using the formula shown below:

$$R_L = \frac{1}{(1+K_L C_o)}$$

The value of R_L is known to represent the nature of adsorption (El Qada et al. 2006). When $0 < R_L < 1$, the adsorption is a favorable process. The adsorption would be unfavorable if $R_L > 1$, linear if $R_L = 1$, and irreversible if $R_L = 0$.

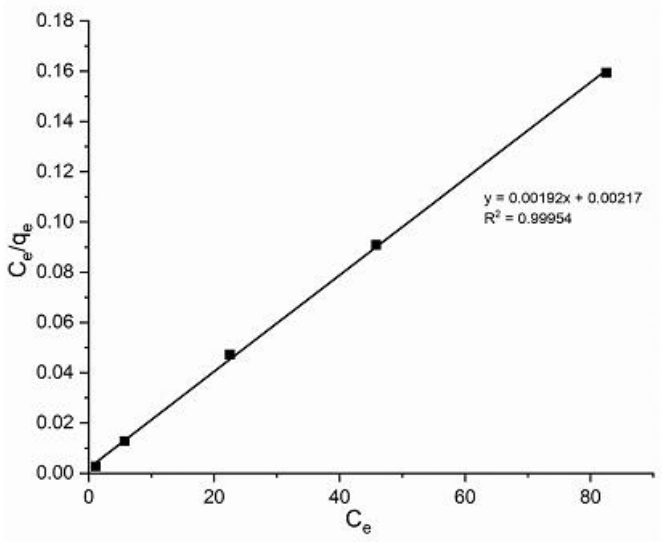

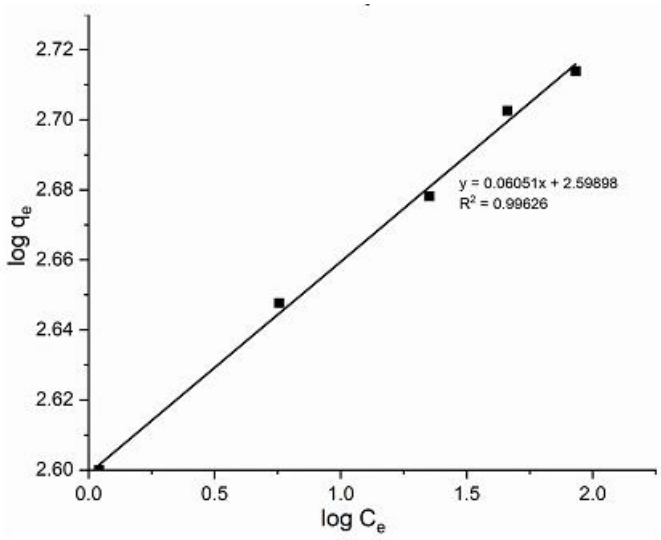

Figure 6.9 Linear plots of Langmuir (top) and Freundlich (bottom) adsorption isotherm for adsorption of MB from aqueous solution by the H-700 sample.

According to the Freundlich isotherm, adsorption takes place on the heterogeneous surface of the adsorbate with varying binding affinities. The linear equation is expressed as:

$$\log q_e = \log K_F + \frac{1}{n}\log C_e$$

K_F and 1/n are Freundlich constants related to the adsorption capacity and intensity of the adsorbent, respectively. The value of n was found to be greater than 1, which indicated a favorable physical process (Kang et al. 2018). The correlation coefficient (R^2) values of Langmuir and Freundlich adsorption isotherm are 0.99954 and 0.99656, respectively, indicating that both models fit well. To give a comparative study with the reported literature table 6.3 is provided.

Table 6.2 Langmuir and Freundlich parameters

Langmuir isotherm				**Freundlich isotherm**		
Q_m (mg/g)	K_L (L/mg)	R^2	R_L	K_F ((mg/g)·(L/mg)$^{1/n}$)	n	R^2
520.8	0.8848	0.99954	(0.002817-0.00188)	397.173	16.52619	0.99626

Table 6.3 Comparison of MB adsorption capacity with the previous literatures.

Feedstock and activation temperature	Activating agents	Methylene blue adsorption (mg/g)	References
CNS- 850 °C	KOH	68.72	(Kumar et al. 2011)
CNS- 500 °C	$ZnCl_2$	476	(Spagnoli et al. 2017b)
Rumex Abyssinicus - 600 °C	H_3PO_4	322	(Fito et al. 2023)
Waste mangosteen peels - 750 °C	$H_3PO_4/FeCl_3$	1362.06	(Fan et al. 2022)
Organge lemon peel – 600 °C	H_3PO_4	38	(Ramutshatsha-Makhwedzha et al. 2022)
Waste mangosteen peels - 450 °C	H_3PO_4	871.49	(Zhang et al. 2021b)
Myristica fragrans shell – 700 °C	KOH	346.85	(Mariana et al. 2021)
Moringa oleifera leaf – 350 °C	NaOH	136.99	(Do et al. 2021)
Cashew nut husk – 700 °C	H_3PO_4	520	This work

6.4.3 Effect of pH

The effect of pH on the adsorption capacity of MB by cashew nut husk-derived activated carbon was studied for the H-700 sample. The pH of the aqueous solution of MB was altered by the dropwise addition of either 0.5 N HCl or 0.5 N NaOH solution. As evident in Figure 6.10, the adsorption capacity of the H-700 sample increased noticeably at basic pH, whereas it decreased in acidic pH. The possible explanation can be based on the surface charge of the activated carbon sample. Zeta potential shows that the surface of H-700 and for S-500 samples were negatively

charged. The mean zeta potential value for the H-700 sample at pH 7 was -32.9 (±0.8) mV, whereas the same for the S-500 sample was -22.7 (±0.7) mV. The surface charge of H-700 at neutral pH was found to be negative and hence had an attractive interaction with the cationic MB dye. With increasing pH, the negative charge density on the surface increases more, leading to better adsorption of MB. At low pH, the H^+ ions compete with MB for adsorption on the active carbon surface. Moreover, the proximity of H^+ ions and cationic MB dye molecules on the surface of the H-700 sample introduces electrostatic repulsion between the adsorbed species. In contrast, the hydroxide ions on the surface at higher pH introduce attractive interaction with the MB dye molecules.

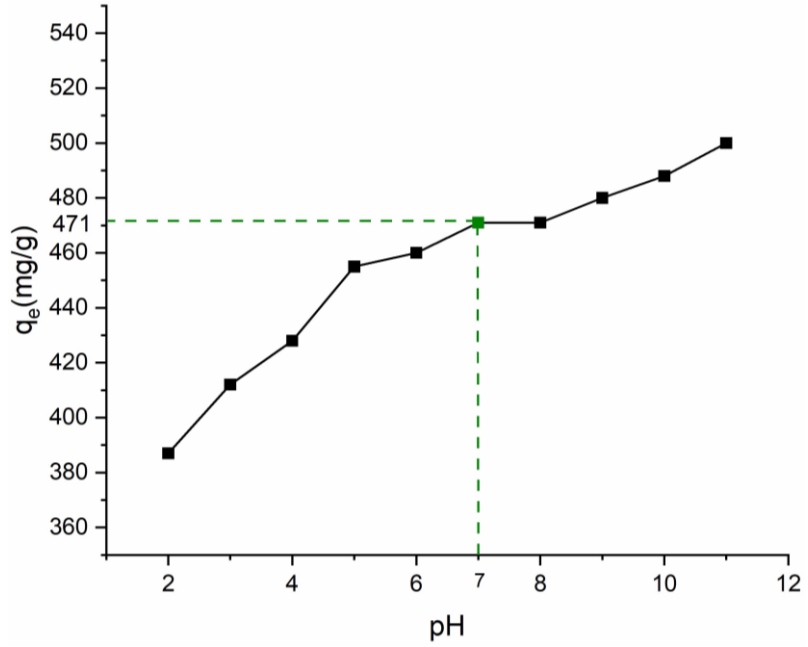

Figure 6.10 Effect of pH on the adsorption capacity of H-700. (C_o = 500 ppm, V = 100 mL, m = 0.1 g, t = 24 h)

The adsorption of MB on the surface of CNH and CNS-derived AC was attributed to the physical trapping in the pores and electrostatic interaction. Pore adsorption takes place as physisorption on the surface of the AC, which will substantially impact the dye adsorption. Due to the phosphoric acid activation, the porous structures of the AC were significantly improved with the increase in its specific surface area. An increase in microporous and mesoporous structures in AC results in better pore diffusion and adsorption. Electrostatic interaction is another mode of adsorption. The zeta potentials

of ACs at neutral pH were negative, while the MB was positively charged in the aqueous solution. Hence, electrostatic interaction between the negatively charged AC and positively charged MB dye molecule leads to the adsorption phenomenon. The adsorption of MB on the surface of CNH and CNS-derived AC was attributed to the physical trapping in the pores and electrostatic interaction. Pore adsorption takes place as physisorption on the surface of the AC, which will substantially impact the dye adsorption. Due to the phosphoric acid activation, the porous structures of the AC were significantly improved with the increase in its specific surface area. An increase in microporous and mesoporous structures in AC results in better pore diffusion and adsorption. Electrostatic interaction is another mode of adsorption. The Zeta potentials of ACs at neutral pH were negative, while the MB was positively charged in the aqueous solution. Hence, electrostatic interaction between the negatively charged AC and positively charged MB dye molecule leads to the adsorption phenomenon. The AC will be effective against other dye molecules too. The porous structure of activated carbon can potentially adsorb most organic dye molecules. However, the efficiency may vary depending on the pH of the solution. Furthermore, the literature reports say that surfaces of the AC in the alkaline solution are predominantly negatively charged and are highly efficient towards positive dye. In an acidic solution, the AC surface becomes positively charged and is efficient towards negative dyes according to the electrostatic adsorption mechanism (Fan et al. 2022; Ullah et al. 2022).

6.4.4 Recyclability

Recyclability of the adsorbent is crucial for practical application to reduce disposal issues of the deactivated adsorbent materials and the cost of replacing them. In this work, the H-700 sample was regenerated and recycled for five consecutive cycles of MB adsorption (Figure 6.11). The adsorbed MB on the surface of H-700 was successfully desorbed using methanol as the desorbing solvent. Only a marginal drop in the MB removal efficiency was observed after the fourth cycle of the adsorption-desorption process. In a typical experiment, the H-700 sample (20 mg) was added to the aqueous solution of MB (50 ppm, 100 mL) taken in an Erlenmeyer flask for stirred magnetically for 24 h at RT to attain equilibrium. The fresh H-700

sample displayed near quantitative removal efficiency of MB. The suspension was subjected to centrifugation to separate the used H-700 sample. The used H-700 sample was then washed with DI water (3×20 mL) and repeatedly refluxed in methanol (3×20 mL) to desorb MB. The H-700 sample was then filtered, washed with fresh methanol, dried in the air, and finally dried at 80 °C for 12 h in a hot-air oven. The recycled H-700 sample was then dried in a muffle furnace at 120 °C for 6 h before being used in the following adsorption cycle. Other than methanol, ethanol can be used with the same efficiency for desorption. Apart from the acute toxicity of methanol for human health, it is typically considered a green solvent for organic synthesis and other processes. Alternatively, other polar solvents, such as ethanol and ethyl acetate, may be used to desorb MB from the surface of AC samples. Photocatalytic degradation can also be employed to degrade the MB dye and desorb it from the surface of AC samples.

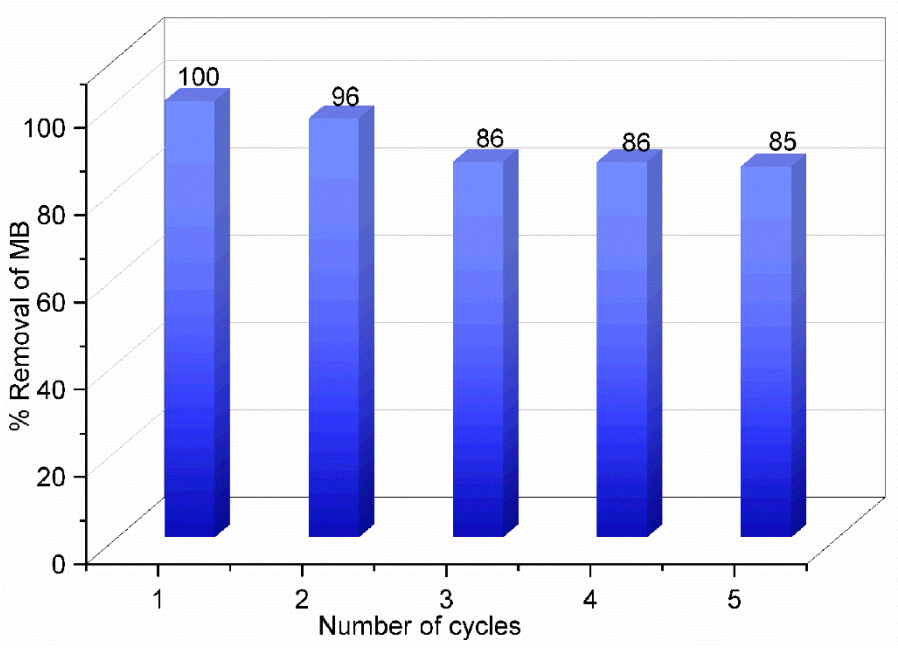

Figure 6.11 Reusability of H-700 towards MB removal (C_o= 100 ppm, V= 100 mL, m= 20 mg, t= 24 h).

6.5 CONCLUSION

CNS and CNH were used as sustainable feedstocks for preparing AC samples by carbonization using orthophosphoric acid as the chemical activating agent. An

activating temperature of 700 °C was found suitable for CNH, whereas the CNS sample was activated at 500 °C. The H-700 and S-500 samples showed a BET surface area of 1511 m^2/g and 1432 m^2/g, respectively. The samples were characterized by other spectroscopic and microscopy methods. The adsorption isotherm of H-700 for methylene blue adsorption showed the best fit for Langmuir isotherm (R^2= 0.9995). Adsorption and isotherm parameters of the synthesized AC samples showed excellent characteristics to be used as an adsorbent. The H-700 sample showed an excellent monolayer methylene blue adsorption capacity of 520 mg/g. The recyclability of the H-700 sample was also promising. The future study will explore the adsorption of other pollutants using ACs produced from CNH and CNS and their photodegradation as a working model for treating wastewater.

CHAPTER 7

SUMMARY AND CONCLUSIONS

The summary and significant findings of the current research study are included in this chapter. A brief description of the potential scope of future work is also included.

7.1 SUMMARY

- There has been significant research over the past few decades for producing furanic compounds from biopolymers and oligomers for their downstream synthetic transformation into value-added specialty chemicals.
- The present work attempted to produce structurally complex and densely functionalizedorganic molecules using the Morita-Baylis-Hillman reaction, Biginelli reaction, and Hantzsch reaction as green transformation. Glucose-derived gluconic acid was employed as a novel green catalyst for synthesizing 3,4-dihydropyrimidinones (DHPMs) and1,4-dihydropyridines (DHPs). 5-(Acetyloxymethyl)furfural (AcMF) was produced from fructose in the glacial acetic acid medium in the presence of a strong Brønsted acid co-catalyst. Activated carbon (AC) was produced from cashew nut shells and cashew nut husks as agricultural wastes using orthophosphoric acid as the chemical activating agent. The AC was then applied for methylene blue (MB) adsorption from the aqueous solution as a model for wastewater treatment.
- MBH reaction is a well-documents, one-pot, atom economic reaction that introduces significant molecular complexity into the MBH adduct. The MBH adducts have shown various pharmacological activities, so studying the substrate scope becomes extremely important. Further, producing renewable novel MBH adducts starting from biomass-derived furfural (FUR) and its 5-substituted analogs is extremely important to expand the derivative chemistry of the biorenewable furaldehydes. The carbohydrate-derived 5-substitued-2-furaldehydes were used as the aldehyde substrate in this work to produce novel MBH adducts. The 5-substitued-2-furaldehydes used in this work includes 5-(ethoxymethyl)furfural (EMF), AcMF, 5-(propionyloxymethyl)furfural (PrMF), 5-(butyryloxymethyl)furfural (BuMF), 5-(benzoyloxymethyl)furfural (BzMF), 5-[(4-nitrobenzoyloxy)methyl]furfural (NBzMF), and 5-[(4-chlorobenzoyloxy)methyl]furfural (CBzMF).

Interestingly, all the reagents and catalysts can be produced renewably from biomass following the existing synthetic methodologies.

- The chemistry of heterocycles has received much attention lately for its use in synthesizing essential molecules with pharmacological properties. The present work used gluconic acid aqueous solution (GAAS) as an efficient acid catalyst to synthesize novel DHPMs and DHPs using biomass-derived renewable 5-substituted-2-furaldehydes. The reaction was optimized for temperature, time, and GAAS loading.
- To increase the commercial potential of biorenewable chemicals, a one-pot, scalable, high-yielding method for producing AcMFs, a hydrophobic and halogen-free congener of HMF, from affordable sugars and carbohydrates is desired. The present work reported using strong Bronsted acid as a co-catalyst for producing AcMF from fructose in an acetic acid medium. The present work explores strong Bronsted acid co-catalysts, such as methanesulfonic acid (MSA), *p*-toluenesulfonic acid (PTSA), amberlyst-15 (A-15), and orthophosphoric acid (H_3PO_4) to produce AcMF from fructose.
- Scalable and economical production of AC from biogenic carbon, especially cellulosic wastes, has immense scope in various industrial settings. Production of AC from agricultural waste helps to mitigate the problem associated with landfilling, burning, and other environmental issues, along with increasing the value of the waste. The production of AC from cashew nut husk (CNH) and cashew nut shell (CNS) has been explored, and the adsorption properties have been studied. The chemical activation was carried out using H_3PO_4 at two different activation temperatures (500 and 700 °C). All four types of AC produced in this work showed excellent specific surface area. The methylene blue (MB) adsorption was carried out to study the adsorption properties of the synthesized AC samples.

7.2 CONCLUSIONS

The primary objective of the thesis was the synthesis of high-value chemicals and materials from biomass-derived resources. The following conclusions have been drawn based on the experimental findings discussed in chapters 3-6.

- A generic synthetic methodology was created for the quick and high-yielding synthesis of 23 MBH adducts using 5-substituted-2-furaldehydes and acrylates generated from biomass. Among the numerous tertiary amines and phosphines investigated, 1,4-Diazabicyclo[2.2. 2]octane (DABCO) was determined to be the most effective organocatalyst. The reaction was first optimized on FUR and later extended to other liquid and solid 5-substituted-2-furfuraldehydes such as 5MF, EMF, AcMF, PrMF, BuMF, BzMF, NBzMF, and CBzMF. The reactions were carried out at room temperature (RT) without the use of solvents, using an equivalent of DABCO catalyst and a slight excess of acrylate. The reactions were completed in a reasonable time. All the MBH adducts were isolated in good to excellent yields. DABCO catalyst was successfully recovered from the aqueous mixture at the end.
- 5-substituted-2-furaldehydes produced from carbohydrates were used to make novel 3,4-dihydropyrimidin-2(1H)-ones, 3,4-dihydropyrimidin-2(1H)-thiones, and 1,4-dihydropyridines (DHPs) in good to exceptional isolated yields using the Biginelli and Hantzsch reaction protocols, respectively. The gluconic acid aqueous solution was proved to be a highly effective catalyst and reaction medium that is also recyclable, affordable, non-toxic, and renewable. Using 5-substituted-2-furfrualdehydes, urea, and ethyl acetoacetate as reagents 3,4-dihydropyrimidin-2(1H)-ones were produced in reasonably decent yields at 60 °C and 6 h using 25 mol% of GAAS. Similarly, switching to thiourea and 50 mol% of GAAS at 80 °C and 12 h, 3,4-dihydropyrimidin-2(1H)-thiones were obtained in good yields. Excellent yields (>84%) of DHPs were obtained using 25 mol% of GAAS (60 °C, 3 h). The scalability of the Biginelli and Hantzsch reaction protocols was demonstrated on a 10 g scale of furfural
- Under optimized parameters the ACMF has been synthesized in a decent yield starting from fructose using strong Brønsted acid co-catalysts such as methanesulfonic acid (MSA), *p*-toluenesulfonic acid (PTSA), amberlyst-15 (A-15) and orthophosphoric acid (H_3PO_4). MSA gave 51% yield from fructose at 100 °C and 45 min.
- The CNS and CNH wastes were efficiently converted to AC by activating at 500 and 700 °C. The H-700 and S-500 gave excellent iodine numbers of 927

mg/g and 827 mg/g. The specific surface area of the samples was 1511 m^2/g and 1432 m^2/g, respectively. The study of adsorption isotherm of H-700 for MB adsorption showed the best fit for Langmuir isotherm with R^2 equals 0.9995. Adsorption and isotherm parameters of synthesized ACs show that they have excellent potential to be used as an adsorbent. Furthermore, H-700 showed a maximum monolayer MB adsorption capacity of 520 mg/g, which makes it an excellent adsorbent for MB and also for other pollutants of similar size.

7.3 FUTURE SCOPE

Novel, multifunctional, heterocyclic compounds have been reported in this work. Since the MBH adducts, DHPMs, and DHPs are known for their pharmacological activities, the biological activity of these novel molecules should be investigated. As a hydrophobic congener of HMF, AcMF has a huge scope for acting as a stable furanic chemical platform for synthesizing renewable fuels, chemicals, and materials of commercial significance. The future study should focus on finding the appropriate catalyst system and reaction conditions for the scalable production of AcMF in acceptable yields in the batch or continuous reactor setup. The reactivity patterns and derivative chemistry of AcMF should also be explored. The AC derived from the wastes of cashew nut industries can be used to remove other water contaminants to demonstrate its versatility as an efficient and inexpensive adsorbent. Other agricultural and municipal cellulosic wastes may be identified that can be conveniently converted into high-quality AC for commercial applications.

REFERENCES

Anchan, H. N., Bhat, N. S., Vinod, N., Prabhakar, P. S., and Dutta, S. (2022). "Catalytic conversion of glucose and its biopolymers into renewable compounds by inducing C–C bond scission and formation." *Biomass Convers. Biorefin., https://doi.org/10.1007/s13399-022-03105-9*.

Anchan, H. N., and Dutta, S. (2021). "Recent advances in the production and value addition of selected hydrophobic analogs of biomass-derived 5-(hydroxymethyl)furfural." *Biomass Convers. Biorefin.*, 13, 2571–2593.

ASTM-D4607-14R21 Standard test method for determination of iodine number of activated carbon, ASTM International, West Conshohocken, PA,. (2021). .

Bai, Y., Wei, L., Yang, M., Chen, H., Holdren, S., Zhu, G., Tran, D. T., Yao, C., Sun, R., Pan, Y., and Liu, D. (2018). "Three-step cascade over a single catalyst: synthesis of 5-(ethoxymethyl)furfural from glucose over a hierarchical lamellar multi-functional zeolite catalyst." *J. Mater. Chem. A*, 6(17), 7693–7705.

Bakhtiarian, M., and Khodaei, M. M. (2021). "Sonochemical synthesis of 1,4-dihydropyridines using a bio-derived magnetic nanocomposite based on the pectin modified with the di-sulfonic acids under mild conditions." *Mater. Today Commun.*, 29, 102791.

Bamgbola, A. A., Adeyemi, O. O., Olubomehin, O. O., Akinlabi, A. K., Sojinu, O. S., and Iwuchukwu, P. O. (2020). "Isolation and characterization of cellulose from cashew (Anacardium occidentale L.) nut shells." *Curr. Res. Green Sustainable Chem.*, 3, 100032.

Bardi, U. (2019). "Peak oil, 20 years later: Failed prediction or useful insight?" *Energy Res. Soc. Sci.*, 48, 257–261.

Basavaiah, D., and Tilak Naganaboina, R. (2018). "The Baylis–Hillman reaction: a new continent in organic chemistry – our philosophy, vision and over three decades of research." *New J. Chem.*, 42(17), 14036–14066.

Basavaiah, D., and Veeraraghavaiah, G. (2012). "The Baylis–Hillman reaction: a novel concept for creativity in chemistry." *Chem. Soc. Rev.*, 41(1), 68–78.

Bhat, N. S., L. Hegde, S., Dutta, S., and Sudarsanam, P. (2022). "Efficient synthesis of 5-(hydroxymethyl)furfural esters from polymeric carbohydrates using 5-

(chloromethyl)furfural as a reactive intermediate." *ACS Sustainable Chem. Eng.*, 10(18), 5803–5809.

Bhat, N. S., Yadav, A. K., Karmakar, M., Thakur, A., Mal, S. S., and Dutta, S. (2023). "Preparation of 5-(acyloxymethyl)furfurals from carbohydrates using zinc chloride/acetic acid catalyst system and their synthetic value addition." *ACS Omega*, 8(8), 8119–8124.

Bicker, M., Kaiser, D., Ott, L., and Vogel, H. (2005). "Dehydration of d-fructose to hydroxymethylfurfural in sub- and supercritical fluids." *J. Supercrit. Fluids*, 36(2), 118–126.

Bora, M., Kadam, K., Wani, P., and Kamble, N. (2022). "$NbCl_5$+$AgClO_4$ as a versatile combined catalyst system for an accelerated synthesis of 1, 4-dihydropyridine scaffolds." *Rasayan J. Chem.*, 15(04), 2596–2604.

Bouchelta, C., Medjram, M. S., Bertrand, O., and Bellat, J.-P. (2008). "Preparation and characterization of activated carbon from date stones by physical activation with steam." *J. Anal. Appl. Pyrolysis*, 82(1), 70–77.

Bozell, J. J. (2008). "Feedstocks for the future – biorefinery production of chemicals from renewable carbon." *Clean: Soil, Air, Water*, 36(8), 641–647.

Cai, N., Cheng, H., Jin, H., Liu, H., Zhang, P., and Wang, M. (2020). "Porous carbon derived from cashew nut husk biomass waste for high-performance supercapacitors." *J. Electroanal. Chem.*, 861, 113933.

Catarino, L., Menezes, Y., and Sardinha, R. (2015). "Cashew cultivation in Guinea-Bissau – risks and challenges of the success of a cash crop." *Sci. Agric. (Piracicaba, Braz.)*, 72(5), 459–467.

Cherubini, F. (2010). "The biorefinery concept: Using biomass instead of oil for producing energy and chemicals." *Energy Convers. Manage.*, 51(7), 1412–1421.

Chopda, L. V., and Dave, P. N. (2020). "Recent advances in homogeneous and heterogeneous catalyst in Biginelli reaction from 2015-19: A concise review." *ChemistrySelect*, 5(19), 5552–5572.

Choudhary, V., Sandler, S. I., and Vlachos, D. G. (2012). "Conversion of Xylose to Furfural Using Lewis and Brønsted Acid Catalysts in Aqueous Media." *ACS Catal.*, 2(9), 2022–2028.

Choudhury, P., Ghosh, P., and Basu, B. (2020). "Amine-functionalized graphene oxide nanosheets (AFGONs): an efficient bifunctional catalyst for selective formation of 1,4-dihydropyridines, acridinediones and polyhydroquinolines." *Mol. Diversity*, 24(1), 283–294.

Crespo, A., El Maatougui, A., Biagini, P., Azuaje, J., Coelho, A., Brea, J., Loza, M. I., Cadavid, M. I., García-Mera, X., Gutiérrez-de-Terán, H., and Sotelo, E. (2013). "Discovery of 3,4-dihydropyrimidin-2(1 *H*)-ones as a novel class of potent and selective A $_{2B}$ adenosine receptor antagonists." *ACS Med. Chem. Lett.*, 4(11), 1031–1036.

Debache, A., Ghalem, W., Boulcina, R., Belfaitah, A., Rhouati, S., and Carboni, B. (2009). "An efficient one-step synthesis of 1,4-dihydropyridines via a triphenylphosphine-catalyzed three-component Hantzsch reaction under mild conditions." *Tetrahedron Lett.*, 50(37), 5248–5250.

Devarajan, N., and Suresh, P. (2019). "MIL-101-SO_3H metal–organic framework as a Brønsted acid catalyst in Hantzsch reaction: an efficient and sustainable methodology for one-pot synthesis of 1,4-dihydropyridine." *New J. Chem.*, 43(17), 6806–6814.

Dezfoolinezhad, E., Ghodrati, K., and Badri, R. (2019). "Polyionene/Br_3 grafted on magnetic nanoparticles as an efficient and eco-friendly catalyst for the metal free synthesis of 3,4-dihydropyrimidin-2(1H)-ones/thiones." *Silicon*, 11(3), 1593–1609.

Do, T. H., Nguyen, V. T., Dung, N. Q., Chu, M. N., Van Kiet, D., Ngan, T. T. K., and Van Tan, L. (2021). "Study on methylene blue adsorption of activated carbon made from Moringa oleifera leaf." *Materials Today: Proceedings*, International Conference & Exposition on Mechanical, Material and Manufacturing Technology (ICE3MT), 38, 3405–3413.

Drewes, S. E., Emslie, N. D., Khan, A. A., and Roos, G. H. P. (1989). "1,2-Addition of activated vinyl carbanions to α,β-unsaturated carbonyls." *Synth. Commun.*, 19(5–6), 959–964.

D'Silva, R. J. (2021). "A case study of cashew industry in Karnataka." A case study International Journal of Case Studies in Business, IT, and Education (IJCSBE), 5(2), 329-341.

Dulie, N. W., Woldeyes, B., Demsash, H. D., and Jabasingh, A. S. (2021). "An insight into the valorization of hemicellulose fraction of biomass into furfural:

catalytic conversion and product separation." *Waste Biomass Valorization*, 12(2), 531–552.

Düll, G. (1895). "Action of oxalic acid on inulin." *Chem. -Ztg.*, 19, 216–220.

Dutta, S. (2023a). "Sustainable synthesis of drop-in chemicals from biomass via chemical catalysis: scopes, challenges, and the way forward." *Energy Fuels*, 37(4), 2648–2666.

Dutta, S. (2023b). "Valorization of biomass-derived furfurals: reactivity patterns, synthetic strategies, and applications." *Biomass Convers. Biorefin.*, 13(12), 10361–10386.

Dutta, S., and Mascal, M. (2014). "Novel pathways to 2,5-dimethylfuran via biomass-derived 5-(chloromethyl)furfural." *ChemSusChem*, 7(11), 3028–3030.

El maguana, Y., Elhadiri, N., Benchanaa, M., and Chikri, R. (2020). "Activated carbon for dyes removal: modeling and understanding the adsorption process." *J. Chem.*, 2020, e2096834.

El Qada, E. N., Allen, S. J., and Walker, G. M. (2006). "Adsorption of methylene blue onto activated carbon produced from steam activated bituminous coal: A study of equilibrium adsorption isotherm." *Chem. Eng. J.*, 124(1–3), 103–110.

Fan, W., Queneau, Y., and Popowycz, F. (2018). "HMF in multicomponent reactions: utilization of 5-hydroxymethylfurfural (HMF) in the Biginelli reaction." *Green Chem.*, 20(2), 485–492.

Fan, Z., Zhang, Z., Zhang, G., Qin, L., Fang, J., and Tao, P. (2022). "Phosphoric acid/FeCl3 converting waste mangosteen peels into bio-carbon adsorbents for methylene blue removal." *Int. J. Environ. Sci. Technol.*, 19(12), 12315–12328.

Fátima, Â. de, Braga, T. C., Neto, L. da S., Terra, B. S., Oliveira, B. G. F., Silva, D. L. da, and Modolo, L. V. (2015). "A mini-review on Biginelli adducts with notable pharmacological properties." *J. Adv. Res.*, 6(3), 363–373.

Feng, Y., Li, Z., Long, S., Sun, Y., Tang, X., Zeng, X., and Lin, L. (2020). "Direct conversion of biomass derived L-rhamnose to 5-methylfurfural in water in high yield." *Green Chem.*, 22(18), 5984–5988.

Fernando, S., Adhikari, S., Chandrapal, C., and Murali, N. (2006). "Biorefineries: current status, challenges, and future direction." *Energy Fuels*, 20(4), 1727–1737.

Fito, J., Abewaa, M., Mengistu, A., Angassa, K., Ambaye, A. D., Moyo, W., and Nkambule, T. (2023). "Adsorption of methylene blue from textile industrial wastewater using activated carbon developed from Rumex abyssinicus plant." *Sci Rep*, 13(1), 5427.

Fort, Y., Berthe, M. C., and Caubere, P. (1992a). "The 'Baylis-Hillman Reaction'mechanism and applications revisited." *Tetrahedron*, 48(31), 6371–6384.

Fort, Y., Berthe, M.-C., and Caubére, P. (1992b). "Selective mono and biscondensations of dialdehydes with methylacrylate." *Synth. Commun.*, 22(9), 1265–1275.

Gao, C., Ma, C., and Xu, P. (2011). "Biotechnological routes based on lactic acid production from biomass." *Biotechnol. Adv.*, 29(6), 930–939.

Gao, Y., Yue, Q., Gao, B., and Li, A. (2020). "Insight into activated carbon from different kinds of chemical activating agents: A review." *Sci. Total Environ.*, 746, 141094.

Gavilà, L., and Esposito, D. (2017). "Cellulose acetate as a convenient intermediate for the preparation of 5-acetoxymethylfurfural from biomass." *Green Chem.*, 19(11), 2496–2500.

Gawhale, N. D., Lokhande, M. N., Uke, S. J., Mardikar, S. P., Pandit, V. U., and Kodape, M. M. (2022). "An expedient synthesis of 3,4-dihydropyrimidin-2(1H)-ones derivatives under solvent free condition using titanium dioxide as a catalyst." *Materials Today: Proceedings*, Polymer & Mediterranean Fiber International, 53, 191–195.

Geczo, A., Giannakoudakis, D. A., Triantafyllidis, K., Elshaer, M. R., Rodríguez-Aguado, E., and Bashkova, S. (2021). "Mechanistic insights into acetaminophen removal on cashew nut shell biomass-derived activated carbons." *Environ. Sci. Pollut. Res.*, 28(42), 58969–58982.

Ghassamipour, S., and Sardarian, A. R. (2010). "One-Pot synthesis of dihydropyrimidinones by dodecylphosphonic acid as solid Bronsted Acid Catalyst under Solvent-Free Conditions via Biginelli condensation." *J. Iran. Chem. Soc.*, 7(1), 237–242.

G.J.M. Gruter, L. E. M., A. S. V. D. S. Dias, F. Dautzenberg, J. Purmova. (2012). "Hydroxymethylfurfural ethers and esters prepared in ionic liquids, US8314260B2."

Gomes, F. N. D. C., Pereira, L. R., Ribeiro, N. F. P., and Souza, M. M. V. M. (2015). "Production of 5-hydroxymethylfurfural (HMF) via fructose dehydration: effect of solvent and salting-out." *Braz. J. Chem. Eng.*, 32, 119–126.

González-García, P. (2018). "Activated carbon from lignocellulosics precursors: A review of the synthesis methods, characterization techniques and applications." *Renewable Sustainable Energy Rev.*, 82, 1393–1414.

Guidotti, B. B., and Coelho, F. (2015). "Sequential Morita–Baylis–Hillman/Achmatowicz reactions: an expeditious access to pyran-3(6H)-ones with a unique substitution pattern." *Tetrahedron Lett.*, 56(46), 6356–6359.

Haleem, A., Ullah, H., Samiullah, Akbar, A., Ahmad, N., Ellahi, M., and Nawaz, M. (2022). "Synthesis and biological activity of Morita Baylis Hillman adducts and their oximes." *Pharm. Chem. J.*, 56(2), 185–190.

Hataminejad, E., Ezabadi, A., and Shameli Akandi, A. (2023). "Novel synthesis of nano-amino acid-based ionic liquid and its application for preparing DHPMs and xanthenes under solvent-free conditions." *Res. Chem. Intermed.*, 49(4), 1275–1295.

Heidarinejad, Z., Dehghani, M. H., Heidari, M., Javedan, G., Ali, I., and Sillanpää, M. (2020). "Methods for preparation and activation of activated carbon: a review." *Environ. Chem. Lett.*, 18(2), 393–415.

Heravi, M. M., Bakhtiari, K., and Bamoharram, F. F. (2006). "12-Molybdophosphoric acid: A recyclable catalyst for the synthesis of Biginelli-type 3,4-dihydropyrimidine-2(1H)-ones." *Catal. Commun.*, 7(6), 373–376.

Hong Yeon-Woo. (2013). "Efficient synthesis of 5-O-acetylhydroxymethylfurfural (AcHMF) as an alternative to HMF, PhD Thesis, Seoul National University."

Hosseini Nasab, N., Raza, H., Shim, R. S., Hassan, M., Kloczkowski, A., and Kim, S. J. (2023). "A facile green synthesis of 3,4-dihydropyrimidin-2(1H)-ones using cysteine as a bio-organic catalyst: Potent urease inhibitors, in vitro evaluation, kinetic mechanism, and molecular docking studies." *J. Mol. Struct.*, 1286, 135638.

Hu, L., Lin, L., Wu, Z., Zhou, S., and Liu, S. (2017). "Recent advances in catalytic transformation of biomass-derived 5-hydroxymethylfurfural into the innovative fuels and chemicals." *Renewable Sustainable Energy Rev.*, 74, 230–257.

Huang, Q., Yang, F., Cao, X., Hu, Z., and Cheng, C. (2019). "Thermally healable polyurethanes based on furfural-derived monomers via Baylis-Hillman reaction." *Macromol. Res.*, 27(9), 895–904.

Huynh, N. T. T., Lee, K. W., Cho, J. K., Kim, Y. J., Bae, S. W., Shin, J. S., and Shin, S. (2019). "Conversion of D-fructose to 5-acetoxymethyl-2-furfural using immobilized lipase and cation exchange resin." *Molecules*, 24(24), 4623.

Ioannidou, O., and Zabaniotou, A. (2007). "Agricultural residues as precursors for activated carbon production—A review." *Renewable Sustainable Energy Rev.*, 11(9), 1966–2005.

Jangid, D. K. (2020). "DABCO as a base and an organocatalyst in organic synthesis: A review." *Curr. Green Chem.*, 7(2), 146–162.

Jiang, C., Cui, S., Han, Q., Li, P., Zhang, Q., Song, J., and Li, M. (2019). "Study on application of activated carbon in water treatment." *IOP Conf. Ser.: Earth Environ. Sci.*, 237(2), 022049.

Jing, Y., Guo, Y., Xia, Q., Liu, X., and Wang, Y. (2019). "Catalytic production of value-added chemicals and liquid fuels from lignocellulosic biomass." *Chem*, 5(10), 2520–2546.

Jogia, M. K., Vakamoce, V., and Weavers, R. T. (1985). "Synthesis of some furfural and syringic acid derivatives." *Aust. J. Chem.*, 38(7), 1009–1016.

John, S. E., Gulati, S., and Shankaraiah, N. (2021). "Recent advances in multi-component reactions and their mechanistic insights: a triennium review." *Org. Chem. Front.*, 8(15), 4237–4287.

Joshi, V., Vyawahare, S., Tekale, S., Shinde, S., Fareesuddin, M., Dake, Dr. S., Shisodia, S., and Pawar, R. (2013). "An efficent synthesis of 4-aryl-substituted 3,4-dihydropyrimidin-2(1H)-ones using nanocomposite ferrite catalyst." *Eur. Chem. Bull.*, 2, 481–484.

Kang, E.-S., Hong, Y.-W., Chae, D. W., Kim, B., Kim, B., Kim, Y. J., Cho, J. K., and Kim, Y. G. (2015). "From lignocellulosic biomass to furans via 5-acetoxymethylfurfural as an alternative to 5-hydroxymethylfurfural." *ChemSusChem*, 8(7), 1179–1188.

Kang, S., Fu, J., Deng, Z., Jiang, S., Zhong, G., Xu, Y., Guo, J., and Zhou, J. (2018). "Valorization of biomass hydrolysis waste: Activated carbon from humins as exceptional sorbent for wastewater treatment." *Sustainability*, 10(6), 1795.

Karapınar, H. S. (2022). "Adsorption performance of activated carbon synthesis by $ZnCl_2$, KOH, H_3PO_4 with different activation temperatures from mixed fruit seeds." *Environ. Technol.*, 43(9), 1417–1435.

Khamkeaw, A., Asavamongkolkul, T., Perngyai, T., Jongsomjit, B., and Phisalaphong, M. (2020). "Interconnected micro, meso, and macro porous activated carbon from bacterial nanocellulose for superior adsorption properties and effective catalytic performance." *Molecules*, 25(18), 4063.

Khan, I., Saeed, K., Zekker, I., Zhang, B., Hendi, A. H., Ahmad, A., Ahmad, S., Zada, N., Ahmad, H., Shah, L. A., Shah, T., and Khan, I. (2022). "Review on methylene blue: Its properties, uses, toxicity and photodegradation." *Water*, 14(2), 242.

Khang, D. S., Hai, T. D., Thi, T. D., and Tuan, P. D. (2020). "Dye removal using cashew nut shell activated carbon." *Vietnam J. Chem.*, 58(6), 832–840.

Khiratkar, A. G., Muskawar, P. N., and Bhagat, P. R. (2016). "Polymer-supported benzimidazolium based ionic liquid: an efficient and reusable Brønsted acid catalyst for Biginelli reaction." *RSC Adv.*, 6(107), 105087–105093.

Khodamorady, M., Sohrabnezhad, S., and Bahrami, K. (2020). "Efficient one-pot synthetic methods for the preparation of 3,4-dihydropyrimidinones and 1,4-dihydropyridine derivatives using BNPs@$SiO_2(CH_2)_3NHSO_3H$ as a ligand and metal free acidic heterogeneous nano-catalyst." *Polyhedron*, 178, 114340.

Kong, X., Zhu, Y., Fang, Z., Kozinski, J. A., Butler, I. S., Xu, L., Song, H., and Wei, X. (2018). "Catalytic conversion of 5-hydroxymethylfurfural to some value-added derivatives." *Green Chem.*, 20(16), 3657–3682.

Kornecki, J. F., Carballares, D., Tardioli, P. W., Rodrigues, R. C., Berenguer-Murcia, Á., Alcántara, A. R., and Fernandez-Lafuente, R. (2020). "Enzyme production of D-gluconic acid and glucose oxidase: Successful tales of cascade reactions." *Catal. Sci. Technol.*, 10(17), 5740–5771.

Koukabi, N., Kolvari, E., Khazaei, A., Ali Zolfigol, M., Shirmardi-Shaghasemi, B., and Reza Khavasi, H. (2011). "Hantzsch reaction on free nano-Fe_2O_3 catalyst :

excellent reactivity combined with facile catalyst recovery and recyclability." *Chem. Commun.*, 47(32), 9230–9232.

Kour, G., Gupta, M., Paul, S., Rajnikant, and Gupta, V. K. (2014). "SiO_2–$CuCl_2$: An efficient and recyclable heterogeneous catalyst for one-pot synthesis of 3,4-dihydropyrimidin-2(1H)-ones." *J. Mol. Catal. A: Chem.*, 392, 260–269.

Krystof, M., Pérez-Sánchez, M., and Domínguez de María, P. (2013). "Lipase-catalyzed (trans)esterification of 5-hydroxy- methylfurfural and separation from HMF esters using deep-eutectic solvents." *ChemSusChem*, 6(4), 630–634.

Kumar, K., Dahiya, A., Patra, T., and Upadhyayula, S. (2018a). "Upgrading of HMF and biomass-derived acids into HMF esters using bifunctional ionic liquid catalysts under solvent free conditions." *ChemistrySelect*, 3(22), 6242–6248.

Kumar, P. S., Ramalingam, S., and Sathishkumar, K. (2011). "Removal of methylene blue dye from aqueous solution by activated carbon prepared from cashew nut shell as a new low-cost adsorbent." *Korean J. Chem. Eng.*, 28(1), 149–155.

Kumar, S., P, D., and Rosen, M. A. (2018b). "Cashew nut shell liquid as a fuel for compression ignition engines: A comprehensive review." *Energy Fuels*, 32(7), 7237–7244.

Lange, J.-P., Heide, E. van der, Buijtenen, J. van, and Price, R. (2012). "Furfural—A promising platform for lignocellulosic biofuels." *ChemSusChem*, 5(1), 150–166.

Lee, C. B. T. L., and Wu, T. Y. (2021). "A review on solvent systems for furfural production from lignocellulosic biomass." *Renewable Sustainable Energy Rev.*, 137, 110172.

Li, X., Jia, P., and Wang, T. (2016). "Furfural: A promising platform compound for sustainable production of C_4 and C_5 chemicals." *ACS Catal.*, 6(11), 7621–7640.

Lim, H. Y., and Dolzhenko, A. V. (2021). "Gluconic acid aqueous solution: A bio-based catalytic medium for organic synthesis." *Sustainable Chem. Pharm.*, 21, 100443.

Liu, X., and Wang, R. (2018). "Upgrading of carbohydrates to the biofuel candidate 5-ethoxymethylfurfural (EMF)." *Int. J. Chem. Eng.*, 2018, e2316939.

Liu, Z., Patel, C., Harvey, J. N., and Sunoj, R. B. (2017). "Mechanism and reactivity in the Morita–Baylis–Hillman reaction: the challenge of accurate computations." *Phys. Chem. Chem. Phys.*, 19(45), 30647–30657.

Lubi, M. C., and Thachil, E. T. (2000). "Cashew nut shell liquid (CNSL) - a versatile monomer for polymer synthesis." *Des. Monomers Polym.*, 3(2), 123–153.

Madivalappa Davanagere, P., and Maiti, B. (2021). "1,3-Bis(carboxymethyl)imidazolium Chloride as a Sustainable, Recyclable, and Metal-Free Ionic Catalyst for the Biginelli Multicomponent Reaction in Neat Condition." *ACS Omega*, 6(40), 26035–26047.

Maheswara, M., Siddaiah, V., Rao, Y. K., Tzeng, Y.-M., and Sridhar, C. (2006). "A simple and efficient one-pot synthesis of 1,4-dihydropyridines using heterogeneous catalyst under solvent-free conditions." *J. Mol. Catal. A: Chem.*, 260(1), 179–180.

Majellaro, M., Jespers, W., Crespo, A., Núñez, M. J., Novio, S., Azuaje, J., Prieto-Díaz, R., Gioé, C., Alispahic, B., Brea, J., Loza, M. I., Freire-Garabal, M., Garcia-Santiago, C., Rodríguez-García, C., García-Mera, X., Caamaño, O., Fernandez-Masaguer, C., Sardina, J. F., Stefanachi, A., El Maatougui, A., Mallo-Abreu, A., Åqvist, J., Gutiérrez-de-Terán, H., and Sotelo, E. (2021). "3,4-Dihydropyrimidin-2(1*H*)-ones as antagonists of the human A_{2B} adenosine receptor: Optimization, structure–activity relationship studies, and enantiospecific recognition." *J. Med. Chem.*, 64(1), 458–480.

Maqsood, T., Dai, J., Zhang, Y., Guang, M., and Li, B. (2021). "Pyrolysis of plastic species: A review of resources and products." *J. Anal. Appl. Pyrolysis*, 159, 105295.

Mariana, M., Mistar, E. M., Alfatah, T., and Supardan, M. D. (2021). "High-porous activated carbon derived from Myristica fragrans shell using one-step KOH activation for methylene blue adsorption." *Bioresour. Technol. Rep.*, 16, 100845.

Mascal, M. (2017). "5-(Halomethyl)furfurals from biomass and biomass-derived sugars." *Production of Platform Chemicals from Sustainable Resources*, Z. Fang, Jr. Smith Richard L., and X. Qi, eds., Singapore: Springer, 123–140.

Mascal, M. (2019). "5-(Chloromethyl)furfural (CMF): A platform for transforming cellulose into commercial products." *ACS Sustainable Chem. Eng.*, 7(6), 5588–5601.

Mascal, M., and B. Nikitin, E. (2010). "High-yield conversion of plant biomass into the key value-added feedstocks 5-(hydroxymethyl)furfural , levulinic acid , and levulinic esters via 5-(chloromethyl)furfural." *Green Chem.*, 12(3), 370–373.

Mascal, M., and Nikitin, E. B. (2008). "Direct, high-yield conversion of cellulose into biofuel." *Angew. Chem.*, 120(41), 8042–8044.

Menegazzo, F., Ghedini, E., and Signoretto, M. (2018). "5-Hydroxymethylfurfural (HMF) production from real biomasses." *Molecules*, 23(9), 2201.

Merin, P., Jimmy Joy, P., Muralidharan, M. N., Veena Gopalan, E., and Seema, A. (2021). "Biomass-derived activated carbon for high-performance supercapacitor electrode applications." *Chem. Eng. Technol.*, 44(5), 844–851.

Mika, L. T., Cséfalvay, E., and Németh, Á. (2018). "Catalytic conversion of carbohydrates to initial platform chemicals: Chemistry and sustainability." *Chem. Rev.*, 118(2), 505–613.

Mondal, J., Sen, T., and Bhaumik, A. (2012). "Fe_3O_4 @mesoporous SBA-15: a robust and magnetically recoverable catalyst for one-pot synthesis of 3,4-dihydropyrimidin-2(1 H)-ones via the Biginelli reaction." *Dalton Trans.*, 41(20), 6173–6181.

Moral-Rodríguez, A. I., Leyva-Ramos, R., Ania, C. O., Ocampo-Pérez, R., Isaacs-Páez, E. D., Carrales-Alvarado, D. H., and Parra, J. B. (2019). "Tailoring the textural properties of an activated carbon for enhancing its adsorption capacity towards diclofenac from aqueous solution." *Environ. Sci. Pollut. Res.*, 26(6), 6141–6152.

Mulushewa, Z., Dinbore, W. T., and Ayele, Y. (2021). "Removal of methylene blue from textile waste water using kaolin and zeolite-x synthesized from Ethiopian kaolin." *Environ. Anal. Health Toxicol.*, 36(1), e2021007.

Nasr-Esfahani, M., Hoseini, S. J., Montazerozohori, M., Mehrabi, R., and Nasrabadi, H. (2014). "Magnetic Fe_3O_4 nanoparticles: Efficient and recoverable nanocatalyst for the synthesis of polyhydroquinolines and Hantzsch 1,4-dihydropyridines under solvent-free conditions." *J. Mol. Catal. A: Chem.*, 382, 99–105.

Ninan, A. R., Babbar, R., Dhiman, S., Singh, T. G., Kaur, K., and Dhiwan, V. (2022). "A Systematic Review on 1, 4-Dihydropyridines and its Analogues: An Elite Scaffold." *Biointerface Res. Appl. Chem.*, 12, 3117–3134.

Nyirenda, J., Zombe, K., Kalaba, G., Siabbamba, C., and Mukela, I. (2021). "Exhaustive valorization of cashew nut shell waste as a potential bioresource material." *Sci. Rep.*, 11(1), 11986.

Nzediegwu, E., and Dumont, M.-J. (2021). "Chemo-catalytic transformation of cellulose and cellulosic-derived waste materials into platform chemicals." *Waste Biomass Valorization*, 12(6), 2825–2851.

Onkarappa, S. B., and Dutta, S. (2019). "High-yielding synthesis of 5-(alkoxymethyl)furfurals from biomass-derived 5-(halomethyl)furfural (X=Cl, Br)." *ChemistrySelect*, 4(19), 5540–5543.

Ontiveros, J. F., Wang, L., Chatel, K., Yue, X., Tan, J.-N., Ali-Rachedi, F., Ahmar, M., Verrier, C., Fusina, A., Nardello-Rataj, V., and Queneau, Y. (2021). "Design and properties of a novel family of nonionic biobased furanic hydroxyester and amide surfactants." *ACS Sustainable Chem. Eng.*, 9(50), 16977–16988.

Oriez, V., Peydecastaing, J., and Pontalier, P.-Y. (2019). "Lignocellulosic biomass fractionation by mineral acids and resulting extract purification processes: conditions, yields, and purities." *Molecules*, 24(23), 4273.

Parthiban, A., and Makam, P. (2022). "1,4-Dihydropyridine: Synthetic advances, medicinal and insecticidal properties." *RSC Adv.*, 12(45), 29253–29290.

Patel, R. I., Sharma, A., Sharma, S., and Sharma, A. (2021). "Visible light-mediated applications of methylene blue in organic synthesis." *Org. Chem. Front.*, 8(7), 1694–1718.

Patil, R. V., Chavan, J. U., Dalal, D. S., Shinde, V. S., and Beldar, A. G. (2019). "Biginelli reaction: Polymer supported catalytic approaches." *ACS Comb. Sci.*, 21(3), 105–148.

Peng, Y., Li, X., Gao, T., Li, T., and Yang, W. (2019). "Preparation of 5-methylfurfural from starch in one step by iodide mediated metal-free hydrogenolysis." *Green Chem.*, 21(15), 4169–4177.

Pérez-Bustos, H. F., Lucio-Ortiz, C. J., Rosa, J. R. de la, Haro del Río, D. A. de, Sandoval-Rangel, L., Martínez-Vargas, D. X., Maldonado, C. S., Rodriguez-González, V., Garza-Navarro, M. A., and Morales-Leal, F. J. (2019). "Synthesis and characterization of bimetallic catalysts Pd-Ru and Pt-Ru supported on γ-alumina and zeolite FAU for the catalytic transformation of HMF." *Fuel*, 239, 191–201.

Phan, H. B., Luong, C. M., Nguyen, L. P., Bui, B. T., Nguyen, H. T., Mai, B. V., Mai, T. V.-T., Huynh, L. K., and Tran, P. H. (2022). "Eco-friendly synthesis of 5-hydroxymethylfurfural and its applications as a starting material to synthesize valuable heterocyclic compounds." *ACS Sustainable Chem. Eng.*, 10(27), 8673–8684.

Qadir, T., Amin, A., Sharma, P. K., Jeelani, I., and Abe, H. (2022). "A Review on Medicinally Important Heterocyclic Compounds." *Open Med. Chem. J.*, 16(1).

Rahimi, J., Niksefat, M., Heidari, M., Naderi, M., Abbasi, H., Tajik Ijdani, M., and Maleki, A. (2022). "Ammonium metavanadate (NH_4VO_3): a highly efficient and eco-friendly catalyst for one-pot synthesis of pyridines and 1,4-dihydropyridines." *Sci. Rep.*, 12(1), 13687.

Ramírez Bocanegra, N., Rivera De la Rosa, J., Lucio Ortiz, C. J., Cubillas González, P., Greenwell, H. C., Badillo Almaráz, V. E., Sandoval Rangel, L., Alcántar-Vázquez, B., Rodríguez-González, V., and De Haro Del Río, D. A. (2021). "Catalytic conversion of 5-hydroxymethylfurfural (5-HMF) over Pd-Ru/FAU zeolite catalysts." *Catal. Today*, Special Contributions to Symposium F3 of XXVII IMRC-2018, 360, 2–11.

Ramutshatsha-Makhwedzha, D., Mavhungu, A., Moropeng, M. L., and Mbaya, R. (2022). "Activated carbon derived from waste orange and lemon peels for the adsorption of methyl orange and methylene blue dyes from wastewater." *Heliyon*, 8(8), e09930.

Rathore, A. S., and Singh, A. (2022). "Biomass to fuels and chemicals: A review of enabling processes and technologies." *J. Chem. Technol. Biotechnol.*, 97(3), 597–607.

Reddy, Ch. V., Mahesh, M., Raju, P. V. K., Babu, T. R., and Reddy, V. V. N. (2002). "Zirconium(IV) chloride catalyzed one-pot synthesis of 3,4-dihydropyrimidin-2(1H)-ones." *Tetrahedron Lett.*, 43(14), 2657–2659.

Rosatella, A. A., Simeonov, S. P., Frade, R. F. M., and Afonso, C. A. M. (2011). "5-Hydroxymethylfurfural (HMF) as a building block platform: Biological properties, synthesis and synthetic applications." *Green Chem.*, 13(4), 754–793.

Rosenfeld, C., Konnerth, J., Sailer-Kronlachner, W., Solt, P., Rosenau, T., and Herwijnen, H. W. G. van. (2020). "Current situation of the challenging scale-up development of hydroxymethylfurfural production." *ChemSusChem*, 13(14), 3544–3564.

Roy, A., Fajardie, P., Lepoittevin, B., Baudoux, J., Lapinte, V., Caillol, S., and Briou, B. (2022). "CNSL, a promising building blocks for sustainable molecular design of surfactants: a critical review." *Molecules*, 27(4), 1443.

Safaei-Ghomi, J., Tavazo, M., and Mahdavinia, G. H. (2018). "Ultrasound promoted one-pot synthesis of 3,4-dihydropyrimidin-2(1H)-ones/thiones using dendrimer-

attached phosphotungstic acid nanoparticles immobilized on nanosilica." *Ultrason. Sonochem.*, 40, 230–237.

Safari, J., Azizi, F., and Sadeghi, M. (2015). "Chitosan nanoparticles as a green and renewable catalyst in the synthesis of 1,4-dihydropyridine under solvent-free conditions." *New J. Chem.*, 39(3), 1905–1909.

Safari, J., and Zarnegar, Z. (2013). "A magnetic nanoparticle supported Ni 2+ -containing ionic liquid as an efficient nanocatalyst for the synthesis of Hantzsch 1,4-dihydropyridines in a solvent-free dry-system." *RSC Adv.*, 3(48), 26094–26101.

S. Aher, D., R. Khillare, K., D. Chavan, L., and G. Shankarwar, S. (2021). "Tungsten-substituted molybdophosphoric acid impregnated with kaolin: effective catalysts for the synthesis of 3,4-dihydropyrimidin-2(1 H)-ones v i a biginelli reaction." *RSC Adv.*, 11(5), 2783–2792.

Sanborn, A. J., and Howard, S. J. (2009). "Conversion of carbohydrates to hydroxymethylfurfural (hmf) and derivatives, US20090156841A1."

Sanchez, N., Fayne, R., and Burroway, B. (2020). "Charcoal: An ancient material with a new face." *Clin. Dermatol.*, 38(2), 262–264.

Sanda, K., Rigal, L., and Gaset, A. (1992). "Optimisation of the synthesis of 5-chloromethyl-2-furancarboxaldehyde from D-fructose dehydration and in-situ chlorination of 5-hydroxymethyl-2-furancarboxaldehyde." *J. Chem. Technol. Biotechnol.*, 55(2), 139–145.

Santos, H., Zeoly, L. A., Rodrigues, M. T. Jr., Fernandes, F. S., Gomes, R. C., Almeida, W. P., and Coelho, F. (2023). "Recent advances in catalytic systems for the mechanistically complex Morita–Baylis–Hillman reaction." *ACS Catal.*, 13(6), 3864–3895.

Shang, Y., Wang, D., and Wu, J. (2009). "Novel $Sc(OTf)_3$/3-HQD catalyst for Morita–Baylis–Hillman reaction." *Synth. Commun.*, 39(6), 1035–1045.

Shapla, U. M., Solayman, Md., Alam, N., Khalil, Md. I., and Gan, S. H. (2018). "5-Hydroxymethylfurfural (HMF) levels in honey and other food products: effects on bees and human health." *Chem. Cent. J.*, 12(1), 35.

Sheldon, R. A. (2018). "The road to biorenewables: Carbohydrates to commodity chemicals." *ACS Sustainable Chem. Eng.*, 6(4), 4464–4480.

Shi, M., and Liu, Y.-H. (2006). "Traditional Morita–Baylis–Hillman reaction of aldehydes with methyl vinyl ketone co-catalyzed by triphenylphosphine and nitrophenol." *Org. Biomol. Chem.*, 4(8), 1468–1470.

Shinde, S., Deval, K., Chikate, R., and Rode, C. (2018). "Cascade Synthesis of 5-(Acetoxymethyl)furfural from Carbohydrates over Sn-Mont Catalyst." *ChemistrySelect*, 3(30), 8770–8778.

Sing, K. S. W. (1985). "Reporting physisorption data for gas/solid systems with special reference to the determination of surface area and porosity (Recommendations 1984)." *Pure Appl. Chem.*, 57(4), 603–619.

Smith, V. A., Rivera, J. F. A., Bello, R., Rodríguez-Aguado, E., Elshaer, M. R., Wodzinski, R. L., and Bashkova, S. (2021). "The role of surface chemistry and polyethylenimine grafting in the removal of Cr (VI) by activated carbons from cashew nut shells." *C*, 7(1), 27.

Spagnoli, A. A., Giannakoudakis, D. A., and Bashkova, S. (2017a). "Adsorption of methylene blue on cashew nut shell based carbons activated with zinc chloride: The role of surface and structural parameters." *J. Mol. Liq.*, 229, 465–471.

Spagnoli, A. A., Giannakoudakis, D. A., and Bashkova, S. (2017b). "Adsorption of methylene blue on cashew nut shell based carbons activated with zinc chloride: The role of surface and structural parameters." *J. Mol. Liq.*, 229, 465–471.

Sujiono, E. H., Zabrian, D., Zurnansyah, Mulyati, Zharvan, V., Samnur, and Humairah, N. A. (2022). "Fabrication and characterization of coconut shell activated carbon using variation chemical activation for wastewater treatment application." *Results Chem.*, 4, 100291.

Susanti, R. F., Wiratmadja, R. G. R., Kristianto, H., Arie, A. A., and Nugroho, A. (2022). "Synthesis of high surface area activated carbon derived from cocoa pods husk by hydrothermal carbonization and chemical activation using zinc chloride as activating agent." *Materials Today: Proceedings*, 2nd International Conference on Chemical Engineering and Applied Sciences, 63, S55–S60.

Tadda, M. A., Ahsan, A., Shitu, A., Elsergany, M., Thirugnanasambantham, A., Jose, B., Razzaque, M., and Norsyahariati, N. (2016). "A review on activated carbon: process, application and prospects." *J. Adv. Civ. Eng. Pract. Res.*, 2, 7–13.

Tajbakhsh, M., Alaee, E., Alinezhad, H., Khanian, M., Jahani, F., Khaksar, S., Rezaee, P., and Tajbakhsh, M. (2012). "Titanium dioxide nanoparticles catalyzed synthesis of Hantzsch esters and polyhydroquinoline derivatives." *Chin. J. Catal.*, 33(9), 1517–1522.

Tan, J.-N., Ahmar, M., and Queneau, Y. (2013). "HMF derivatives as platform molecules: aqueous Baylis–Hillman reaction of glucosyloxymethyl-furfural towards new biobased acrylates." *RSC Adv.*, 3(39), 17649–17653.

Tan, J.-N., Ahmar, M., and Queneau, Y. (2015). "Bio-based solvents for the Baylis–Hillman reaction of HMF." *RSC Adv.*, 5(85), 69238–69242.

Tezer, Ö., Karabağ, N., Öngen, A., Çolpan, C. Ö., and Ayol, A. (2022). "Biomass gasification for sustainable energy production: A review." *Int. J. Hydrogen Energy*, 47(34), 15419–15433.

Trox, J., Vadivel, V., Vetter, W., Stuetz, W., Kammerer, D. R., Carle, R., Scherbaum, V., Gola, U., Nohr, D., and Biesalski, H. K. (2011). "Catechin and epicatechin in testa and their association with bioactive compounds in kernels of cashew nut (Anacardium occidentale L.)." *Food Chem.*, 128(4), 1094–1099.

Tursi, A. (2019). "A review on biomass: Importance, chemistry, classification, and conversion." *Biofuel Res. J.*, 6, 962–979.

Ubando, A. T., Felix, C. B., and Chen, W.-H. (2020). "Biorefineries in circular bioeconomy: A comprehensive review." *Bioresour. Technol.*, 299, 122585.

Ullah, F., Ji, G., Irfan, M., Gao, Y., Shafiq, F., Sun, Y., Ain, Q. U., and Li, A. (2022). "Adsorption performance and mechanism of cationic and anionic dyes by KOH activated biochar derived from medical waste pyrolysis." *Environ. Pollut.*, 314, 120271.

Vassilev, S. V., Baxter, D., Andersen, L. K., and Vassileva, C. G. (2010). "An overview of the chemical composition of biomass." *Fuel*, 89(5), 913–933.

Verevkin, S. P., Emel'yanenko, V. N., Stepurko, E. N., Ralys, R. V., Zaitsau, D. H., and Stark, A. (2009). "Biomass-derived platform chemicals: thermodynamic studies on the conversion of 5-hydroxymethylfurfural into bulk intermediates." *Ind. Eng. Chem. Res.*, 48(22), 10087–10093.

Vottero, E., Carosso, M., Pellegrini, R., Piovano, A., and Groppo, E. (2022). "Assessing the functional groups in activated carbons through a multi-technique approach." *Catal. Sci. Technol.*, 12(4), 1271–1288.

Wan Daud, W. M. A., Ali, W. S. W., and Sulaiman, M. Z. (2003). "Effect of activation temperature on pore development in activated carbon produced from palm shell." *J. Chem. Technol. Biotechnol.*, 78(1), 1–5.

Wang, J. (2021). "Study on the performance identification of openCV in cashew nut shell-based activated carbon." *IOP Conf. Ser.: Earth Environ. Sci.*, 769(3), 032030.

Wang, L., Tan, J.-N., Ahmar, M., and Queneau, Y. (2019a). "Solvent issues in the Baylis-Hillman reaction of 5-hydroxymethyl furfural (HMF) and 5-glucosyloxymethyl furfural (GMF). Towards no-solvent conditions." *Pure Appl. Chem.*, 91(7), 1149–1158.

Wang, L., Tan, J.-N., Ahmar, M., and Queneau, Y. (2019b). "New functionalized scaffolds from hydroxymethylfurfural and glucosyloxymethylfurfural by Morita–Baylis–Hillman reaction with cycloalkenones." *C. R. Chim.*, 22(9), 615–620.

Wang, P.-Z., Chen, J.-R., and Xiao, W.-J. (2019c). "Hantzsch esters: An emerging versatile class of reagents in photoredox catalyzed organic synthesis." *Org. Biomol. Chem.*, 17(29), 6936–6951.

Wang, Y., Wang, H., Kong, X., and Zhu, Y. (2022). "Catalytic conversion of 5-hydroxymethylfurfural to high-value derivatives by selective activation of C−O, C=O, and C=C bonds." *ChemSusChem*, 15(13).

Wazir, A. H., Haq, I. ul, Manan, A., and Khan, A. (2022). "Preparation and characterization of activated carbon from coal by chemical activation with KOH." *Int. J. Coal Prep. Util.*, 42(5), 1477–1488.

Williams, M. T. J., Morrill, L. C., and Browne, D. L. (2020). "Expedient organocatalytic aza-Morita–Baylis–Hillman reaction through ball-milling." *ACS Sustainable Chem. Eng.*, 8(48), 17876–17881.

Witsuthammakul, A., and Sooknoi, T. (2012). "Direct conversion of glycerol to acrylic acid via integrated dehydration–oxidation bed system." *Appl. Catal., A*, 413–414, 109–116.

Xia, H., Xu, S., Hu, H., An, J., and Li, C. (2018). "Efficient conversion of 5-hydroxymethylfurfural to high-value chemicals by chemo- and bio-catalysis." *RSC Adv.*, 8(54), 30875–30886.

Xiong, C., Sun, Y., Du, J., Chen, W., Si, Z., Gao, H., Tang, X., and Zeng, X. (2018). "Efficient conversion of fructose to 5-[(formyloxy)methyl]furfural by reactive extraction and in-situ esterification." *Korean J. Chem. Eng.*, 35(6), 1312–1318.

Xu, J., Chen, L., Qu, H., Jiao, Y., Xie, J., and Xing, G. (2014). "Preparation and characterization of activated carbon from reedy grass leaves by chemical activation with H_3PO_4." *Appl. Surf. Sci.*, 320, 674–680.

Xu, J., Miao, X., Liu, L., Wang, Y., and Yang, W. (2021). "Direct synthesis of 5-methylfurfural from D-Fructose by iodide-mediated transfer hydrogenation." *ChemSusChem*, 14(23), 5311–5319.

Xu, Y.-H., and Li, M.-F. (2021). "Hydrothermal liquefaction of lignocellulose for value-added products: Mechanism, parameter and production application." *Bioresour. Technol.*, 342, 126035.

Yadav, V. G., Yadav, G. D., and Patankar, S. C. (2020). "The production of fuels and chemicals in the new world: critical analysis of the choice between crude oil and biomass vis-à-vis sustainability and the environment." *Clean Technol. Environ. Policy*, 22(9), 1757–1774.

Yang, T., and Lua, A. C. (2003). "Characteristics of activated carbons prepared from pistachio-nut shells by physical activation." *J. Colloid Interface Sci.*, 267(2), 408–417.

Yang, W., Grochowski, M. R., and Sen, A. (2012). "Selective reduction of biomass by hydriodic acid and its in situ regeneration from iodine by metal/hydrogen." *ChemSusChem*, 5(7), 1218–1222.

Yang, W., and Sen, A. (2011). "Direct catalytic synthesis of 5-methylfurfural from biomass-derived carbohydrates." *ChemSusChem*, 4(3), 349–352.

Yu, C., Liu, B., and Hu, L. (2001). "Efficient Baylis−Hillman reaction using stoichiometric base catalyst and an aqueous medium." *J. Org. Chem.*, 66(16), 5413–5418.

Yu, D., Liu, X., Jiang, J., Liu, Y., Tan, J., and Li, H. (2021). "Catalytic synthesis of the biofuel 5-ethoxymethylfurfural (EMF) from biomass sugars." *J. Chem.*, 2021, e9015481.

Yuan, H., Zhang, K., Xia, J., Hu, X., and Yuan, S. (2017). "Gallium (III) chloride-catalyzed synthesis of 3,4-dihydropyrimidinones for Biginelli reaction under solvent-free conditions." *Cogent Chemistry*, (C. Smith, ed.), 3(1), 1318692.

Zafeer, M. K., and Bhat, K. S. (2023). "Valorisation of agro-waste cashew nut husk (Testa) for different value-added products." *Sustain. Chem. Clim. Action*, 2, 100014.

Zhang, Q., Wan, Z., Yu, I. K. M., and Tsang, D. C. W. (2021a). "Sustainable production of high-value gluconic acid and glucaric acid through oxidation of biomass-derived glucose: A critical review." *J. Cleaner Prod.*, 312, 127745.

Zhang, X., Lin, L., Zhang, T., Liu, H., and Zhang, X. (2016). "Catalytic dehydration of lactic acid to acrylic acid over modified ZSM-5 catalysts." *Chem. Eng. J.*, 284, 934–941.

Zhang, Y., Wang, B., Zhang, X., Huang, J., and Liu, C. (2015). "An Efficient Synthesis of 3,4-Dihydropyrimidin-2(1H)-Ones and Thiones Catalyzed by a Novel Brønsted Acidic Ionic Liquid under Solvent-Free Conditions." *Molecules*, 20(3), 3811–3820.

Zhang, Z., Xu, L., Liu, Y., Feng, R., Zou, T., Zhang, Y., Kang, Y., and Zhou, P. (2021b). "Efficient removal of methylene blue using the mesoporous activated carbon obtained from mangosteen peel wastes: Kinetic, equilibrium, and thermodynamic studies." *Microporous Mesoporous Mater.*, 315, 110904.

Zhao, Y., Lu, K., Xu, H., Zhu, L., and Wang, S. (2021). "A critical review of recent advances in the production of furfural and 5-hydroxymethylfurfural from lignocellulosic biomass through homogeneous catalytic hydrothermal conversion." *Renewable Sustainable Energy Rev.*, 139, 110706.

Zhou, B., Yang, J., Li, M., and Gu, Y. (2011). "Gluconic acid aqueous solution as a sustainable and recyclable promoting medium for organic reactions." *Green Chem.*, 13(8), 2204–2211.

Zolfagharinia, S., Kolvari, E., and Salehi, M. (2017). "Highly efficient and recyclable phosphoric acid functionalized zirconia encapsulated-Fe_3O_4 nanoparticles: clean

synthesis of 1,4-dihydropyridine and 1-amidoalkyl-2-naphthol derivatives." *React. Kinet., Mech. Catal.*, 121(2), 701–718.

Zuo, M., Lin, L., and Zeng, X. (2023). "The synthesis of potential biofuel 5-ethoxymethylfurfural: A review." *Fuel*, 343, 127863.

LIST OF PUBLICATIONS

1. **Anchan, H. N**., & Dutta, S. (2023). Renewable synthesis of novel acrylates from biomass-derived 5-substituted-2-furaldehydes by Morita-Baylis-Hillman reaction. *ChemistrySelect*, *8*(13), e202300264.
2. **Anchan, H. N.**, Naik, P. C., Bhat, N. S., Kumari, M., & Dutta, S. (2023) Efficient synthesis of novel biginelli and hantzsch products sourced from biorenewable furfurals using gluconic acid aqueous solution as the green organocatalyst. *ACS Omega*, *8*(37), 34077-34083
3. **Anchan, H. N.**, Jadhav, S., & Dutta, S. (2023) Activated Carbon from Cashew Nut Husk and Cashew Nut Shell Wastes: Synthesis, Characterization and Adsorption Studies. *ChemistrySelect*, *8*(44), e202302831.

OTHER PUBLICATIONS

1. **Anchan, H. N.,** & Dutta, S. (2021). Recent advances in the production and value addition of selected hydrophobic analogs of biomass-derived 5-(hydroxymethyl)furfural. *Biomass Conversion and Biorefinery*, 13, 2571-2593.
2. **Anchan, H. N**., Bhat, N. S., Vinod, N., Prabhakar, P. S., & Dutta, S. (2022). Catalytic conversion of glucose and its biopolymers into renewable compounds by inducing C–C bond scission and formation. *Biomass Conversion and Biorefinery*, 1-34.
3. Dutta, S., Bhat, N. S., & **Anchan, H. N**. (2022). Nanocatalysis for Renewable Aromatics. *Heterogeneous Nanocatalysis for Energy and Environmental Sustainability*, *1*, 61-90.

7. CONFERENCE ATTENDED

1. Presented oral presentation on TEQIP-III sponsored international conference on "**Energy and Environmental Technologies for Sustainable Development**" organized by Department of Chemical Engineering, MNNIT Allahabad, Prayagraj.

Mrs. Harshitha N Anchan
Shree sathya narayana kripa, Hejamady, udupi district-574103
Mo. 9108139566; Email: anchanharshitha17@gmail.com

Personal Information:

Date of Birth: August 17, 1995

Sex: Female

Nationality: Indian

Languages: 1. English: (Proficient), 2. Hindi: (Proficient), 3. Kannada (Proficient), 4. Tulu, 5. Sanskrit: Basic.

Mailing Address: 605 Science Block, Dept. of Chemistry, NITK, Surathkal, Mangaluru-575025, Karnataka, India.

Educational Qualifications:

SSLC, Karnataka Seconcondary Education Examination Board, Sri Narayana Guru Eng. Med. High School, Mulky Mangalore Taluk (2010-2011) (**94.56%**)

Sri Narayana Guru Composite Pre University College Mulky, Department Of Pre-University Education , Government of Karnataka (2012-2013) (**92%)**

Bachelor of Science (2013-2016) in Chemistry, Physics, and mathematics from the Vijaya College, Mulki (under Mangalore university) India. Secured **Fourth rank in university (96.7%)**.

Master of Science (2016-2018) in Chemistry from National Institute of Technology (NITK), Karnataka, India. **(9.28/10)**.

Awards & Honors:

1. Karnataka State Eligibility Test (K-SET) in 2018 December.
2. GATE (2019), AIR is 712
3. CSIR-UGC-NET JRF (Junior Research Fellowship) in 2018 December.

4. TMA Pai gold medallist (best outgoing student in Degree College).
5. Sir C. V. Raman fellowship awarded by the Karnataka State Government (5000/- per annum) for three years (2015-2017).

Previous Research Experience:

Summer intership in Indian Institute of Technology, Madras (IITM), Karnataka, India

Title of project : Dynamics of self-assembled cordination complexes prepared from palladium(II) or cis-protectected palladium (II) and N,N'-(1,3-phenylene)dinicotinamide.

M. Sc. Research (major project) in National Institute of Technology Karnataka (NITK), Karnataka, India (Dec, 2017- May, 2018)

Title of project : Synthesis and Characterization of Nickel hydroxide/oxide nanofluids.

Professional Skills:

- Multi-step organic synthesis, green chemistry and catalysis, high pressure and high temperature reactions.
- Hands-on experience in handling high pressure-glass reactors
- Hands-on experience in analytical instruments (FT-IR, UV-Vis, and TGA).
- A regular compute operation in MS word, Excel, power point presentation, Chem Draw, Mestrelab Mestrenova, SciFinder, Bruker Topspin, Adobe products, etc.